2019

Surface-enhanced Raman Spectroscopic Imaging of Bacteria within Fresh Produce In Situ

Michael Hickey

SURFACE-ENHANCED RAMAN SPECTROSCOPIC IMAGING OF BACTERIA WITHIN FRESH PRODUCE *IN SITU*

A Dissertation Presented

by

MICHAEL E. HICKEY

Submitted to the Graduate School of the

University of Massachusetts, Amherst in partial fulfillment

of the requirements for the degree of

DOCTOR OF PHILOSOPHY

September 2019

Department of Food Science

SURFACE-ENHANCED RAMAN SPECTROSCOPIC SURVEILLANCE OF BACTERIA WITHIN FRESH PRODUCE *IN SITU*

A Dissertation Presented

by

MICHAEL E. HICKEY

Approved as to style and content by:

_____

Lili He, Chair

_____

Matthew D. Moore, Member

_____

Mingxu You, External Member

_____

Eric A. Decker, Department Head

Department of Food Science

DEDICATION

This proposal is dedicated to my Mom and my Dad. Thank you for seeing me all the way through.

ACKNOWLEDGEMENTS

I thank God for being my reminder that the journey is more important than the ending. I thank my Mom and my Dad for always making sure that I had everything that I needed to succeed. I never felt forgotten throughout the darker moments of graduate school because my parents were always thinking of me and checked-in regularly to make sure that I was healthy and safe. Their moral support is really what kept me building at times when it all seemed to be falling apart faster than I could sustain. They were always there for me during the best and worst times and, in the end, that support is what got me through to the end. Without the loving support of my parents, I wouldn't have accomplished anything. My brothers and sister were my best escape from the stresses of graduate school and they were always the most encouraging. It's easy to forget that we're doing impressive work in the lab when the stress seems to get the best of us. My family was always there to remind me that my time in graduate school was well-spent and that the research struggles were well-worth the trouble in the end.

My advisor, Dr. Lili He, has been an inspiration to me since the first time that we met. I'll always be grateful for her leadership inside and outside of the lab. She always wore a smile and radiated that, 'take a deep breathe,' attitude that I needed to make it through the program. Dr. He was always adamant to our team that research should not consume our lives and that it is important to go outside to spend time doing things that we enjoy. She taught me when it is time to take things seriously and when to be less strict with my time. Her advice has made me a more efficient scientist and has helped me to

find joy in jobs that used to overwhelm me with stress. Most of all Dr. He was willing to take me onto her team and for that I'll be forever grateful that she took that chance on me. My peers in the lab were also invaluable to my experiences during the program. I made a lot of good friends and valuable collaborations that will last my lifetime. Research science at the Ph.D. level can sometimes stir-up heated debates between lab members but, when I reflect on everything, I really value the shared-passion of common interests in the lab and I'm grateful to have been surrounded by such an awesome team.

Nearly every member of the department has influenced me in one way or another. Dr. Eric Decker has been a tremendous department head and was one of the first faculty in the program to communicate with me years ago. I want to thank him for entrusting me with the responsibilities of a teaching assistantship. Dr. Ronald Labbe and Dr. Yeonhwa Park served as Graduate Program Directors during my time at the university and did an excellent job of communicating with me to make sure that I met the necessary requirements for graduation; or sometimes just to have lighthearted conversations in the hallway. Dr. Guodong Zhang, Dr. Julian McClements, and Dr. Maria Corradini each taught courses of mine at UMass that I'll keep with me forever. Dr. Zhang for his tell-it-like-it-is attitude that I desperately needed to help navigate the field properly. Dr. McClements for his genuine philosophical approach to teaching that I believe is legendary to our department. Dr. Corradini for her very human and down-to-earth approachability that always brought a calm when I needed it. She took notice of me at times when I was struggling in the research lab and she could have ignored it and walked away. Instead she approached me to remind me that I was doing everything right and to keep my head up and keep trying.

Dr. Fergus Clydesdale and Dr. Robert Levin have both contributed so much to the department that I continue to benefit from their legacies. Dr. Clydesdale is still active in the department and I'm grateful for his leadership. Dr. Levin was the advisor of my first research advisor, Dr. Jung-Lim Lee, when I started working in Delaware back in 2011. It has been a special experience learning so many of Dr. Levin's protocols at another university before bringing back that legacy for work within the halls of UMass. It goes to show what an amazing program that we have in Amherst. The department and the students are invested symbiotically in one-another and the relationship travels across generations all over the world. I hope that my research contributions will one day have the same effect on incoming young scientists. These two faculty have been a humbling inspiration to me.

I am grateful to Jean Alamed and Fran Kostek. The Ph.D. program is rather sink-or-swim and, paired with my initial teaching assistant responsibilities and lack of knowledge about the building during my earliest days in the program, these two people were my lifelines. Jean always made sure that I found everything that I needed for teaching labs. I can think of several occasions where she raced over to the store to get things that I couldn't find and at least one occasion where she worked excessively late into the day to make sure that my chemicals were up-to-code for an important experiment. She certainly has a reputation in my book for saving the day. Fran was my go-to source for knowledge of the department. She knew everyone and everything. If I needed a hundred copies of an exam for a class that was in five minutes – Fran would make it happen. She kept me out of trouble when I was still learning the ropes more times than I can count.

Dr. Jung-Lim Lee was the first professor to offer me an opportunity to work in food science research. Years ago, I was turned-away for an undergraduate research position in an organic chemistry lab. That professor told me, “I’ll tell you what – There is an internship opportunity [this other] university. It’s hard work and you’ll have to give-up your summer. But if you prove yourself there, I’ll give you a chance in my lab next fall.” That opportunity was in Dr. Lee’s lab. Dr. Lee didn’t second guess me or turn me away, he simply gave me the opportunity. Out of that evolved a very strong professional relationship and to this day he remains one of my closest personal friends. I never took the opportunity in the organic chemistry lab. Instead, I stayed-on in Dr. Lee’s lab and worked for free after the internship ended. I learned a lot about from him about the fields of food science, microbiology, and biotechnology. He taught me the importance of conducting quality research, even at the expense of output quantity. I take a lot of pride in the scientific values that he instilled in me and our team. He will always be a trustworthy collaborator and close family friend.

I want to thank my committee for all of the time that they donated to my dissertation. I proctored the student interview with Dr. Matthew Moore when he was considering joining the UMass family and everyone loved his sense of humor, his depth of knowledge, and his down-to-earth demeanor. Dr. Moore served on the committee for my verbal exam and has always shared his wealth of graduate school and microbiological knowledge with me when I needed it. Dr. Mingxu You deserves acknowledgement for taking time out of his schedule to evaluate my research efforts at UMass. He has a wealth of experience in analytical and biomedical applications and I am extremely grateful that he volunteered his time to serve on my committee. Dr. Lynn McLandsborough served on

my verbal exam committee, as well. She was one of the first faculty that I interacted with during my time at UMass. I always enjoyed talking with her about the idiosyncrasies of microbiological research and I will always be grateful that she was willing to share her lab space with me during my early months at the university.

Brett Sansbury's contributions to my everyday life have been indispensable throughout this study. She was my closest friend throughout my hardest times during this program. Brett and I shared our dog, Achilles, throughout this entire process. Each having to experience loss and solitude throughout our graduate studies, simultaneously. We, understatedly, have had our share of hard times these past few years. We were burglarized, in several car accidents, faced with serious threats to our dog's health, and each forced to handle these hardships alone, by cell phone communication. Through it all, Brett has become a reminder to me that a life in isolation is no life at all. She has always been there for me when I needed her most, during the happiest times and the most stressful. She, and our dog Achilles, are the most important parts of my life. They have brought me the most hope for a fulfilling life and have been my escape when I needed to take a breather away from the bench of a research lab. Without them, I would not have made it through graduate school.

ABSTRACT

SURFACE-ENHANCED RAMAN SPECTROSCOPIC SURVEILLANCE OF BACTERIA WITHIN FRESH PRODUCE *IN SITU*

SEPTEMBER 2019

MICHAEL E. HICKEY, B.S., DELAWARE STATE UNIVERSITY

M.S., DELAWARE STATE UNIVERSITY

PH.D. UNIVERSITY OF MASSACHUSETTS, AMHERST

Directed by: Professor Lili He

The growth curves for *E. coli* O157:H7 (#043888) are reported. We make the case that the onset of stationary growth is the optimal point at which a bacteria culture is considered suitable for quantitative Raman analyses. The optimal conditions for 3-mercaptophenylboronic acid coating of bacteria cells is also reported. Fundamental drawbacks of the status-quo approach have been elucidated and overcome, based on measurable improvements to the experimental methodology. This approach is shown to be suitable for the evaluation of bacterial rinse-washing efficacy by means of Raman light-scattering. The data were compared to label-free applications and the measurable differences between each approach were defined. Future use of 3-mercaptophenylboronic acid labelling for SERS analyses of bacteria should strictly follow the methods that we outlined within this paper. A real-time method to surveil mass bacterial communities

directly *in situ* is also reported. The approach was successfully employed to indiscriminately monitor mass bacteria populations directly among plant tissue.

TABLE OF CONTENTS

Page

LIST OF TABLES

Table Page

LIST OF FIGURES

Figure Page

CHAPTER 1

INTRODUCTION

1.1. Raman Spectroscopy

1.1.1. Rayleigh and Raman light-scattering

Spectroscopy is the spectral analysis of photon-collisions with matter. Collisions between photons and matter are detected by a silicon-based charge-coupled device which can register an entire spectrum of scattered light in one acquisition. Photon collisions with matter generally result in light-scattering at wavelengths and frequencies which are equal to that which was evident prior to the interaction; this is the result of *elastic* photon collisions called Rayleigh light-scattering. However, some photons that encounter matter cause molecules to exhibit vibrational -excitation or -rotations which cause light-scattering patterns that are unique to molecular structure; this is the result of *inelastic* photon collisions called Raman light-scattering. Raman scattered photons (*i.e.* scattered Raman frequencies) typically exhibit lower energies and frequencies than were exhibited prior to their excitative contact with matter (*i.e.* exciting frequencies). Raman scattering of photons is therefore weaker than Rayleigh light-scattering and can be challenging to detect for spectral analyses.

1.1.2. Types of Raman light-scattering

Raman scattering of inelastic photon collisions with matter are generally expressed in one of two forms. The first and stronger form occurs when a portion of the

photon's energy is transmitted to the colliding matter upon impact, causing the matter to increase in its energy state; this is the result of a *red shift* that we identify as Stoke's Raman scattering. The second weaker form occurs when a portion of the material's energy is transmitted to the colliding photon upon impact, causing the photon to increase in its energy state; this is the result of a *blue shift* that we identify as anti-Stoke's Raman scattering. The form of the inelastic collision that is ultimately expressed depends on the temperature, the types of photons being administered, as well as the analyte upon which they are employed. These parameters can be voluntarily manipulated based on the research objectives of the user. The Raman scattering that is to be discussed in this dissertation will be Stoke's Raman scattering in which an analyte will be excited by one intense monochromatic light frequency (*i.e.* a laser beam) for energy transmission into a predetermined material for the expression of a distinct light-scattering spectral pattern of interest.

1.1.3. Significance of Raman light-scattering

Inelastic Raman scattering can be difficult to detect because most photons scatter elastically (*i.e.* Rayleigh scattering) following their collision with matter. Only about 10^{-5} % of exciting photon frequencies exhibit Raman interactions when colliding with an analyte. However, the Rayleigh scattering pattern of photons is less dependent on the *composition* of the colliding matter than that of Raman scattering patterns. The Raman scattering of photons is strongly dependent on the molecular composition of the interacting matter which direct Raman emittance based on molecular composition, conformation, rotation, and vibration following photonic excitation. The specific pattern

of Raman scattered photons often represents important information about the photon-matter interaction itself, reflecting specific qualities of the interacting matter which can be examined quantitatively through spectral analyses. Raman spectra can be reverse-engineered to identify an analyte, to study the conformational qualities of a substance, or to elucidate the molecular vibrational-behavior of an analyte when exposed to photonic excitation. Raman light-scattering patterns are therefore worth investigating despite restrictions in their detection.

1.1.4. Advantages of Raman spectroscopy

Raman spectroscopy is often associated with gas chromatography, high-performance liquid chromatography, mass spectrometry, and infrared spectroscopy. Each of these alternative methods possesses its own unique advantages. The major advantage of Raman spectroscopy is its potential for targeted molecular analyses without the need to separate an analyte from its substrate. Infrared spectroscopy is the only method which can compete in this respect. Both Raman and infrared spectroscopy are employed to analyze the vibrational behavior of molecules under photonic excitation. However, Raman spectroscopy is the study of molecular-polarization vibrations which *scatter* light while infrared spectroscopy is the study of molecular charge distance-dependent vibrations (*i.e.* dipole moments) which *absorb* light. Raman spectroscopy generally exhibits higher sensitivity to homo-nuclear molecular bonds (*e.g.* C-C or C=C) while infrared spectroscopy is generally more sensitive to hetero-nuclear functional group vibrations and polar bonds (*e.g.* OH stretching in H_2O). The methods are often employed as complements to each other because some molecules are more compatible with one of

these two spectroscopic analyses than the other. Raman spectroscopy is therefore irreplaceable in the targeted, non-destructive study of molecules which possess low-compatibility with infrared spectroscopic analyses.

Raman spectroscopy enables the direct, *in situ* study of an analyte among its original substrate. Most alternative approaches require the destructive separation or purification of an analyte from its substrate. Raman scattering also allows scientists to precisely image the location of an analyte respective to the geography of its substrate above the inchscale. The instrument operates at room temperature and does not require column or solvent-dependent separation to analyze multiple components simultaneously. Raman instruments have been mobilized for portable field applications but mapping features have not yet been included in these devices. Raman imaging is panoramic-based and does not limit the user to one microscopic field-of-view; as in seen in alternative optical approaches. The approach is 1,000x more sensitive than fluorescent analyses, offering significant advantages for the detection of low analyte concentrations. Furthermore, fluorescent analyses generally require dark-field parameters which disconnect the luminescence from that of the substrate. Raman imaging overlays the geographic and chemical qualities of an analyte with the high-resolution, detailed imagery of its substrate. Raman lasers are generally near-infrared and therefore enable a unique depth-penetration of photons for analytical profiling at the x, y, and z-axes; this can be variable depending on the opacity of the substrate. Thus, Raman depth profiling enables scientists to non-destructively detect an analyte which has internalized within a substrate and precisely identify its location *in situ*. The unique advantages of Raman

spectroscopy can be analyzed in real-time and the versatility of the approach converges with a variety of multidisciplinary applications.

1.1.5. Disadvantages of Raman spectroscopy

Raman samples are strongly subjected to natural entropy and the lack of control over the physics therein is often the root of the method's drawbacks. Raman spectroscopy does not possess separatory features, such as those seen in chromatography. The laser line is generally very narrow, and the targeted precision of the approach is therefore a potential drawback, as the analyte of interest must be aligned directly under the laser line to produce a detectable signal. Not all molecules will exhibit Raman modes when contacted with a laser and are therefore incompatible with the approach altogether. Molecules which are compatible with Raman analyses often require controlled substrates (*e.g.* Au-coated, reflective glass) to produce sufficient Raman light-scattering for detection. Thus, complex substrates such as natural plant tissues are extremely difficult to collect Raman signals without enhancement mechanisms. Enhancers typically included nanostructures which are comprised of metallic noble metals and the structures must be within close contact of the analyte to register a detectable signal. False-negative detection is an ever-present challenge that Raman technologists must overcome. There is a wide-spread need for standardization in the field, as well. Different instruments or software will sometimes register different spectra from the same sample. Free nanoparticles will never fall in precisely the same way, twice – which can profoundly influence Raman analyses. Many groups prepare their own nanostructures in-house, which can significantly alter the Raman spectra of an analyte, and even purchasing nanoparticles

from different commercial suppliers can yield different Raman results. There is a double-standard in the field of Raman spectroscopy wherein the same aspects of the approach that are branded as ‘drawbacks’ can also be seen as ‘advantages’ in versatility and precision.

1.1.6. Surface-enhanced Raman spectroscopy

Raman light-scattering emissions can be enhanced by the presence of noble metal nanostructures (*e.g.* gold, platinum, silver) which possess plasmon resonance frequencies which are favorable for Raman mode molecular excitation. Two major theories have been recognized as plausible explanations of this phenomenon but the mechanisms by which Raman light-scattering patterns are enhanced under these circumstances remain inconclusive. The first theory is founded around the electromagnetic properties of noble metal structures. Many scientists believe that perpendicular photon-noble metal structure collisions create Langmuir waves –rapid electron oscillations on the nano structure surface– which act as molecular polarization forces. Polarization forces (*i.e.* plasmon polaritons) induce molecular vibrations which are reminiscent of Raman excitation as the noble metal electron clouds oscillate toward equilibrium at the nanoscale. Thus, the quantity of Raman scattered photons is increased dramatically because the molecular analyte is preserved in its Raman excitation mode. Raman light-scattering is difficult to analyze when the molecular analyte is not exhibiting Raman excitation; these are optimal conditions for Rayleigh scattering. The second theory explains surface-enhancement in Raman scattering which operates independently of plasmon polariton activity. Certain molecules can adsorb to noble metal surfaces through electron-donor-acceptor complexes

(*i.e.* charge transfer). Molecular orbital occupancies among the analyte are transitioned which alter the energy state of the molecules being analyzed. Noble metal nanostructures would therefore act as charge-transfer intermediates which allow Raman frequencies to excite the analyte as efficiently as ultra-violet light to exhibit Raman light-scattering. Each surface-enhanced Raman light-scattering mechanism is believed to stand-alone or cooperate in unison depending on the circumstances.

1.1.7. Ligand applications in Raman spectroscopy

Ligands are ions or molecules which are attached to a metal atom by coordinate bonding (*i.e.* dative covalent bonding). Coordinate bonds are similar to traditional covalent bonding –two different atoms each contributing one electron to establish one mutual bond– except both electrons in the bond pair are donated by one atom for reception by the second atom. Surface-enhanced Raman spectroscopy relies on nanoscale metallic materials to increase the detection of Raman scattered photons. Ligands are often incorporated into Raman analyses due to their natural binding capacity with metal atoms. Ligands can also be specialized for selective binding to an intended analyte. Closer interactions between nanometals and analyte of interest results in stronger Raman signaling. Ligands can therefore be designed to closely bridge a target analyte together with nanometals for concentrated and enhanced Raman analyses.

Foodborne illness is a common threat to public health among consumers world-wide. Food products can act as growth mediums that provide sustenance to a variety of microorganisms. Environmental pathogens can take refuge within food matrices and have the potential to harm consumers on a mass-scale. Approximately 48 million people are

victims of foodborne outbreaks in the United States every year, resulting in about 128 thousand hospitalizations and 3 thousand consumer fatalities (CDC, 2010). The Food and Agriculture Organization of the United Nations has stated that the current global agricultural-output needs to be increased by at least 70% by the year 2050 to sustain the human population (FAO, 2009). The evidence suggests that a greater number of consumer health crises will emerge in the coming years if food safety measures are to remain unchanged. The United States Congress has addressed this issue by passing the Food Safety Modernization Act (Public Law 11-353, 2011) which the Food & Drug Administration described as "the most sweeping reform of [the nation's] food safety laws in more than 70 years" (FDA, 2016). Regulators cited a need for (a) new safety standards and (b) enhanced inspection capabilities in food systems, as two of the bill's top-priorities. In support of this effort, we propose the use of surface-enhanced Raman spectroscopy as a tool to detect, characterize, and track bacteria in leafy produce as a means of preventing costly food recalls or mass consumer health crises.

1.2. Relevant Food Safety Concerns

1.2.1. Leafy vegetables and foodborne illness

Raw foods of animal origin are generally act as the most severe sources of foodborne illness (Painter et al., 2013). Fruits and vegetables are viewed as having low health-risks in comparison and are often thought to be a lower priority in foodborne illness research. However, leafy greens are the most likely food to cause foodborne illness (Tomson, 2013). In one example, a U.S. *Escherichia coli* O157:H7 outbreak in spinach products (Dole Food Company, Inc.) occurred in 2006 causing over 200 people

to be infected, resulting in 3 consumer deaths (CDC, 2006). Larger outbreaks are typically linked to processed markets because corporate products tend to reach massive consumer populations. Vegetables can be distributed in either fresh or processed markets. A fresh market would consist of the plant being picked by-hand in the field, bundled in its original form, and sold as-is without any treatment or further processing. A processed market would consist of the harvested plant being exposed to sterilization, processing, or packaging techniques through a food distribution facility. These food processing pathways can inflict minor physical damage to the leafy vegetable matrix. When the biochemistry of the leaves themselves are compromised in this way, microorganisms are more likely to access the internal tissue of the product where they are better protected against antimicrobial applications.

Spinach leaves will serve as one medium in our investigation of the nature of bacteria in plant tissues *in situ*. The commodity yields over $6.2 million in the U.S. annually and is on track to grow in value by about 4% every year (USDA, 2016). Although some spinach products are imported internationally, spinach that is consumed in the U.S. is generally grown domestically (Lucier et al., 2004). Most U.S. spinach output can be traced back to California (70%), Arizona (21%), Texas (4.3%), and New Jersey (3.5%), with Colorado and Maryland being the minority (<1% combined) (USDA, 2016). Foodborne illness stemming from spinach consumption is generally the result of *E. coli* or *Salmonella* species. Consumers infected by these pathogens exhibit fever, nausea, digestive distress, and severe physical pain. These symptoms can lead to hospitalization or even death. Contamination in spinach can occur during environmental growth, irrigation, harvest, transportation, and handling or storage procedures during food

processing. Bacteria take shelter in leaf tissues through anatomical openings such as pores, physical abrasions, or vascular tissue. Leaves also exhibit physical creasing or wrinkling patterns which offer bacteria a safe-haven, protecting them from antimicrobial applications. Therefore, biological pathogens in leafy vegetables possess a niche opportunity to harm consumers even when preventative measures are carried out appropriately.

1.3. Surveillance of Biological Hazards in Foods

1.3.1. Importance of SERS in microbial detection

Surveillance of biological pathogens is a top-priority among food companies and federal agencies. Foodborne outbreaks can drive-down corporate financial markets for several months before reaching a recovery (USA Today, 2007). This drives business outside of domestic companies to international competitors and can leave a permanent, negative-brand in the collective consciousness of consumers. Biological pathogens thus harbor a wealth of potential as weapons of mass destruction, in terms of consumer health and global economics. Researchers have developed technologies that can target these pathogens for surveillance in food-related systems (Table 1). Surfaced-enhanced Raman spectroscopy (SERS) is a laboratory tool that utilizes laser technology to establish a spectra-based ‘fingerprint’ of a given sample (Zheng and He, 2014). The spectra are established based on light dispersions that pass-through detection filters as a result of laser contact with an analyte and certain nanoparticles can allow SERS to detect as few as one single molecule in a sample (Kneipp et al., 1997). Microbiological studies have shown that SERS can detect and distinguish bacteria down to the subspecies level (Jarvis

and Goodacre, 2004). SERS is therefore emerging as one of the most rapid, sensitive, specific, and user-friendly strategies to detect hazards in food.

SERS stands-out as a superior biological detection strategy because the method allows for the monitoring of a target organism both (a) *in situ* and (b) in real-time. Bacteria can be detected in aqueous solutions using SERS without the need for sophisticated bacterial cell-labels, showing promise for applications in the beverage industry (Zhou et al., 2015). Solid food matrices are complex and present challenges to biological detection strategies. These food matrices must be broken-down, homogenized, or purified to isolate inhabiting-microorganisms for accurate detection (Wu et al., 2013). Sunduram and colleagues (2013) were able to detect bacteria in chicken by rinsing the sample and analyzing the drainage using SERS. Until now, however, detection strategies to monitor bacteria in solid food matrices directly *in situ* have not been established. Recently though, Yang and colleagues (2016) were able to detect chemical hazards within the matrix of spinach leaves *in situ* using SERS. SERS detection of the spinach leaf matrix did not interfere with peaks that were representative of the pesticides being analyzed in their study. Related research in SERS detection of microorganisms has shown that bacteria consistently produce a peak at the 780 'Raman shift cm^{-1}' range due to N-acetyl-d-glucosamine that is present in the cell wall (Jarvis and Goodacre, 2004). The characteristic peak of bacterial detection using SERS also appears to be applicable to plant tissues for *in situ* detection.

1.3.2. General concepts of interest in pathogenic surveillance of foods

Detection of bacteria can be accomplished by a number of different methods. New methods of bacteria detection emerge every year. There are often a number of concerns that linger through this line of research such as: (i) will the method of detection be cost-effective, (ii) will the method of detection be able to identify the bacteria, (iii) will the method of detection be compatible with the speed of production, (iv) how many samples can be screened by an employee in a given day, (v) how experienced does the user need to be in order to conduct the screening, (vi) how low is the limit of detection, and (vii) how much work should go into preparing the sample for screening before the actual assay procedures? Depending on the food product that is produced, some of these questions gain merit over others. For example, if a chicken product is of concern, the limit of detection should be very low, and the detection method should be specific to the species level of bacteria. This is because pathogens can proliferate to lethal levels in poultry in a very short time. If the product is an ice cream, the focus is more on the isolation of bacteria from different instruments and less on the ice cream itself; otherwise the source of the outbreak might go undetected and continue to halt production.

1.3.3. Culture-based methods, pros and cons

Food companies and research into pathogenic detection strategies yearn to migrate from culture-based methods toward higher-technologies. However, the culture-based strategy of bacterial detection remains to be a strongly relevant tool for bacterial analysis and food companies of all sizes still embrace the practice out of necessity. Culture-based analyses of bacteria such as plate counts allow microbiologists a

quantitative visual product of microorganisms. In true microbiology studies -these being studies which focus specifically on the anatomy/physiology of the bacterium itself- culture based methods are essential. In food protection and safety studies however, the culture-based strategies of detection are far too time consuming. The growth of bacteria on agar plates can take days and often time some bacteria will not be cultivable, even when provided the optimal growth conditions. Bacteria in nature are fragile to the influence of mankind. Minor changes in habitat can render bacteria dormant or physically broken. During even the strongest isolation and growth yield of bacteria by this strategy, bacteria cannot be identified by more than colony color; virtually meaningless data. Further studies are then required which can take additional hours just to identify a bacterium to the genus-level. There is always opportunity for contamination and human error. Frankly, detection of *E. coli* by culture-based methods leaves more open-ended questions than the food industry is equipped to answer such as: (i) what type of *E. coli*, (ii) is it pathogenic, (iii) if identified to the subspecies, what serotype is it? From this global society of industrial agriculture emerges a need for near-immediate surveillance of microorganisms and culture-based methods are inadequate in this respect.

1.3.4. Immuno-based detection strategies

The closest alternative to culture-based detection strategies is an immunological assay known as enzyme-linked immunosorbent assay (ELISA). This offers technologists the opportunity to analyze surface cellular components on bacteria in a matter of hours on a vertical gel. The assay itself is highly affordable but the preparation of the sample from a food source is essentially impossible. Say there is more than one bacteria in food

sample, the gel will represent data for more than one bacteria. How do you separate the gel band-data for accurate accountability by species? The answer would be culture-based growth on an agar plate to separate the colonies prior to gel analyses. Once again, this approach is of no use to the food industry which moves at a pace that far exceeds this methodology. In a perfect world, where the gel data could in fact elucidate to the species level, this would require a particular expertise in laboratory analyses. To put it frankly, there is no secret that the end-goal of the pathogenic surveillance strategies are to eliminate the need for expensive employees. In most cases, it is in the best interest of a company to move toward business models which are technology-based rather than employing cadres of skilled workers.

1.3.5. Genetic detection strategies

Genetic-based surveillance strategies of bacteria emerged in the 1980's with the establishment of the polymerase chain reaction (PCR). PCR has served as the first generation of a range of gene-based amplification mechanisms such as loop-mediated isothermal amplification (LAMP) and recombinase polymerase amplification (RPA). PCR is the gold standard pathogenic surveillance strategy for larger food companies at the present time. Because the method has been around for over thirty years, undergraduate students are now educated on the subject. Food companies can fill these technologist-level positions at little cost and the materials which are required for operation are reasonable compared to the noveler alternatives that have surfaced in recent years such as those based on nanochip analyses. PCR is very cost-effective in that academics publish optimized protocols which are specific to bacterial species

surveillance online for under $50 or in many cases free, open-access and the procedures are continually optimized every year. In the best of cases, genetic based surveillance strategies can detect bacteria from a food source in under an hour. The problems with gene-based detection strategies are simply that sample preparation takes too long.

This is why outbreaks of foodborne illness continue to occur at lethal rates in the US. For example, if a company is moving several tons of spinach per day from the processing plant to grocery shelves, the percentage of the product that is screened for pathogenic bacteria is extremely low. Yes, the employment of a reliable and educated technologist is fairly inexpensive, but to screen a sufficient amount of product for pathogenic presence will require many of these employees. This is because a typical shift is 8-12 hours and the worker has personal rights to a break or two in addition to lunch. Realistically, any one technologist can really only screen maybe 5 samples per hour by PCR. In a perfect world, maybe the employee can work constantly to prepare samples for PCR without stopping to produce a dozen or-so samples in one hour. But it isn't realistic for the employee to work at a pace that is equal to the efficiency of a machine. In a real-world situation, a technologist would screen say one sample per every thousand for example. This would leave 99.9% of samples left unchecked in this example. The reason for this approach is because it isn't reasonable for the technologist to check every sample; there isn't enough time in the day. There is a real need to focus on plant tissues in-the-field, as well as a need to more precisely understand the nature of bacteria directly within leafy tissues; the true source of the problem at hand.

1.3.6. Long-term significance of SERS research in food production

High-throughput surveillance strategies that don't require human intervention are the final goal of pathogenic detection research in the food industry. Ideally, all foods would be monitored for pathogens at every stage of production. This of course is not our current reality but research in this area should serve as a bridge toward this goal otherwise the data will likely be obsolete in a matter of only a few decades. SERS is a detection strategy that exceeds all others in detection specificity, protocol duration speed, ease and simplicity of sample preparation, and limit-of-detection. There are significant limitations in SERS technology that still need to be overcome. However, SERS holds potential to detect and identify bacteria within a solid food sample *in situ* and in real-time. The only step that is required to prepare a sample is the addition of noble nanoparticles, when the protocol is optimized. There is clearly a long-term opportunity for SERS to bridge the gap that takes the food industry to high-throughput, autonomous pathogenic surveillance. At the same time, the reduction of foodborne outbreaks would be unprecedented if the protocol were proven applicable to a wide-range of food sources. Even the strongest gene-based detection strategies have a limit of detection of about 10 bacterial cells per gram of food. SERS protocols have been optimized to a limit of detection of one molecule. When optimized, SERS sensitivity of detection is unmatched in the food industry but there is substantial work to be done to take this method mainstream. This study will serve as a major gateway and milestone for pathogenic defense on a mass-scale in the interest of public health.

SERS application as a pathogen surveillance strategy is important to the US agriculture and food industry. Most microbial surveillance studies have focused on

animal related products. However, leafy vegetables are the most likely produce to cause a foodborne outbreak. We are convinced that SERS is compatible with the detection of bacteria in plant tissues. The annual market for spinach alone is around 262 million dollars in the US, according to the USDA National Agricultural Statistics Service. Currently, food companies rely on genetic amplification technologies to surveil pathogens in solid foods. However, this process requires the solid food matrix to be broken-down, homogenized, filtered, purified, and prepared by a biotechnology specialist. Such results consume time and resources for only one sample. Therefore, it is reasonable to speculate that even the most experience technician can screen only a few dozen samples in one day and with each step there is a risk of human error. SERS detection of bacteria in a sample is near-immediate and does not require a great deal of expertise once the protocol is optimized.

The use of SERS as an immediate, *in situ*, real-time detection strategy of bacteria in solid foods is a cost-effective development that is worth pursuing (Table 1). Greater quantities of produce should be screened on an hourly basis to enhance the governments traceability capacity when outbreaks do occur. This will trickle-down to benefit consumers on a mass-scale as critical points of pathogenic control will be reformed to higher-throughput and more specialized surveillance strategies. There is a wealth of unanswered questions that impede this progress, however. The focus of this dissertation is to establish a root-foundation for this line of research: *in situ* surveillance of bacteria in plant tissues.

Table 1. Strategies to surveil biological hazards in food to highlight the strengths and weaknesses of each method.

Detection Method or Assay	**Identification Strategy**	**Detection Specificity**	**Protocol Duration**	**Quantitative Sensitivity**	**Sample preparation**	***in situ* capability**
Culture media	Growth colony	Low	Days	N/A	Short time	-
Chemical testing	Chemical	Moderate	Days	N/A	Short time	-
Enzyme-linked immunosorbent assay	Immuno-components	Moderate	Hours	1000 CFU/g	Long time	-
Polym. chain reaction	Genetic	High	Hours	10 CFU/g	Long time	-
Isothermal amplification	Genetic	High	Minutes	10 CFU/g	Long time	-
Recomb. amplification	Genetic	High	Minutes	10 CFU/g	Long time	-
Surface-enhanced Raman spectroscopy	**Light-scattering**	**High**	**Minutes**	**1 CFU/g**	**Short time**	**+**

N/A: Not Applicable

1.4. Objectives

The Overall Objective of this study is to develop a reproducible protocol in which bacteria can be surveilled indiscriminately *en masse* using surface-enhanced Raman spectroscopy directly among food matrixes. We generated the following hypothesis-driven strategy in order establish a proof-of-concept and proof-of-application, as well as to elucidate specific opportunities for innovation in future studies:

Objective 1: Identify which SERS approach is most suitable for *in situ* surveillance of bacteria populations (label vs. label-free).

We tested the hypothesis that *in situ* SERS bacterial-surveillance is optimal when cells are labeled. Available literature suggests that label-free SERS surveillance of bacteria is achievable and is suitable for species-level discrimination *in situ*. However, there is a variety of exceptions when translating the approach to *in situ* imaging among complex substrates. We utilized 3-mercaptophenylboronic acid and propidium iodide as SERS labels to compare bacteria cells.

Objective 2: Optimize label-based SERS bacterial surveillance parameters to increase the reproducibility of *in situ* applications.

We tested the hypothesis that bacteria cells could be more efficiently labeled with 3-mercaptophenylboronic acid. Literature on the subject called for additional experiments to improve binding efficiency of 3-mercaptophenylboronic acid to bacteria cells. Stronger binding was necessary to advance the technology past the proof-of-concept stage toward proof-of-application studies.

Objective 3: Indiscriminately screen bacterial populations *en masse* directly among agriculture using surface-enhanced Raman spectroscopy.

We tested the hypothesis that entire bacterial populations could be imaged *in situ* among edible agriculture. The approach was founded upon bacteria cell labeling which could be applied to study cell adhesion properties during rinse washing applications. This methodology would offer insight into the microbial nature of food at a level which is comparable to electron and fluorescent microscopies.

CHAPTER 2

LITERATURE REVIEW

2.1. Overview of the Literature

2.1.1. Review papers concerning the general Raman technology

Raman approaches can take several major forms, including: Fourier Transform and charge-coupled device-based resonance and enhanced analyses (Baena and Lendl, 2004). Enhanced analyses of Raman light-scattering can be achieved using surface-enhanced (SERS), tip-enhanced (TERS), surface-enhanced hyper Raman (SEHRS), ultra violet-excited (UVSERS), and surface-enhanced resonance (SERRS) Raman scattering (Tian, 2005). Advanced applications for Raman technology, across many scientific disciplines, have been reviewed in excess over the past decade (Kudelski, 2008; Hering *et al.*, 2008; Hudson and Chumanov, 2009; Izake, 2010; McNay *et al*., 2011; Yamamoto, 2014). The work that is described within this dissertation focuses on charge-coupled device-based, surface-enhanced Raman spectroscopic analyses of bacteria cells.

2.1.2. Review papers concerning Raman investigations into bacteria cells

Raman analyses of bacteria are generally only achievable when utilizing surface-enhancement mechanisms. Surface-enhanced Raman spectroscopic investigations of bacteria initially relied upon nano-roughened substrates to achieve detectable spectral peaks (Tripp, Dluhy, and Zhao, 2008). These approaches progressed toward the utilization of mobilized nanosubstrates (*i.e.* nanoparticle colloids) which were employed

upon smooth substrates that contained bacteria cells (Jarvis and Goodacre, 2008). The reputation of Raman technology grew significantly as an approach could be utilized to detect and identify microbial species based on reproducible chemical spectra-based signatures (Sauer-Budge *et al*., 2012), even at the scale of one single bacterial cell (Li *et al*., 2012). Raman-based investigations of bacteria have been summarized at-depth in several recent review articles (Mosier-Boss, 2017; Liu *et al.*, 2017; Chisanga *et al*., 2018). Raman-based analyses of bacteria and other hazards have also been investigated rather extensively for their implementation into food safety practices (Craig, Franca, and Irudayaraj, 2013; Zheng and He, 2014; Pang, Yang, He, 2016; Zhao *et al*., 2018). The work that is described in within this dissertation focuses on the Raman-based analysis of bacteria which are relevant to the food industry.

2.1.3. Microbiological applications & outlook

Raman spectroscopy applications are gaining popularity in microbiology. Bacteria, spores, and bacteriophage each possess properties which are compatible with Raman technology (Alexander, Pellegrino, Gillespie, 2003; Goeller and Riley, 2007). Federal agencies around the world have taken notice and are eager to incorporate portable Raman analyses into their standard operating procedures (Luo and Lin, 2007). There is a wealth of opportunities to mobilize the technology for environmental applications (Halvoroson and Vikesland, 2010). Benchtop work in the laboratory is becoming increasingly specialized for precise biochemical analyses (Yang *et al*., 2011). Antibiotic effects on the biochemistry of microorganisms is a high-profile subject in public health circles and Raman technology is contributing to these efforts (Bebu *et al*., 2011). Some

bacteria secrete extracellular products which are unique by species and can be targeted by SERS for identification (Carlson *et al*., 2012). Bacterial spores have been reported to produce species-specific Raman spectra, in both wet and dry conditions, which are quantifiable using portable devices (Chan *et al*., 2004; Zhang *et al.*, 2005; Cowcher, Xu, Goodacre, 2013). Others have targeted bacteria with genetic precision (Vo-Dinh *et al*., 1994) by incorporating polymerase chain reaction-like primers with noble nanometals to produce SERS readings of specific bacterial presence (Driskell *et al*., 2008; Gracie *et al*., 2014).

SERS investigations of bacteria have proven efficacy among real-world applications. For example, SERS can be utilized to diagnose urinary tract infections (Jarvis and Goodacre, 2004). Specific algorithms can be coded in which enable computational systems to autonomously identify bacteria based on Raman spectra (Liu *et al*., 2007). There are reports that SERS can be utilized to identify reduction pathways among bacteria cells (Ravindranath *et al*., 2011) and some have achieved high-resolution Raman imaging of bacteria cell walls at the nanoscale (Oleson *et al*., 2017).

2.2. Major Classes of SERS for Bacterial Investigations

2.2.1. Nanoroughened substrates for Raman interpretations of bacteria

Raman technology is less straightforward than chemical applications, when it comes to biological applications. There is an inherent variability in Raman parameters between scientists when it comes to surface-enhancement efforts, but the sheer size of bacteria cells in comparison to monomeric molecules greatly amplifies data ‘error’ between users. Nanoroughened substrate morphologies are therefore a central focus of

the field as scientists work toward optimizing and standardizing Raman-based approaches for the interpretation of bacteria cells. Raman substrates can take a variety of forms but generally include a base support and metal coating (Vo-Dinh *et al*., 1999). Early efforts to fabricate bacteria-compatible SERS substrates were generally silicon-based and were coated in various forms of silver (Ag) or gold (Au) nanoparticle colloids (Primasiri *et al*., 2005; Jarvis, Brooker, Goodacre, 2006), nanorod arrays (Shanmukh *et al*., 2006; Chu, Huang, Zhao, 2008), or nanoclusters (Patel *et al*., 2008). Scientists moved ahead using plastic films in place of silicon wafers (Kao *et al*., 2008) and began to target specific biomarkers rather than whole-cells alone (Cheng *et al*., 2009). Nanopatterning increased in sophistication with single substrates hosting multiscale signal enhancers (Yan *et al*., 2009) or brail-like precision among nanostructure arrangements (Gopinath *et al*., 2009). The precise arrangement of nanostructures among SERS substrates are a critical factor (Kahraman *et al*., 2008), as nanostructures are immobilized therein and their interactions with bacteria cells are variable (Yang *et al*., 2010). These nanostructures can be coated with antibiotics to screen for bacterial presence based on Raman shifting patterns therein (Liu *et al*., 2011; Wu *et al*., 2013). Some have reported the use of multiple nanometals (Sivanesan *et al.*, 2014) or nanostructures within the same substrate (*i.e.* nanoparticles upon nanowires) to enhance bacterial SERS detection (Preciao-Flores *et al*., 2011). The fabrication of specialized ‘chips’ are starting to gain traction in the field as SERS reach in microbiology continues to expand (Wang *et al*., 2015; Yang *et al*., 2018).

2.2.2. Label-free Raman analyses of bacteria cells

Bacteria have mostly been studied without cellular labels when using Raman technology. The method originally involved the combination of bacteria with sodium borohydride-based silver (Ag) nanoparticles and a cyanide rinse to achieve a cellular Raman signature (Zeiri *et al*., 2002). Some claimed that this approach provided scientists with 'whole-organism fingerprints' of bacterial species (Jarvis, Brooker, and Goodacre, 2004) and provided spectral information regarding intracellular molecular contents of bacteria cells (Zeiri *et al*., 2004). Raman analyses of bacteria quickly became more specialized as scientists were eager to apply the technology toward the prevention of imminent real-world dangers. For example, bacteria-contaminated bioterror-related aerosols were studied for their collectable properties, in terms of compatibility with Raman analyses (Sengupta *et al.*, 2005). Conditions for bacterial Raman analyses were tested in terms of species, trophicity, excitation wavelength, and chemical compositions within the colloidal milieu (Laucks *et al.*, 2005; Zeiri and Efrima, 2005). Various authors began to screen identical bacteria species for Raman spectra and the data were beginning to show spectral consistencies (Sengupta, Mujacic, Davis, 2006).

Nanoparticle interactions with bacteria are a constant issue when targeting cells with Raman spectrometers. The surface-enhancement phenomena for Raman generally requires the target analyte reside within 10μm a laser-exposed noble metal nanostructure. However, SERS has been reported using other materials such as zinc (Zn), as well (Dutta, Sharma, and Pandey, 2009). The nanoparticle-cell contact-yield is therefore relatively unpredictable during label-free analyses. Many have turned to tip-enhancement to overcome this limitation (Neugebauer *et al*., 2006) while others have made the case that

stronger nanoparticle-cell contact-yields do not always translate to stronger Raman signals (Çulha *et al.*, 2008). The surface charge of bacteria cells can be reduced to encourage nanoparticle contact (Zhou *et al*., 2014). Nanoparticle precipitation within cellular compartments has also been reported as a means of investigating intracellular components within bacteria (Jarvis *et al*., 2008; Willets, 2009). Label-free surface-enhanced Raman scattering of bacteria cells will often register different spectra within the same sample and therefore require multiple readings by a variety of approaches to conclusively identify an unknown strain (Efrima and Zeiri, 2008). There have been reports in which bacteria and yeast were differentiated within one label-free mixture (Çulha *et al*., 2010). Nanoparticle colloids are available for commercial purchase from a variety of distributors and there are reports of scientists manufacturing their own in-house which often contributes to data variations between SERS investigators (Knauer *et al*., 2010). Nanoparticle-entrapment devices enable the concentration of free nanostructures with the target analyte (Cheng *et al*., 2014) while others have reported that *in situ* formation of nanoparticles among cells enables the discrimination of live and dead bacteria (Zhou *et al*., 2015).

Raman technology is often celebrated in the literature for its ability to identify bacteria species. However, this approach is often accomplished under highly controlled conditions rather than detection in nature. Challenges surrounding label-free data reproducibility also remain to be an issue as more scientists manufacture their own nanostructures (Dong *et al*., 2012) and report unique spectral varieties (Fan *et al*., 2011). Reproducibility is has become a top-priority in SERS bacteria studies (Prucek *et al*., 2012) but some reports still emerge without sufficient nanostructure descriptions

(Stephen *et al*., 2012). Label-free bacterial SERS studies continue to be refined and scientists are building precise theories behind the direct metabolomic cause of such SERS peaks (Premasiri *et al*., 2016) at the single-cell scale (Dina *et al.*, 2017).

2.2.3. Label-based Raman analyses of bacteria cells

Bacteria labelling for SERS analyses is less-common than label-free investigations. Cellular labelling is generally introduced as a means of: a) isolating a specific target, b) discriminating various targets from each another, or c) enhancing the yield at which cells are detected by the Raman system. Not all cellular labels are SERS-active and those which produce Raman spectra generally act as *indicators* rather than offer insight into the biochemical nature of the analyte. For example, antibodies are commonly employed to selectively conjugate nanoparticles with target cells (Naja *et al*., 2007). Coating cells with conjugates can enable higher nanoparticle contact yields with bacteria cells (Kahraman *et al*., 2009) while others have reported encapsulations of nanoparticles within biopolymeric labels for adherence to bacteria cells (Sundaram *et al*., 2013). Label applications are gaining traction in SERS bacterial studies and their focuses are broadening beyond spectral analyses toward ecological influences among microbial analytes (Lin *et al*., 2014). Bacteria labels are also employed in the form of magnets. Magnet-based labels enable scientists to selectively isolate and concentrate a target within a mixture (Zhang *et al*., 2012). Magnetic nanostructures of various morphologies can be employed as traditional enhancers of Raman light scattering but can also be conjugated with immunological components such as antibodies (Guven *et al*., 2011). Labelling bacteria cells for SERS analysis offers unique advantages in terms of

specificity and Raman intensity, but there are several aspects which remain unclear and require strict interpretation (*e.g.* influence on cell viability or quantitation).

Microfluidics in microbiology coincides well with Raman technology. The major hurdles of bacterial Raman detection often resonate around the improbable nature of simultaneous laser, cell, and nanoparticle contact. Microfluidic engineering increases the likelihood that each component, which is necessary for Raman detection, is aligned within an organized space. The microfluidic approach is not confined to label-based SERS analyses of bacteria and is likely the optimal puzzle-piece which will enable label-free analyses of bacteria cells among portable, field-based investigations. However, the efforts which have conjoined microfluidics with Raman technology for bacteria analyses have generally been limited to label-based cellular investigations. At the time of writing, the public data regarding microfluidic SERS of bacteria is rather exciting. There have been reports of single-cell SERS analyses using nanoprobes and a dielectrophoretic device (Lin *et al*., 2014). Others have reported microfluidic separation of bacteria among a microfluidic chip for SERS-based interpretation (Walter *et al*., 2011). Flow-through devices have been reported in which liquid can be continuously sifted for target bacteria by utilizing antibody-based strainers within microfluidic channels (Knauer *et al*., 2012). More recently, microfluidic SERS devices have been fabricated in which limit-of-detection claims reached Log 2 CFU/mL (Madiyar *et al*., 2015) and field-based demonstrations have been achieved in under 5 minutes utilizing human blood (Cheng *et al.*, 2013). Microfluidic-based approaches themselves often struggle to reach mainstream applications due to the specialized nature of their fabrication. However, companies will inevitably transition toward this type of offering in Raman technology as the field

progresses into microbiology. Most companies in the sector offer nanoroughened substrates and vend portable devices, strictly based on their marketing advantages. The promise behind microfluidic SERS for bacteria analyses is too powerful to be ignored by federal agencies and will eventually become the status-quo in the field of detection due to their inherent standardization qualities.

CHAPTER 3

GROWTH KINETICS FOR *ESCHERICHIA COLI* O157:H7 (#043888) TO ESTABLISH TRUE QUANTITATIVE EXPERIMENTS

3.1. Abstract

The growth curves for *E. coli* O157:H7 (#043888) are reported. Initial inocula-populations were judiciously controlled to demonstrate its strict relationship with growth rate. The onset of stationary growth is the optimal point at which a bacteria culture is considered suitable for quantitative Raman analyses. There is a clear disparity among the literature as to how bacteria cells should be handled for Raman analyses, in this respect. Bacteria populations are often generalized based on growth duration and optical density (absorbance). Proper handling conditions are demonstrated for a model *E. coli* strain that is utilized for Raman analyses to appropriately justify the validity behind judgements of cellular quantification or related conclusions herein.

3.2. Introduction

Bacterial analyses take several forms, including: a) presence/absence, b) non-/viable, c) non-/cultivable, d) live/dead, and e) quantitative analyses. Quantitative analyses offer dimension to bacterial investigations that 'positive/negative' approaches do not. Factors can be measured and interpreted in terms of severity, degree of influence, variation, and distribution. Several quantitative approaches offer precise insight into cell

populations, but bacteria are traditionally interpreted using colony counts upon agarose surfaces.

Misconceptions lurk within microbiological methods in terms of the quantitative nature of bacterial experiments. For example, there is a common rule-of-thumb in which bacteria can be incubated overnight or for 16 hours to reach stationary growth. The example is circumstantially true but will not apply to most cases. One bacteria species will grow differently than a second bacteria species. Presence vs. absence investigations of bacteria species require less stringent regulation but quantitative interpretations of bacteria require judicious regulation of important parameters.

Stationary growth is generally the most suitable growth phase for bacterial quantification. Exponential bacterial growth involves rapid cell division that is amplified across nearly every cell within the microcosm. Daughter cells are often conjoined which will appear as one colony among an agar plate and the population will altogether change within minutes. Stationary phase enables microbiologists to, at the highest rate of likelihood, investigate individual bacteria cells among a population of other individual cells with a relatively constant overall population quantity.

Our experimental efforts are founded upon Raman spectroscopic analyses. Traditional culture-based approaches will not register non-viable cells and quantitative efforts of that nature often offer avoidable experimental error. Raman laser interactions occur with an analyte indiscriminately of individual circumstances. Thus, quantitative precision with bacteria cultures must be controlled as accurately as possible. Here, we established a mathematical relationship between incubation duration, initial bacterial populations within inocula, stationary growth influence on experimental error, and

spectrophotometric optical densities. The data is specific to *Escherichia coli* O157:H7 (#043888) and offers exceptional reproducibility in the quantitative investigation of this bacteria.

3.3. Materials and Methods

3.3.1. Bacterial culture and initial growth curvature

Non-toxin *Escherichia coli* O157 (Strain: 043888; American Type Culture Collection®, Rockville, Maryland, USA) was cultivated on tryptic soy agar (Becton, Dickinson and Company, Difco™, Franklin Lakes, New Jersey, USA) for 24 hrs under 37 ˚C incubation. One bacterial colony was transferred from an agar growth plate to 10 mL of tryptic soy broth (Becton, Dickinson and Company). The broth culture was incubated at 37 ˚C with 125 rpm agitation overnight. The turbidity of the broth culture was analyzed for optical density (absorbance at 600 nm λ) using a spectrophotometer (BioSpec-mini, Shimadzu Corp., Kyoto, Japan) on an hourly basis. The colony-forming population was also monitored on an hourly basis. *E. coli* cultures were transferred from the broth culture to TSA plates at a volume of 100 μL for spread-plating. Colony counts were plotted with respect to optical density absorbance values, in relationship to incubation duration. The initial population within the inocula became clearer through several trials and the standard relationship was further clarified, see results.

3.3.2. Elucidating growth kinetics based on initial inocula population

E. coli cultures were prepared following the previously described approach. It was determined that a single, two-day-old colony on TSA would reach stationary phased

growth at an average of 7 hrs when incubated by the above approach. The procedure was optimized to specifically register Log 8.5 CFU/mL following the approach, with respect to optical density absorbance. The culture was then diluted to a specific inoculation concentration of Logs 4, 3, 2, 1, and 0 CFU/mL to assess the growth rate of the species, based specifically on initial population. Optical density absorbance readings were collected for each sample on an hourly basis, following the previously described methods.

3.4. Results and Discussion

3.4.1. Establishing a growth curve from a colony

Spectrophotometry proved that *Escherichia coli* O157:H7 (#043888) growth cultures reach stationary phased growth around an absorbance value of 1 (Figure 1). We therefore concluded that 0.969_A was the constant threshold for the onset of stationary growth for this *E. coli* with variance dependent upon the initial cell population within the inocula. Our initial screening proved that the average two-day agar-based growth colony consisted of approximately Log 5 CFU/mL within the 10 mL broth culture medium. Thus, inoculation of an *E. coli* agar-based growth colony requires 7 hours of incubation in order for the culture to reach stationary growth.

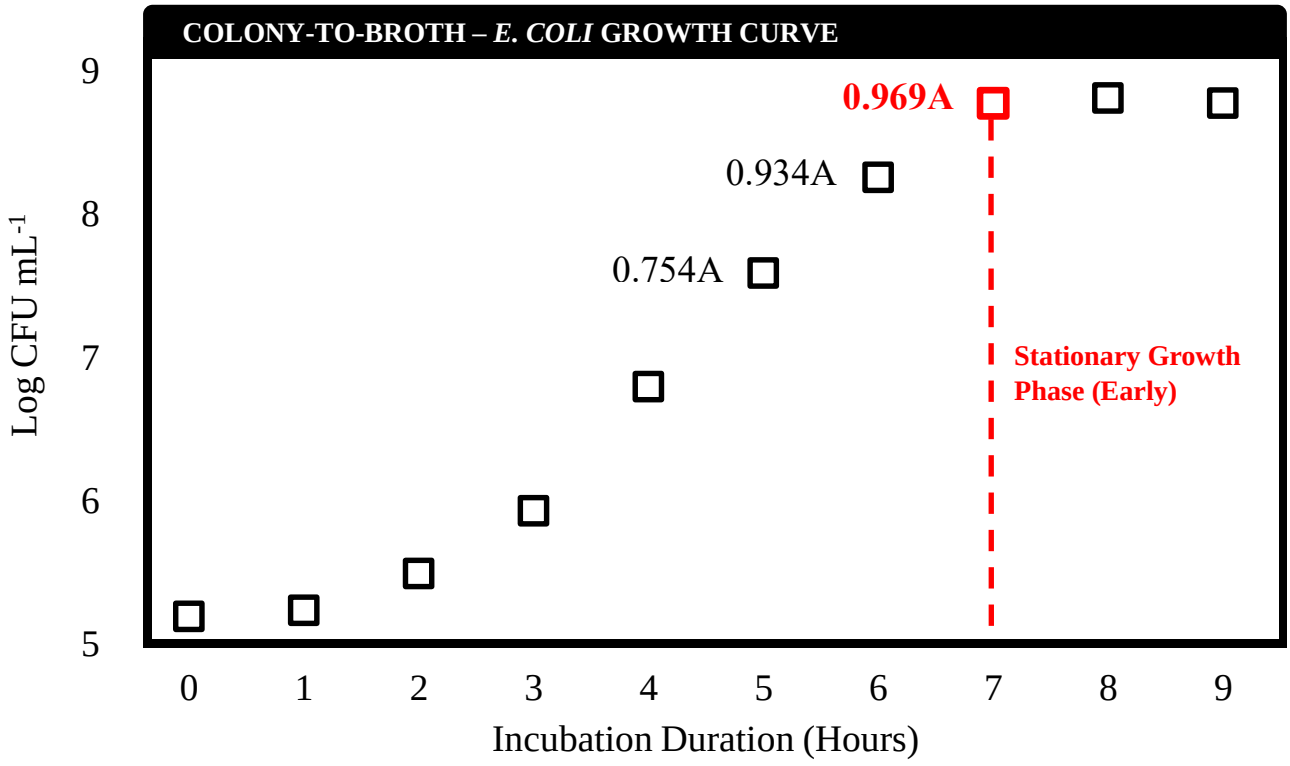

Figure 1: *Escherichia coli* O157:H7 (ATCC: 043888) hourly growth curve at 125 rpm agitation during 37°C incubation. The curve is representative of a second-generation streak-colony inoculated into TSB and monitored by manual-spread plating in duplicate on TSA.

There is a risk that bacteria cells are still dividing or conjoined if the culture is utilized prior to the onset of stationary growth. The absorbance value for the growth culture continued to increase beyond the stationary growth threshold. This proves that the species continues to divide after the onset of stationary growth and fractionates the population between cultivable and non-cultivable cells. The trend is visually apparent to the naked-eye by the formation of cell collections which are suppressed to the bottom of the culture container (i.e. test tube). We therefore proved that over-incubation of the culture will result in consistent colony forming unit quantities but higher quantities of total cells. Raman analyses are not forgiving to this level of experimental error in the same way as culture-dependent analyses. Bacteria cells will register under the Raman laser line regardless of viability. This is one of the most critical errors that is evident among published literature of this kind and we therefore wanted to ensure that this data be presented as transparently as possible throughout this paper.

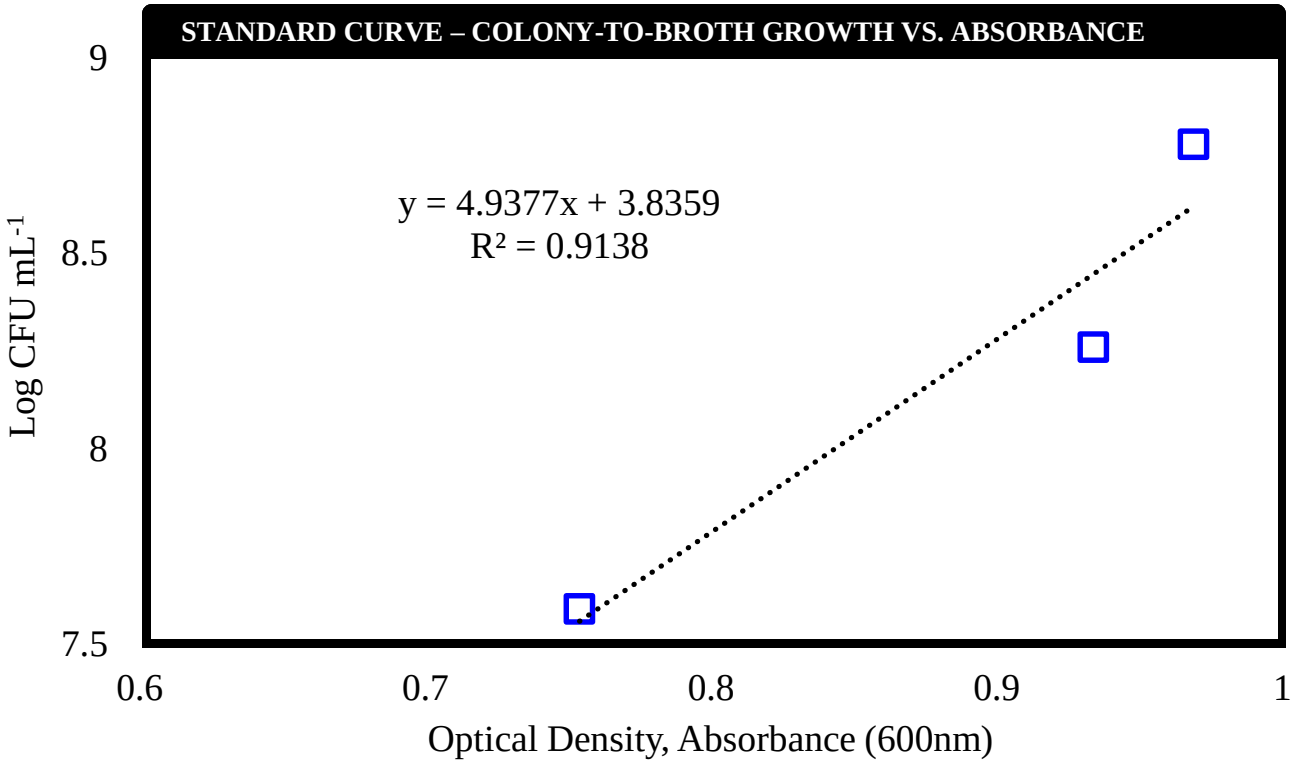

Figure 2: Colony forming unit readings in relation to optical density data, based on absorbance readings of *E. coli* O157:H7 (ATCC: 043888) during late-exponential growth. The values directly correspond to the data that is represented in the previous figure.

3.4.2. Establishing a quantitative inocula

Colony-to-broth cultivation of bacteria populations introduces substantial error to quantitative analyses. The theory behind this error is founded upon: a) the variation between cell quantities per colony, and b) the inherent inconsistency at which cell populations are relocated by the user. Thus, the exact population at which the cells are inoculated is always inconsistent by this approach and is therefore discouraged for quantitative analyses. This unfortunately remains to be an 'acceptable norm' of practice in this field. We see in Figure 2 that the R^2 value for this approach was 0.914. However, trying to reproduce this approach, we achieved a higher R^2 value of 0.934 (Figure 3). We then had a clear understanding of the incubation time at which one growth colony would reach stationary growth and exactly how many bacteria cells that threshold represented.

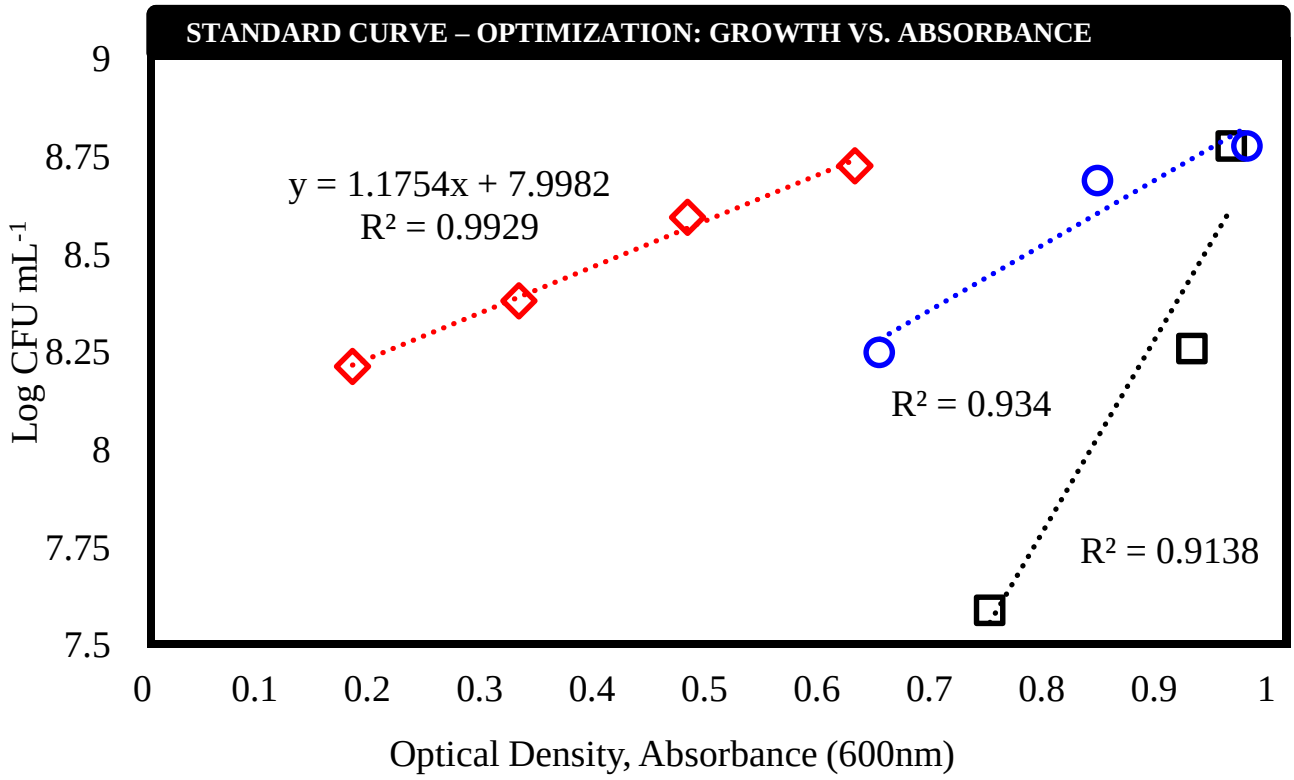

Figure 3: Colony forming unit readings in relation to optical density data, based on absorbance readings of *E. coli* O157:H7 (ATCC: 043888). The data which is represented in red was established using a stationary growth-staged bacterial culture. Methods were established based on the R^2 equation determined in the previous experiment (blue and black).

We therefore reached an end-value of R^2 0.993 which was consistent throughout the duration of the study. The relationship between spectrophotometric absorbance and viable cell population proves that consistent command of bacteria population quantities can be manipulated with high precision as long as the initial inocula population is judiciously managed and viable. Initial cell populations are critically important during quantitative investigations of bacteria. Decimal dilutions are fundamental to bacterial analyses and experimental error is therefore increasingly pronounced as the initial culture is manipulated by the user. We therefore aimed to establish a consistently credible starting-point for analyses. Data that is shown in Figure 3 proves that spectrophotometry can only reliably indicate *E. coli* populations within the 8 Log range. Thus, the culture needs to be fixed within a specific optical density at a specific 8 Log quantity as a base from which the sample can be diluted to an even 8 Log. Issues arise in this respect because an even Log 8 CFU/mL culture falls below the spectrophotometric absorbance range. We therefore needed to fix the culture to an even Log 8.5 CFU/mL using a spectrophotometer for dilution down to an even Log 8 CFU/mL (Figure 4).

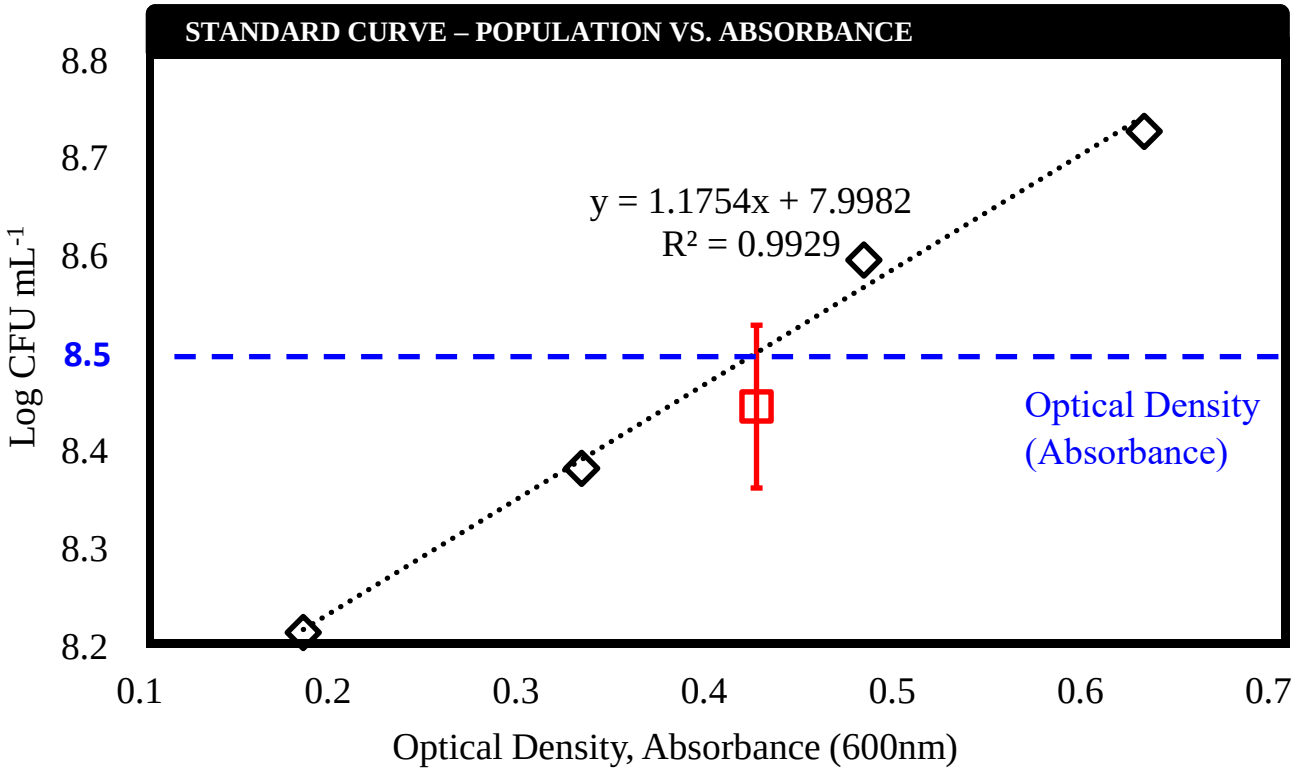

Figure 4: Determine the sensitivity/consistency of this practice during early-stationary growth phase.

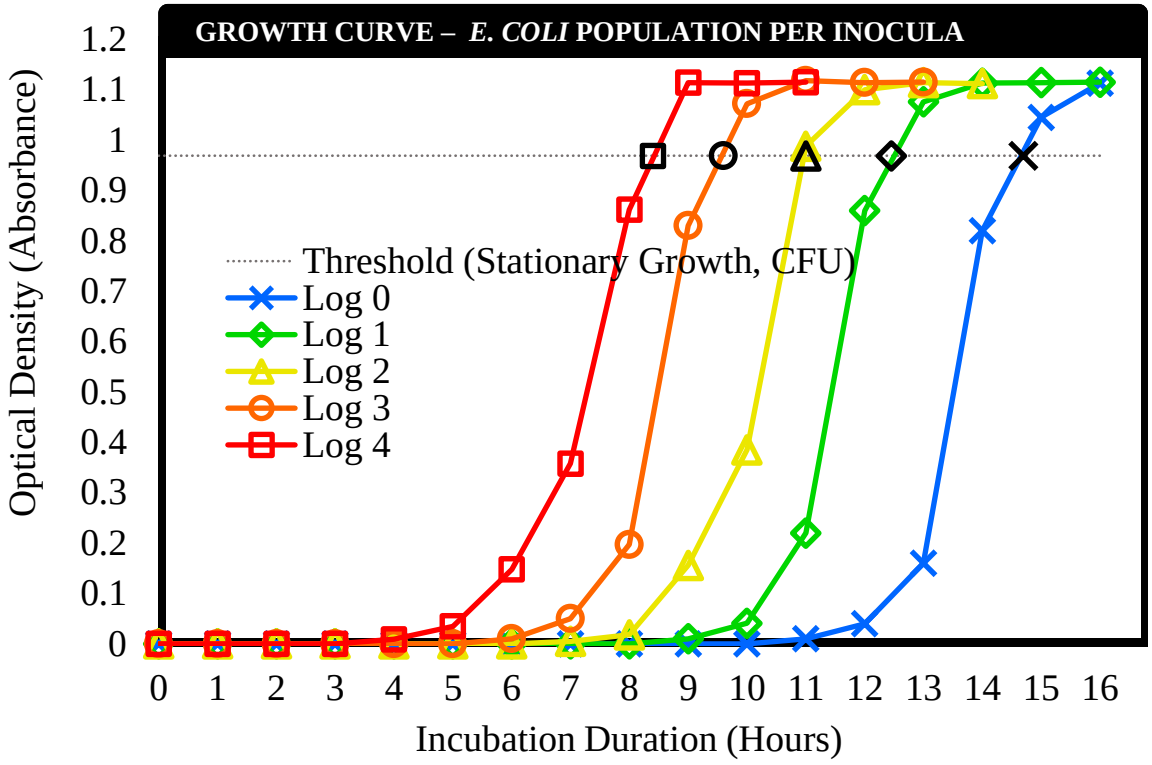

Figure 5: Growth curves for *E. coli* O157:H7, #043888 in TSA. Measurements were made using a spectrophotometer at 600nm wavelength. The key point is the difference in growth rate based on the initial inoculation population of *E. coli* cells.

The approach conclusively allowed us to manipulate the growth curve of the *E. coli* strain in a way that was controlled precisely for quantitative investigations. We were able to determine exactly how many viable cells were being inoculated into a broth culture and exactly when to utilize the culture for accurate quantitative analyses (Figure 5). It is critical that scientists utilize this approach when investigating bacteria cells quantitatively by Raman spectroscopy. The standard curve data proves that Log 1 CFU/mL and above provided precise indications of growth curve predictions (Figure 6). However, utilizing a Log 0 CFU/mL culture introduced unfavorable error within the trendline.

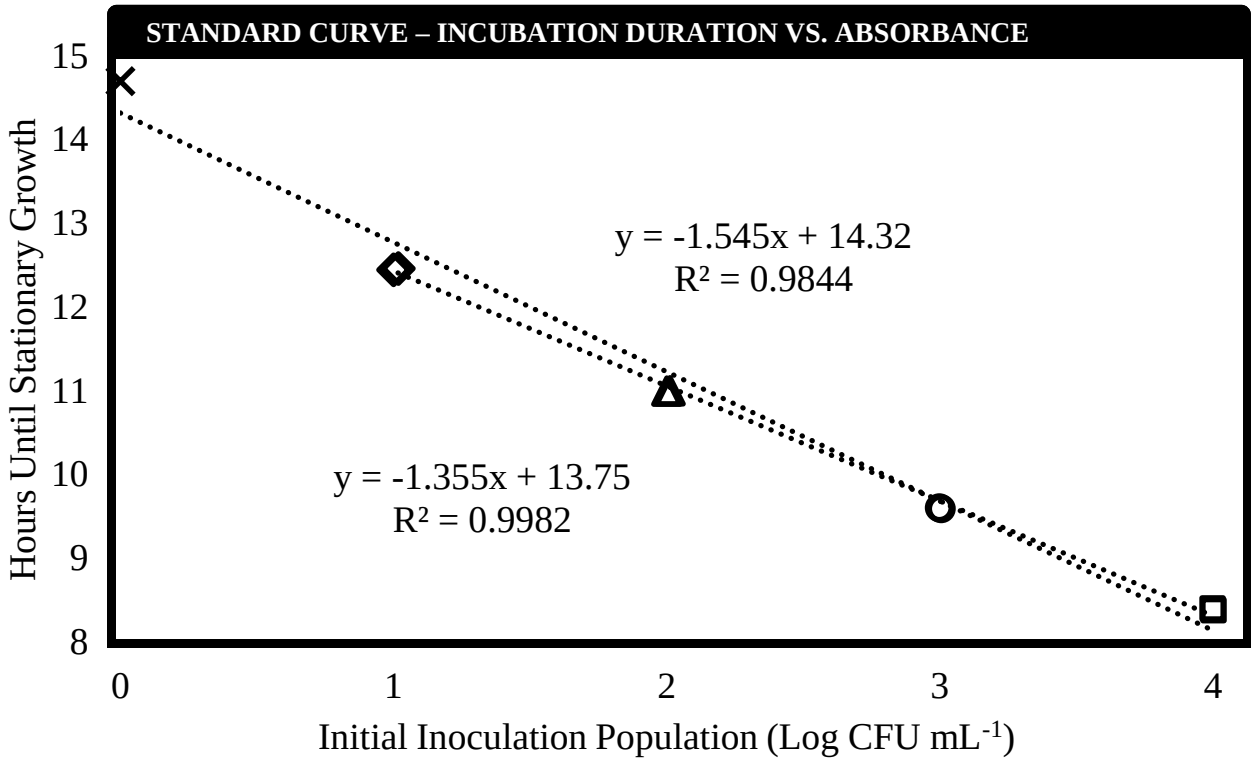

Figure 6: Standard curve to establish a relationship between the growth rate of *E. coli* O157:H7, #043888 in TSB with respect to the initial population of cell inoculate. The black data points were identified in previous figures.

3.5. Conclusions

Culture preparations of known-bacteria for Raman analyses require strict attention to conclusively produce reproducible quantification-data. Raman experiments *in vitro* must always follow this strict blueprint if the data is to be interpreted for quantification-trends: (i) Bacteria should be cultured on agar; (ii) a single bacterial colony should be relocated to broth for shake-incubation; (iii) the onset of stationary phased growth should be identified based on incubation duration, with respect to optical density absorbance; (iv) the bacteria should then be relocated via broth-to-broth inoculation with a *known* population of viable bacteria cells, from stationary culture; (v) the culture should be incubated to a known onset of stationary growth and should be used immediately. Raman light-scattering is not biased to duplicate cells, damaged cells, dormant cells, lysed cells, or whole-cells. Field-studies will not have this luxury of control and that will automatically contribute to data error, understandably. However, *in vitro* investigations need to be treated with strict attention to produce reliable and reproducible findings for adoption world-wide. Therefore, the model that is presented herein should be accepted as standard for all quantification-related SERS investigations of bacteria populations.

CHAPTER 4

EVALUATING THE 3-MERCAPTOPHENYLBORONIC ACID CHEMICAL LABEL FOR OPTIMAL SURFACE-ENHANCED RAMAN SPECTROSCOPY OF BACTERIA POPULATIONS

4.1. Abstract

Bacteria cells have been successfully captured and tagged with 3-mercaptophenylboronic acid for analyses using surface-enhanced Raman spectroscopy (SERS). There is potential for this approach to be adjusted in such a way that bacteria can be coated with the chemical label for SERS mapping of their cellular distribution, in ways which are similar to fluorescent microscopy. We report the optimal conditions for 3-mercaptophenylboronic acid coating of bacteria cells to bridge an important gap toward further applications. We make the case that this approach is now suitable for the evaluation of rinse-washing efficacy by means of SERS imaging. The procedure was also found to implement harm to bacterial ecology and the trend was quantitatively different based on the initial cell population being labeled. SERS imaging by this approach measured all labeled bacteria cells, regardless of viability. Non-culturable cells are therefore detectable by this SERS approach and can even produce stronger SERS spectral peaks than viable cells. We recommend that further 3-mercaptophenylboronic acid labeling applications for the SERS of bacteria follow the new methods which are outlined in this paper. Avoiding so could result in unbound 3-mercaptophenylboronic acids registering false-positive data when contacted by the Raman laser line.

4.2. Introduction

Microorganisms are generally analyzed *in situ* using fluorescent and electron microscopy. Fluorescent microscopy enables scientists to monitor microorganisms in real-time directly *in situ* but the target organism must exhibit some degree of fluorescence. Electron microscopy can render high-definition images of microorganisms *in situ* at the nanoscale but the result is merely a 'freeze-frame' of the sample at one specific point in time. The preparation of these samples can also take several days depending on the substrate and there is currently no potential for real-time microbial analyses using electron microscopy. Surface-enhanced Raman spectroscopy (SERS) is showing promise for field analyses of non-fluorescent bacteria in real-time and expertise surrounding the technique is rapidly developing (Pahlow et al., 2015).

SERS applications are broadening throughout the field of microbiology (Halvorson and Vikesland, 2010; Mosier-Boss, 2017). SERS is capable of producing spectral 'bar codes' which are specific to the species level (Patel et al., 2008). Laser precision has enabled the targeted SERS study of intracellular and extracellular bacterial components (Jarvis et al., 2008). Bacteria can be studied using SERS with and without chemical or biological labels among a variety of conditions (Liu et al., 2017). We and others have utilized mercaptophenylboronic acids as labels to indiscriminately monitor bacteria based on Raman scattering (Figure 7) (Pearson et al., 2018; Wang et al., 2015).

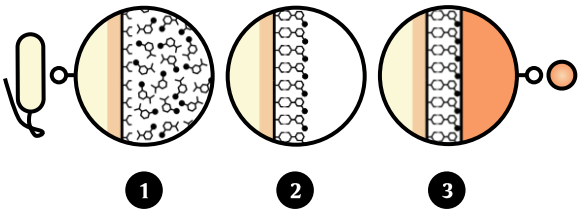

Figure 7: Illustration of bacteria cells being (1) coated with 3-mercaptophenylboronic acids, (2) rinsed of unbound labels, and (3) subsequently coated with gold (Au) nanoparticles. Strong Au-S interactions offer incentive for nanoparticles to interact with the target analyte.

Boron possesses an empty *p* orbital which enables boronic acids to better accept an electron pair from diols along the cell wall of bacteria (Rao et al., 2016). Mercaptans bind strongly to gold (Au) nanoparticles which render mercaptophenylboronic acids suitable for bacterial SERS analyses, as noble metal nanoparticles exponentially enhance Raman scattering.

Mercaptophenylboronic acid labeling of bacteria cells is a strong starting-point for Raman analyses of microbial ecosystems. The approach has been applied to cell capture or separatory assays for bacterial analyses (Wang et al., 2017; Gao et al., 2018; Pearson et al., 2018). However, the reactivity of boronic acids are quite complex (Larkin et al., 2006) and unanswered questions still linger around the approach in terms of binding efficacy, as well as influence on cell viability. False positive and negative signals are also a constant concern when administering labels for SERS analyses. Unbound labels can contribute to false-positive signals while bound labels hold the potential to lack distinct peaks which are representative of cellular attachment. Mercaptophenylboronic acids possess strong potential for the development of remote microbial sensors if the approach can be optimized for mobile analyses.

Here, we measured specific parameters which are essential to mercaptophenylboronic acid applications in SERS bacterial analyses. Our results elucidated several factors of concern which have been overlooked in previous efforts of this kind: a) reversibility of cell-bound labels, b) optimizing binding efficiency, c) strengthening Raman signals, d) binding-duration influence on Raman intensity, as well as e) the influence of mercaptophenylboronic acid on cellular viability. We advance the precision and understanding of mercaptophenylboronic acid bacterial labeling while

shedding new light on previously unknown consequences of the methodology. This approach can now be applied to cell coating procedures for the surveillance of bacteria populations in ways which are competitive to fluorescent microscopy.

4.3. Materials and Methods

4.3.1. Bacterial culture and handling conditions

Escherichia coli O157:H7 (non-toxin producing strain: 043888; American Type Culture Collection®, Rockville, Maryland, USA) cells were cultured upon tryptic soy agar (Becton, Dickinson and Company, Difco™, Franklin Lakes, New Jersey, USA) under 37 ˚C incubation. Single colonies were relocated from agar growth plates to 10 mL of tryptic soy broth (Becton, Dickinson and Company). Broth cultures were stored at 37 ˚C under 125 rpm shaking-incubation until stationary growth. Broth cultures were then diluted to a predetermined turbidity (optical density absorbance at 600 nm λ) using a spectrophotometer (BioSpec-mini, Shimadzu Corp., Kyoto, Japan) to maintain consistent cell quantities for experimentation. Cultures were utilized at the growth stage throughout the duration of this study. Experimental cultures were initially adjusted to Log 8 CFU mL^{-1} to act as a starting-point for decimal dilutions during quantitative analyses.

4.3.2. Coating bacteria with a cellular SERS label

Bacteria cells were separated from each broth solution following 23 ˚C centrifugation at 9,000 rpm for 3 min, using 1 mL aliquots. Bacterial pellets were then resuspended in ammonium bicarbonate [800 µL, 50 mM] (Thermo Fisher Scientific Inc., Waltham, Massachusetts, USA). The cultures were washed-free of tryptic soy broth exactly three times by the approach. 3-mercaptophenylboronic acid (3-MPBA) [110 mM]

(AstaTech Inc., Bristol, Pennsylvania, USA) was used as the model cell label in this study and was initially dissolved in absolute ethanol (200 proof) (Thermo Fisher Scientific Inc.) for stock storage under 4 °C stabilization. The bacterial suspension was then mixed with 3-MPBA (100 µL) to initialize the cellular labelling process. Sodium hydroxide [100 mM] (Thermo Fisher Scientific Inc.) was then utilized as an esterification trigger for 3-MPBA binding to bacteria cells *in vitro*. The optimal sample solutions for SERS (1 mL) consisted of known experimental-concentrations of bacteria, ammonium bicarbonate [40 mM], 3-MPBA [10 mM], and sodium hydroxide [10 mM]. A solution containing ammonium bicarbonate [50 mM] and sodium hydroxide [10 mM, respective to experimental conditions] was then utilized as a rinse solution following the pellet-centrifugation protocol that was described previously. This rinse strategy was essential to ensure that unbound 3-MPBA was diluted out of the system that might otherwise register false-signals during Raman analyses. Ultrapure water from a Millipore water purification system (Millipore Co., Burlington, Massachusetts, USA) was also investigated as a rinse agent following 3-MPBA coating to evaluate the stability of the boronate ester bond with bacteria cells under unfavorable conditions.

4.3.3. Sample preparation for SERS analyses of bacteria

Spherical bare gold (Au) nanoparticles (AuNPs) (50nm ø) [0.20 mg mL^{-1}, 2 mM sodium citrate] (nanoComposix Inc., San Diego, California, USA) were applied to enhance the Raman scattering of 3-MPBA for SERS bacterial analyses. Bacteria were screened for SERS on BioGold^{TM} (Au)-coated microarray slides (75 x 25 mm) (Thermo Fisher Scientific Inc.). Each analytical component (bacteria suspension and AuNPs) were

deposited upon the microarray slides at equal volumes. Analyte administration sequences upon the microarray slides were evaluated to elucidate the optimal conditions for SERS analyses: a) AuNPs dried first, bacteria suspension applied second; b) bacteria suspension dried first, AuNPs applied second; and c) both AuNP and bacteria suspensions mixed together for simultaneous drying. The inocula were dried under room temperature (23 ˚C) incubation within a 1300 Series Class II, Type A2 Biological Safety Cabinet (Thermo Fisher Scientific Inc.) before SERS analyses were performed.

4.3.4. SERS parameters and analyses

Samples were coordinated into microscopic focus using 20x/0.40NA (Numerical Aperture) and 100x/0.90NA objective lenses. Raman spectra were assembled using a DXR2xi Raman Imaging Microscope System (Thermo Fisher Scientific Inc.) based on photon scattering patterns from a 780 nm (λ) laser line. Each spectrum was generated following 0.1 sec collection-exposures through a 50 μm slit-aperture at 3 mW laser strength. Samples were SERS imaged using the OMNICxi Raman Imaging Software v1.6 (Thermo-Nicolet, Madison, Wisconsin, USA). Raman intensity threshold values were variable depending on individual spectral trends and the collection region. Spectra were comparatively analyzed based on discriminatory features which were identified using the TQ Analyst 9.0 platform (Thermo-Nicolet) and were averaged *en masse* using the OMNICxi software directly. The spectra shown in this paper were generated by converging all individual SERS readings into one average spectrum, unless noted otherwise.

4.3.5. Scanning electron microscopy

Bacteria were coated with 3-MPBA and administered onto a (Au)-coated microarray slide glass following methods that were previously described. The samples were immersed in 2% glutaraldehyde for 6 hrs incubation within a 4 °C chamber. The glutaraldehyde was diluted to 2% using HEPES buffer [0.1 M] prior to its administration. Absolute ethanol was administered at increasing concentrations for dehydration. The samples were mounted using two-sided carbon tape and sputter coated with gold AuNPs (2 nm, ø). Electron micrographs were constructed using and FEI Magellan extreme high-resolution (XHR) 400 FE scanning electron system (Nanolab Technologies Inc., Milpitas, California, USA).

4.4. Results and Discussion

4.4.1. Binding 3-MPBA to bacteria for SERS

Bacteria were suspended in ammonium bicarbonate and treated with 3-MPBA to chemically label the cells for SERS analyses. The chemical labeling procedure enabled SERS bacteria detection upon (Au) coated glass (Fig. 8). We previously showed that an ammonium bicarbonate suspension was sufficient to anchor bacteria cells upon a 3-MPBA coated chip. However, this approach required different conditions as any unbound chemical labels can register false-positive signals during SERS analyses. Keeping chemical labels bound to bacteria cells, and removing unbound labels from the sample, is important for SERS approaches of this kind to advance toward real field applications. It is known that 3 -mercaptophenylboronic esters favor alkaline conditions (Iwatsuki et al., 2007) and produce slightly different SERS spectra than 3-MPBA. SERS spectra of 3-

MPBA exhibit two strong peaks near the 998 cm^{-1} and 1070 cm^{-1} positions as a result of phenyl ring stretching (Chen et al., 2019). Diol-bound 3-mercaptophenylboronic esters produce nearly identical spectra with a minor peak at the 1024 cm^{-1} range among SERS spectra, as a result of in-plane ν_{18a} C–H bond-bending (Szafranksi et al., 1998). We previously utilized sodium hydroxide to compensate for decreases in pH that could contribute to 3-MPBA hydrolysis away from bacteria cells (Pearson et al., 2018).

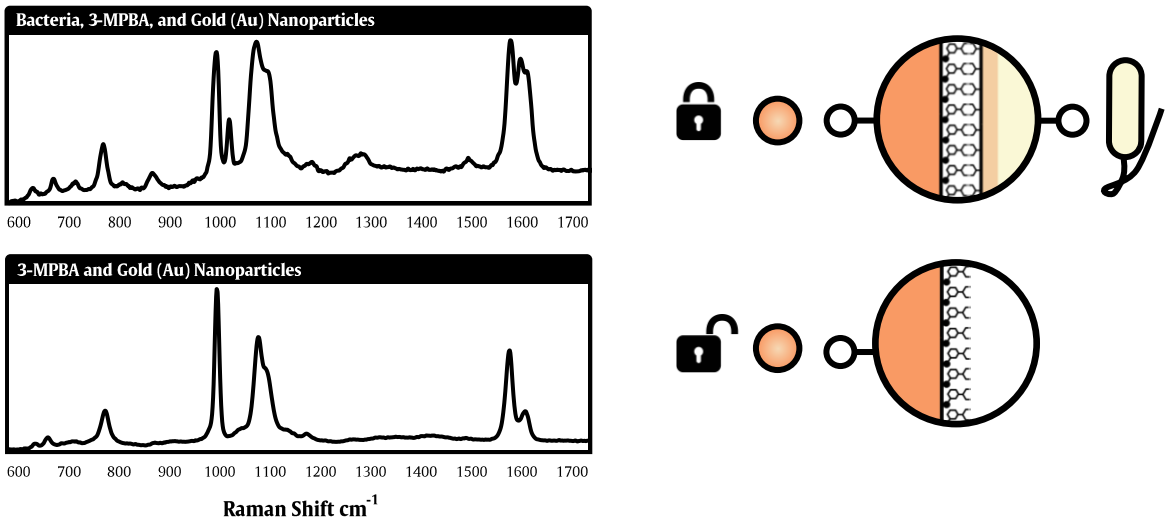

Figure 8: SERS spectra of 3-MPBA when bound or unbound to bacteria. The presence of the 1024 cm^{-1} Raman shift indicated esterification to a secondary diol.

Boronic esters can hydrolyze away from cells which could reduce the potential of SERS to detect chemically labeled bacteria. We therefore wanted to stress-test the chemical labeling procedure by exposing precoated bacteria cells to water (Fig. 9). The labeling procedure was quite robust, with bacteria producing 3-MPBA SERS spectra after 5 thorough rinse water applications. The peak at 998 cm^{-1} was less prominent following the second rinse water application. However, the peak intensity was consistent throughout the remaining washes. Three important conclusions can be derived from this data. First, SERS peak intensities by this procedure can vary depending on hydrolytic factors and each experiment should be evaluated carefully in this respect. Second, hydrolytic factors can cause unbound 3-MPBA to register significant false-positive SERS signals if the bacteria cells have not been rinsed with water at least once. Third, rinsing bacteria that were precoated with 3-MPBA more twice or more can result in consistent SERS spectral data even when the cells are resuspended in water several times. Our findings show that hydrolytic exposures can help to ensure that consistent and reliable SERS readings are achieved when bacteria are coated with boronic esters.

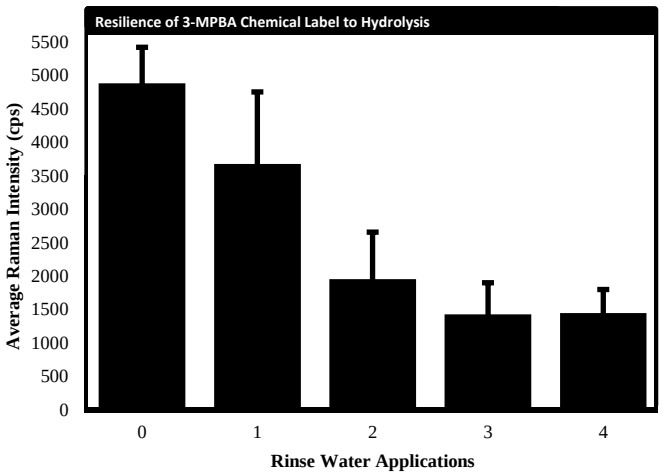

Figure 9: SERS analyses of the 998 cm^{-1} peak among 3-MPBA labeled bacteria showed some evidence of hydrolysis away from bacteria cells which could negatively influence SERS data. However, the overall approach was consistent throughout several rinse water applications, supporting the robustness of the 3-MPBA SERS approach and elucidating the need for water applications when quantitatively gauging peak intensity as an indicator of bacterial distribution.

Binding duration is a key factor of interest when using SERS to analyze chemically labeled bacteria cells over time. The hydrolytic tendencies of 3-MPBA led us to investigate the resiliency of the chemical label over a prolonged duration. Bacteria cells were coated with 3-MPBA, rinsed free of unbound labels, and were left to incubate for 24 hrs (Fig. 10). The procedure was executed using live bacteria and cells that were inactivated via bleach [6 ppm total chlorine] for 10 min; bleach exposure to Log 8.5 CFU mL^{-1} bacteria resulted in 99.998% sterilization. SERS spectra were collected following each of the four rinse washes with an ammonium bicarbonate/sodium hydroxide solution. Living bacteria cells again exhibited consistent peak intensities among SERS spectra when exposed to rinse washes. However, dead bacteria cells expressed higher peak intensities that were diminished by subsequent rinse wash applications. The data revealed that 3-MPBA was able to bind to inactivated cells at higher yields than living cells, suggesting that cellular damage provided stronger access to intracellular components. The bleach inactivated cells lost SERS spectral intensity following rinse washing applications, suggesting that chemically labeled cellular debris were being washed away from the sample. Changes in SERS spectral intensity among chemically labeled bacteria populations can serve as an indicator of cellular vitality.

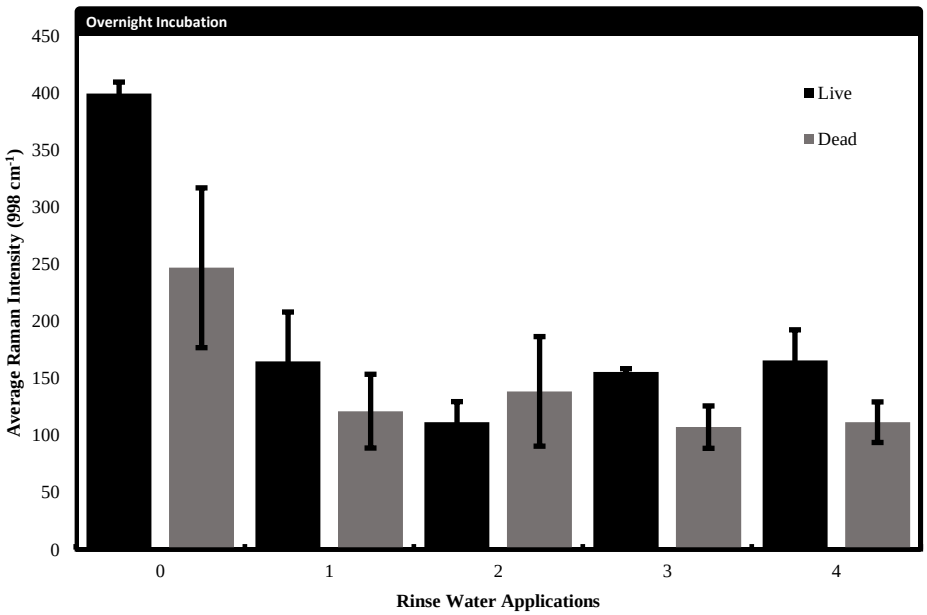

Figure 10: Live and dead bacteria were coated with 3-MPBA for SERS analyses following several rinse water applications. Live bacteria exhibited consistent SERS spectral intensities at the 998 cm^{-1} region while dead bacteria exhibited stronger peak intensities which partially diminished throughout rinsing cycles.

4.4.2. Sample preparation for SERS analyses

Nanoparticle contact with bacteria cells can vary depending on sample preparation proceedings which can influence SERS spectra. We investigated this potential variability by suspending bacteria cells in 3-MPBA for approximately 10 min and 24 hrs for administration onto gold (Au) coated glass before, during, and after nanoparticle deposition into the sample (Fig. 11). Prolonged exposure of bacteria to 3-MPBA solution resulted in weaker SERS peak intensity than short exposure. Furthermore, simultaneous administration of chemically labeled bacteria cells and nanoparticles increased SERS peak intensity by three-fold, when compared against separate applications. This is an important concept to consider because real field applications will unlikely allow simultaneous administration of bacteria inocula and nanoparticle depositions, in situations where bacteria already reside among their natural substrate. However, laboratory investigators might find the data to be useful for comparison to traditional nanosubstrate-based methods (Premasiri et al., 2005). SERS peak intensity of chemically labeled bacteria cells should be cautiously analyzed with respect to their potential variability in counts per second. Chemical labels can bind at different yields with individual bacteria cells and their subsequent nanoparticle interactions are also subject to variability.

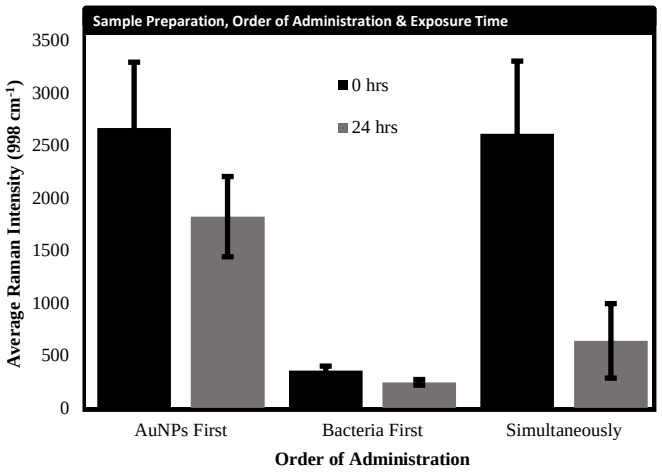

Figure 11: Prolonged incubation of bacteria with 3-MPBA was less efficient than immediate chemical labeling of cells when screening for SERS spectra. Applying bacteria or gold (Au) nanoparticles separately from one another resulted in lower SERS spectral intensities than when each component was administered simultaneously.

4.4.3. Cellular viability when coated with 3-MPBA

Chemical labeling of bacteria is unnatural and can interfere with cellular viability. We previously showed that labeling bacteria with 3-MPBA can reduce cell viability by as much as 1 Log CFU mL^{-1} (Pearson et al., 2017). This experiment was based on 3-MPBA interactions with Log 8 CFU mL^{-1} *Salmonella enterica*. Here, we aimed to evaluate the influence of 3-MPBA labeling proceedings among smaller bacteria populations. Tenfold differences in *E. coli* populations were exposed to the same concentrations of 3-MPBA, ammonium bicarbonate, and sodium hydroxide (Fig. 12). The data revealed that bacteria populations must reach at least Log 5 CFU mL^{-1} for cells to survive the labeling procedure. Bacteria populations below Log 5 CFU mL^{-1} were sterilized entirely when exposed to the labeling solution. Growth-colony data therefore proved that cell labeling with 3-MPBA is not a 'one size fits all' approach to SERS bacterial analyses. Our labeling approach yielded nearly identical SERS spectral data, regardless of chemical label concentrations between 25-200 mM 3-MPBA (data not shown), suggesting that lower label concentrations can still yield sufficient results. SERS studies that require viable bacteria must include customized concentrations of chemical labeling components with direct respect to cell population.

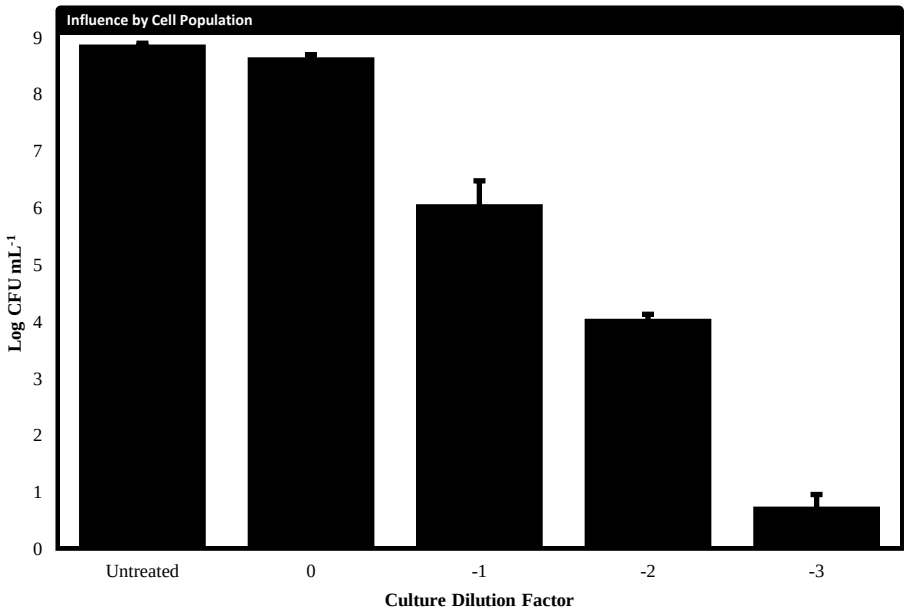

Figure 12: Bacteria of various cell concentrations were exposed to equal concentrations of 3-MPBA to assess the influence of the chemical label upon cell vitality.

4.4.4. Imaging 3-MPBA labeled bacteria cells

Bacteria inactivation by the 3-MPBA labeling procedure is a concern if cellular debris are registered by the Raman system as false-positive indicators of whole-cell detection. Scanning electron microscopy analyses revealed that the 3-MPBA coating can be corrosive to cells, leaving intact bacterial ghosts (Fig. 13). The corrosive properties of the procedure are likely enhanced by the addition of gold (Au) nanoparticles which are employed to enhance Raman scattering frequencies. Gold (Au) nanoparticles form a strong bond with mercaptans and therefore have the potential to break-off cell components which are under pressure by the fluidic nature of the sample. Degradation might also be substantiated by the use of gold (Au) coated substrates where bacteria cells can be anchored in one place and subjected to corrosive forces, rather than flow freely within a solution.

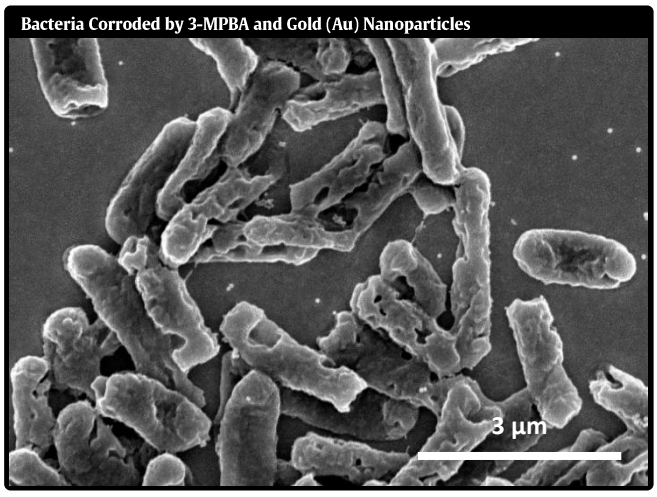

Figure 13: Scanning electron micrographs of bacteria cells which were damaged as a result of the 3-MPBA chemical labeling procedure.

SERS has can detect single molecules (Le Ru and Etchegoin, 2012) and our imaging data supported the notion that the spatial resolution of the Raman system is sufficient for the detection of individual bacteria cells (Fig. 14) (Guicheteau et al., 2010). Here, we report a novel perspective upon single-cell SERS detection whereby overall bacteria populations influenced the detection of individual cells. Bacteria were precoated with 3-MPBA and diluted to smaller cell populations for high-magnification SERS analyses. Larger cell populations produced robust 3-MPBA SERS spectra. However, smaller cell populations progressively produced less robust 3-MPBA SERS spectra as the sample was diluted. We can therefore conclude that the vicinity outside of the photon incident point influences the SERS data. Bacteria which are not directly contacted by the Raman laser line can therefore improve the detection of a second cell that has been directly contacted by incoming photons. The data also suggests that this phenomenon is not contributing to false-positive bacteria detection signals. Regions where bacteria were absent did not produce 3-MPBA SERS spectra. SERS detection values for bacteria can be characterized by several standards: a) cells per surface area, b) cells per inocula, or c) cells per initial sample volume. Here, we will refer to the cell population by CFU per analyzed region; inocula. Lower magnification SERS analyses revealed a detection limit of approximately Log 4 CFU per region (Fig. 15). SERS images that were compiled using a lower objective lens resulted in larger laser diameters than when higher objective lenses are employed (Paipetis et al., 1996). Lower objective lenses also enable for the SERS of larger surfaces areas in less time. However, larger surface areas require larger pixel sizes for rapid analyses, leaving many bacteria cells unregistered by the system altogether. Lower magnification SERS analyses of bacteria can therefore result in false-

negative cell detection. SERS can be coupled with an optical microscope which aids in instrumental alignment and cell detection. As the technology advances to more complex substrates, however, bacteria will not always be optically visible. Understanding our approach will help users to locate invisible bacteria cells for conclusively credible SERS analyses.

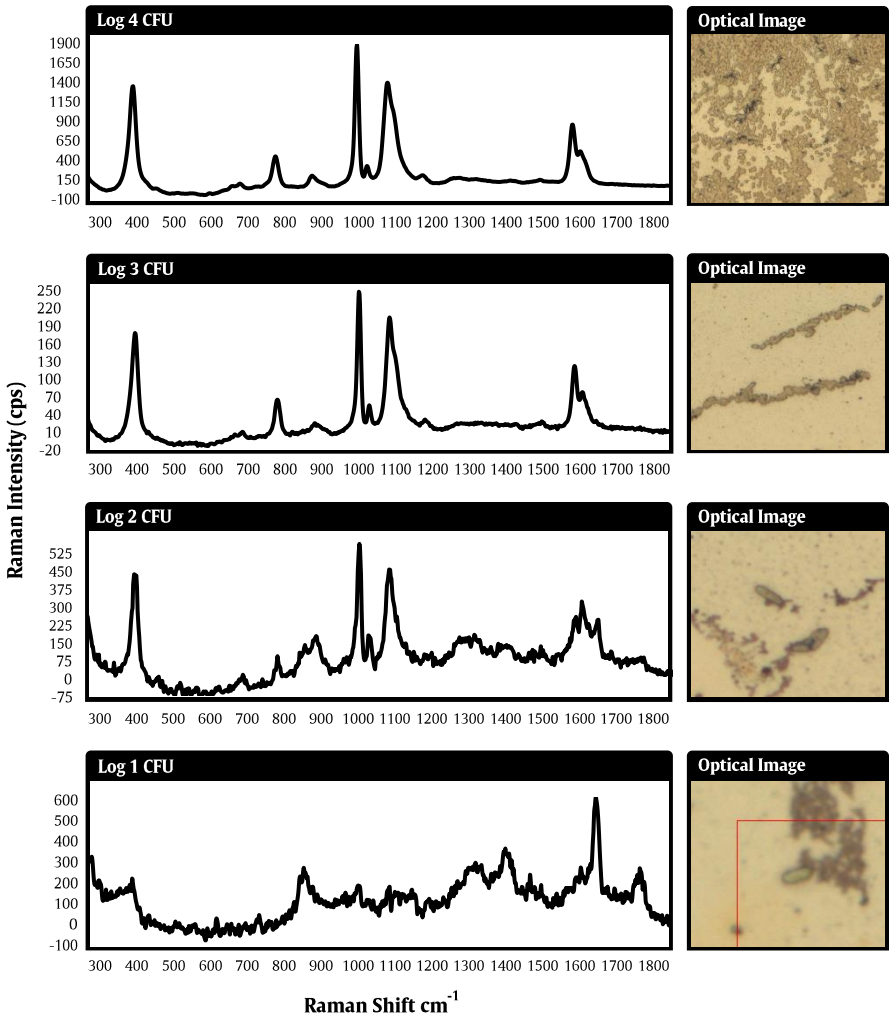

Figure 14: Bacteria were coated with 3-MPBA and diluted for SERS analyses at the single cell level. The sample was diluted using an ammonium bicarbonate / sodium hydroxide solution to prevent hydrolysis of the boronic ester.

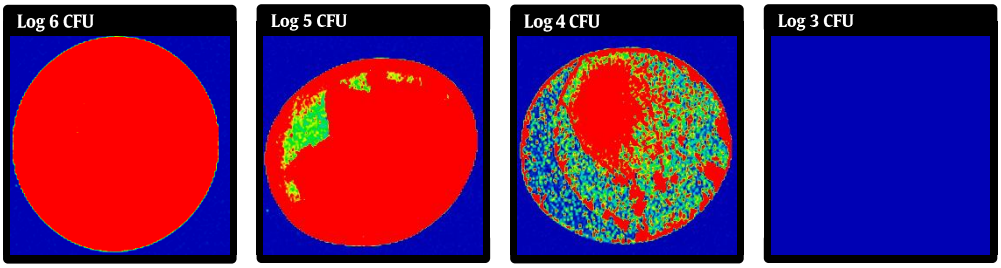

Figure 15: Bacteria were coated with 3-MPBA and diluted for SERS analyses at the whole-inocula scale, using a lower microscope objective lens. The limit of SERS detection was hundred-fold lower than single-cell analyses which utilized a higher objective lens.

4.5. Conclusions

Our approach prevented hydrolysis of the chemical label through several intensive rinse wash applications and produced consistent SERS spectra when unbound labels were rinsed from the system. Simultaneous administrations of prelabeled bacteria cells and AuNPs produced the most robust SERS peaks, compared to separate applications for each component. Bacteria endured the labeling procedure differently, depending on the cell population being treated. Populations below Log 5 CFU mL^{-1} were unable to exhibit binary fission when exposed to the labeling conditions. Electron micrographs revealed signs of corrosion among labeled cell populations that resulted in stronger SERS signals among dead cells than viable cells. SERS labeling applications should be customized when possible, corresponding to each bacteria population being measured.

CHAPTER 5

COMPARISON OF LABEL-FREE AND LABEL-BASED APPROACHES FOR SURFACE-ENHANCED RAMAN MICROSCOPIC IMAGING OF BACTERIA CELLS

5.1. Abstract

In situ analyses of bacteria populations are generally limited to transparent substrates, fluorescent cells, or electron micrographs. Surface-enhanced Raman spectroscopic (SERS) approaches are emerging whereby bacteria cells can be measured based on their biochemical composition (label-free) or with the aid of a chemical label to enhance the SERS signal. Combining a microscope, SERS microscopy is capable of imaging bacteria populations *en masse* based on specific spectrophotometric peaks. Here, we compared the label-free and label-based approaches to study *Escherichia coli* O157:H7 which was utilized as a model bacterium for SERS analyses upon a gold (Au) coated microscope slide glass. Gold (Au) nanoparticles were utilized to enhance Raman scattering during this study and 3-mercaptophenylboronic acid was utilized as a model chemical label for comparison against label-free conditions. The result shows that SERS images of bacteria cells yield measurable differences in precision, depending on the application of chemical labels. Chemical labels enabled SERS imaging of whole bacteria populations with single-cell precision. Bacteria that were coated with labels were also easier to bring into focus using high-magnification optical microscopy, without the need for immersion oil. Label-free analyses of single-cells were lower in geographic precision

but provided clear opportunities to study the natural biochemistry of bacteria cells with strong accuracy. SERS analyses of label-free bacteria cell components were conclusively improved *in vitro* on a time-dependent basis. This concept can serve as an important benchmark when biochemically profiling or characterizing bacteria cells based on SERS. Electron micrographs proved that chemical labels can be utilized to increase nanoparticle contact with bacteria cells and reduce free nanoparticles which contribute to background noise in SERS spectra. We also demonstrate the use of both 3-mercaptophenylboronic acid and propidium iodide to discriminate live and dead bacteria through the simultaneous collection of data from these two chemical labels. Label-free approaches to SERS bacteria analyses are better suited for biochemical characterization and label-based approaches are better suited when accounting for individual cells among a population.

5.2. Introduction

Due to recent instrumentational development, Raman microscopy is emerging as a fast and high-resolution technique for chemical imaging based on integration of characteristic vibrational frequencies. Enhanced by noble metal nanostructures (*e.g.* gold, silver), surface enhanced Raman scattering (SERS) imaging facilitates highly sensitive and selective imaging capability that has been utilized to study both prokaryotic and eukaryotic cells. For example, Ko et al., (2018) demonstrated that Salmonella spp. can be selectively detected using nanoparticle-conjugated antibodies upon SERS compatible lithographs. De Marchi et al. (2019) showed that SERS substrates can be integrated with bacterial culture media for metabolic analyses. Park et al. (2009) demonstrated SERS compatibility with mammalian cells using functional nanoprobes, leading to more

specific targeting of biochemical markers such as that of cancer cells (Hu et al., 2007; Lee et al., 2014). Overlaying the chemical image with optical image gives more insight of the target analyte distribution and interaction with the surrounding matrices (Sauer-Budge et al., 2012; Schmid et al., 2013).

Two approaches are normally taken in SERS imaging, label-free and label-based (Fig. 16). Label-free approach measures the intrinsic Raman signature of the target analyte interacted with the SERS substrate. Label-based approach utilizes a highly sensitive and distinctive SERS label that can response to the target analyte. Both approaches are highly dependent on the interaction with the SERS substrates, and therefore manipulating and controlling the way that SERS substrate interact with the target analyte is very important. The objective of this study is to compare both approaches to study bacteria populations on a surface in situ in terms of signal variation and precision of imaging single cells. *Escherichia coli* O157:H7 was utilized as a model bacterium, and gold nanoparticles (AuNPs) were utilized to enhance Raman scattering during this study. We employed 3-mercaptophenylboronic acid (3-MPBA) to serve as a model chemical label when utilizing SERS to image the distribution of bacteria cells among a population. Boronic acids indiscriminately bind with vicinal diols under alkaline conditions (Murakami et al., 2000; Otsuka et al., 2003; Golabi et al., 2017). Mercaptans form strong bonds with gold but the interactions are strongly influenced by the properties of the gold surface, the pH of the environment, and the duration of their interaction (Xue et al., 2014). These conditions fortunately align when using boronic acids to measure bacteria cell populations using SERS. The efficacy of boronic acid-based bacterial SERS labels were proven through a variety of studies and show remarkable promise for

interdisciplinary applications throughout the field (Wang et al., 2015; Wang et al., 2017; Pearson et al., 2017; Pearson et al., 2018). The boronic esters were utilized as a capturing agent which can anchor bacteria to a surface for SERS mapping and their Raman spectra were analyzed for statistical variation among bacteria cells. In this paper, we precoated bacteria cells with the 3-MPBA label *in vitro*, rather than a surface for cell capture, to map cell populations among a gold (Au) coated slide glass via SERS imaging. Precoating bacteria cells with 3-MPBA enabled us remove unbound chemical labels from the sample and to compare the precision of label and label-free SERS imaging of bacteria populations. In addition, the use of two chemicals labels, 3-mercaptophenylboronic acid and propidium iodide to discriminate live and dead bacteria was also evaluated. The advantages and limitations of both approaches were also discussed.

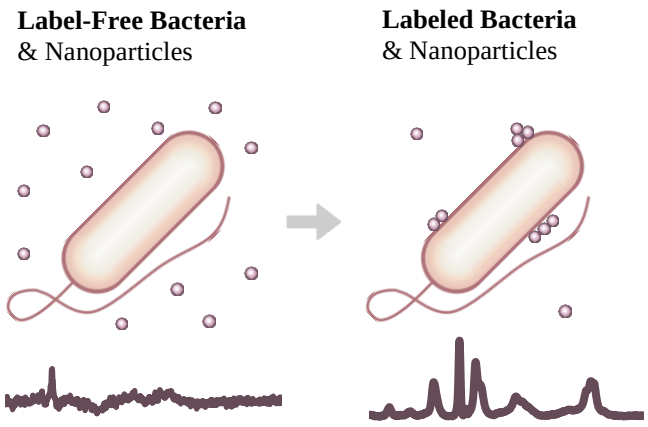

Figure 16: Metallic nanoparticles interact differently with bacteria, depending on cell surface chemistry. SERS analyses of bacteria are therefore customizable, depending on the mission of the user (*e.g.* biochemical characterization vs. surveillance).

5.3. Materials and Methods

5.3.1. Bacterial culture and handling conditions

Non-toxic *Escherichia coli* O157 (Strain: 043888; American Type Culture Collection®, Rockville, Maryland, USA) were cultivated on tryptic soy agar (Becton, Dickinson and Company, Difco™, Franklin Lakes, New Jersey, USA) for 24 hrs under 37 ˚C incubation, to serve as a model bacteria population for SERS imaging. One bacterial colony was transferred from the agar growth plate to 10 mL of tryptic soy broth (Becton, Dickinson and Company). The broth culture was incubated at 37 ˚C with 125 rpm agitation until the earliest onset of stationary-phased growth. The turbidity of the broth culture was immediately adjusted to a predetermined optical density (absorbance at 600 nm λ) using a spectrophotometer (BioSpec-mini, Shimadzu Corp., Kyoto, Japan) to maintain accurate quantities of colony forming units (CFU) throughout experimentation. *E. coli* cultures were analyzed at precisely the same point on the growth curve consistently throughout the duration of this study, to minimize any biochemical variations in bacterial cell physiology between experiments. The samples were consistently adjusted to an initial population of Log 8 CFU mL^{-1} to serve as a base-culture for ten-fold dilution adjustments during quantitative analyses. Tryptic soy broth supernatants were separated from the bacteria following 23 ˚C centrifugation of the culture for 3 min at 9,000 rpm. The remaining bacterial pellet-masses were suspended in ammonium bicarbonate [50 mM, 800 µL] (Thermo Fisher Scientific Inc., Waltham, Massachusetts, USA) by aid of a vortex mixer. Bacteria cultures were rinsed of tryptic soy broth remnants by these methods exactly three times.

5.3.2. Sample preparation for SERS analyses

Citrate-stabilized 50 nm (ø) [0.25 mg mL^{-1}] spherical AuNPs (Nanopartz Inc., Loveland, Colorado, USA) were used to enhance Raman scattering in this study. We utilized [1 mM] 3-mercaptophenylboronic acid (3-MPBA) (AstaTech Inc., Bristol, Pennsylvania, USA) as a non-specific chemical label for bacteria analyses. The 3-MPBA was dissolved in ethyl alcohol [200 proof] (PHARMCO, Greenfield Global, Brookfield, Connecticut, USA) for 100 µL inoculation into the ammonium bicarbonate bacteria suspension. Sodium hydroxide [100 mM] (Thermo Fisher Scientific Inc.) was administered for at five 20 µL increments to encourage 3-MPBA esterification among the bacteria cells. The final solutions (1 mL) thereby consisted of known *E. coli* populations, ammonium bicarbonate [40 mM], 3-MPBA [10 mM], and sodium hydroxide [10 mM]. A solution containing ammonium bicarbonate [50 mM] and sodium hydroxide [10 mM] was then utilized as a rinse solution following the bacteria-rinsing procedure that was described previously, to remove unbound 3-MPBA from the sample. Samples were analyzed for SERS on the surface of gold (Au) coated microscope slides, consisting of *E. coli* cells and AuNPs at equal volumes. The inocula were dried under 23 ˚C incubation within a 1300 Series Class II, Type A2 Biological Safety Cabinet (Thermo Fisher Scientific Inc.) before SERS analyses were performed.

5.3.3. SERS microscopy and image analysis

All samples were brought into focus using either 20x/0.40NA or 100x/0.9NA microscope objective lenses. SERS spectra were collected using a DXRxi Raman

imaging microscope (Thermo Fisher Scientific Inc.) with a 780 nm (λ) laser line. Each spectrum was generated based on 0.1 sec collection-exposures using a 3 mW laser line through a 50 µm slit-aperture. Chemical imaging was achieved by integrating at least four thousand spectra. The laser spot size was approximately 2.38 µm and 1.06 µm (ø), respective to the use of lower and higher magnification lenses. Single-cell SERS microscopy was conducted using a 2 µm pixel step-size and lower magnification images were constructed using a 40 µm pixel step size. Images were analyzed using the OMNICxi Raman SW software (Thermo-Nicolet, Madison, Wisconsin, USA). Spectra were comparatively analyzed based on discriminatory features which were identified using the TQ Analyst 9.0 software (Thermo-Nicolet).

5.3.4. Scanning electron microscopy

Bacteria were administered onto the surface of gold (Au) coated microscope slides following the methods which were described above, to validate the SERS and optical data via electron microscopy. The cells were fixed for observation using 2% glutaraldehyde for 6 hrs at 4 °C incubation. The fixation media was prepared by diluting glutaraldehyde in fresh [0.1M] HEPES buffer and chilled to 4 °C prior to application. Gradient concentrations of molecular-grade ethanol were used to dehydrate the sample after fixation. The sample mounts were grounded using two-sided carbon tape for electron imaging. AuNPs (2 nm, ø) were administered onto the samples via sputter deposition to prevent electrostatic charge accumulation which could interfere with the generation of accurate electron micrographs. Electron micrographs were generated using

an FEI Magellan extreme high-resolution (XHR) 400 FE scanning electron microscope system (Nanolab Technologies Inc., Milpitas, California, USA).

5.3.5. Sample preparation for discrimination between live and dead cells using multicomponent labeling

A known concentration of bacteria cells was isolated from a broth culture and washed three times using sterile deionized water, following the previously described methods. The bacteria were then exposed to various concentrations of chlorine bleach (The Clorox Company, Oakland, California, USA) for 10 min to determine which concentration would damage bacteria cells without shattering them into fragments. The samples were again washed three times with water and the supernatants were removed. The bacterial pellets were suspended in 500 µL of propidium iodide [2 mg mL^{-1}] (Invitrogen, Carlsbad, California, USA) for 5 min gyration on a nutation mixer (Thermo Fisher Scientific Inc.) at room temperature. The cells were washed in water three times to remove residual propidium iodide. The optimal chlorine bleach concentration ([6 ppm total chlorine] 12 min exposure) was determined by optical analyses of the cell debris and/or propidium iodide pigment intensity therein. For proof-of-concept purposes, it was a priority to keep the cells intact. The cells were then labeled using 3-mercaptophenylboronic acid following the previously described methods. SERS mapping of the multiple components was achieved using the previously described parameters with the exception of the pixel-size being 2 µm and AuNPs from nanoComposix (San Diego, California, USA).

5.4. Results and Discussion

5.4.1. Surface-enhanced Raman spectra of label-free vs. labeled bacteria cells

SERS spectra of label-free and label-based bacteria and AuNP controls were shown in Fig. 17 and 18. Each spectrum generated by converging at least four thousand SERS spectra on the basis of average Raman intensity (counts per second). In general, label free spectra exhibit lower intensity and more variation than the label-based spectra. Specifically, peaks in the label-free spectra are originated with intrinsic biochemicals of cells. For example, the most studied Raman shifting near 735 cm^{-1} is originated from adenine in bacteria (Premasiri et al., 2016). Other peaks show more variations in pattern and intensity, largely influenced by the AuNP background. SERS of AuNPs which are bound to 3-MPBA generally emitted two major peaks at the 998 cm^{-1} and 1070 cm^{-1} positions. These vibrational assignments reflect phenol ring stretching among the chemical label (Chen et al., 2019). The phenyl ring group among 3-MPBA produces very robust SERS peaks which are consistent with our previous investigations (Pearson et al., 2017; Pearson et al., 2018). When bacteria are involved with AuNPs and 3-MPBA, Raman shifting produced two prominent peaks at 1024 cm^{-1} and 1550 cm^{-1} that differed from the negative control. These peaks represented in-plane ν_{18a} C–H bond-bending which occurs when phenylboronic acids are esterified to a substrate while being simultaneously excited by the Raman laser line (Szafranski et al., 1998; Sun et al., 2014). This is a valuable concept as SERS innovations progress toward *in situ* chemical labelling, beyond *in vitro* constraints. Unbound chemical labels can produce false-positive signals during SERS imaging. It is therefore beneficial when bound labels produce different spectra than unbound chemical labels. However, the 1024 cm^{-1} peak

might also indicate di-/trimerization which can occur at increasing yields when 3-MPBA is abundant within alkaline conditions where other diols are scarce (Nishiyabu et al., 2011).

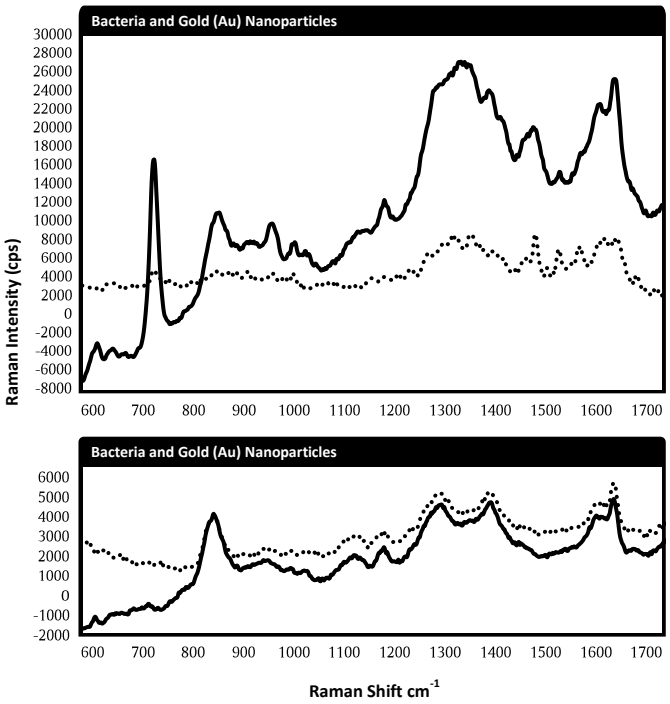

Figure 17: SERS spectra which are representative of label-free bacteria cells, compared to that of a AuNP control. Nanoparticles often caused ‘noise’ which overpowered the bacterial indicator peak due to fewer cell contact yields and lower peak intensities.

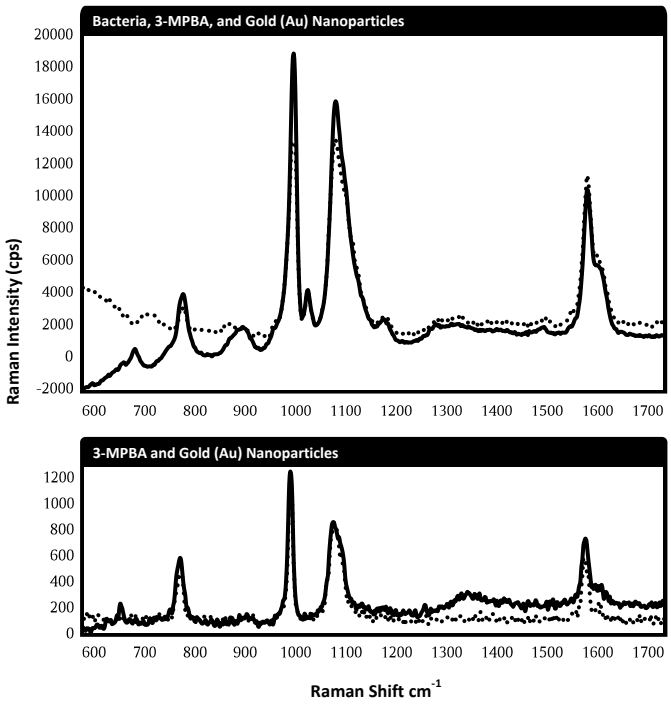

Figure 18: SERS spectra which are representative of bacteria cells that were coated with a 3-mercaptophenyl boronic ester. Nanoparticles sometimes caused ‘noise in the spectra but the analyses were uninhibited due to the sharper, more robust peaks which exhibited strong Raman intensity.

5.4.2. Scanning electron micrographs of label-free vs. labeled bacteria cells

To gain more insight into the nanoparticle and bacteria interaction, scanning electron microscopy was performed on the label-free and labeled bacteria with AuNPs (Fig. 19). Label-free bacteria were coated with fewer nanoparticles than labeled cells which resulted in an abundance of free nanoparticles across the surface of the sample. The AuNPs also aggregated less frequently under label-free conditions than label-based conditions. Many label-free bacteria cells were bare of nanoparticles altogether. Bare bacteria cells do not exhibit surface-enhanced Raman scattering mechanisms and therefore only exhibit traditional Raman scattering. The efficiency of surface-enhanced Raman photon scattering is dependent upon nanoparticle interactions with the analyte. Traditional Raman scattering is difficult to detect because most photons exhibit elastic Rayleigh scattering; photons which do not exhibit shifts in wavelength. Nanostructured noble metals dramatically increase the quantity of inelastically scattered photons through their induction of Langmuir waves, making Raman analyses more feasible. Label-free SERS analyses of bacteria are still suitable for biochemical characterization, but less so for tracking whole cells. Extracellular bacterial secretions can also be targeted by the system, in this respect. Cellular contact yields with nanostructures appear to be a primary bottleneck among label-free surface-enhanced Raman analyses of bacteria.

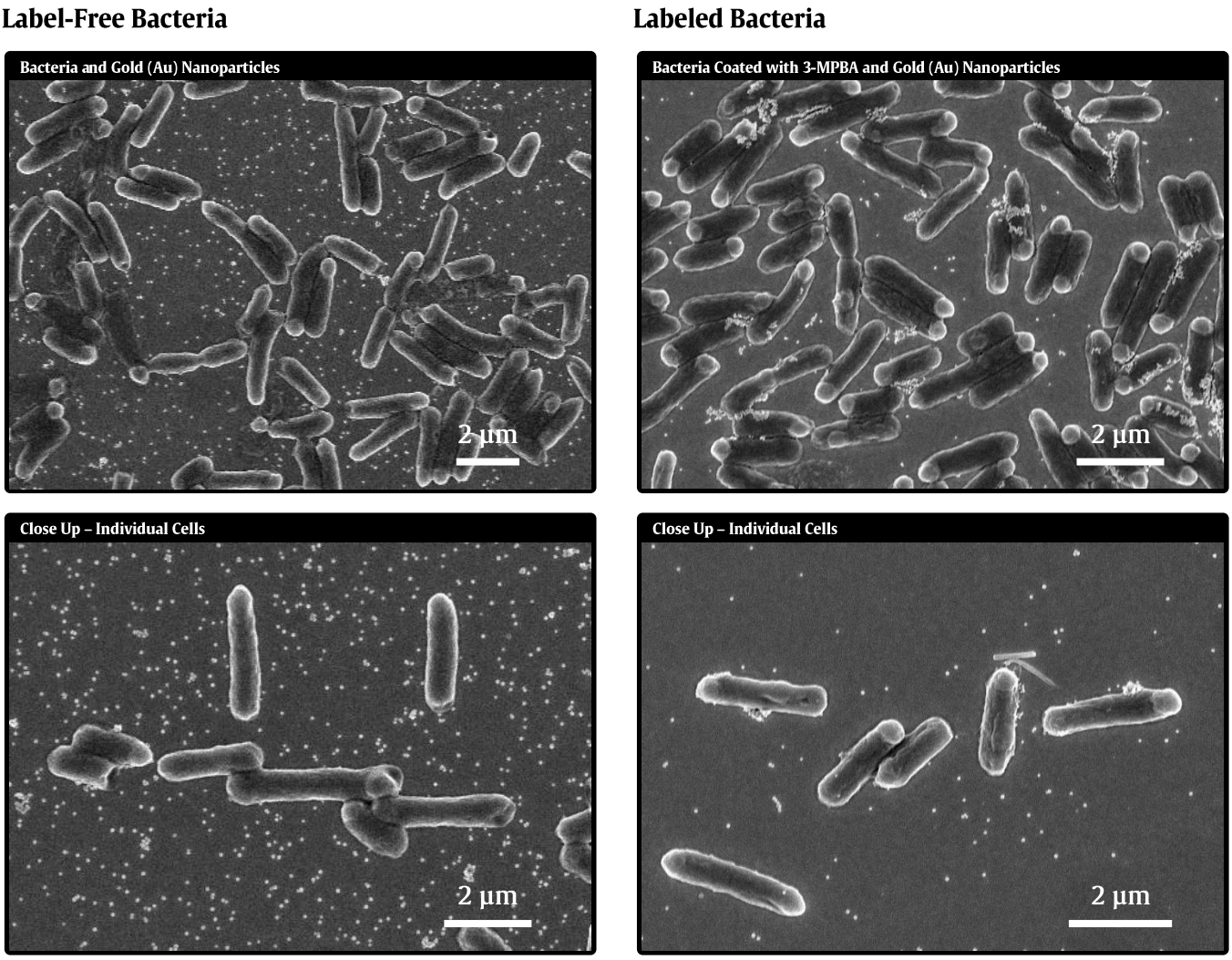

Figure 19: Electron micrographs of the bacteria samples as they were analyzed using SERS. Nanoparticles exhibited less contact with label-free cells than labeled cells, resulting in an abundance of free nanoparticles across the substrate. Nanoparticle contact with labeled cells was stronger, resulting in fewer free nanoparticles in the surrounding sampling regions.

Labeled bacteria were coated with more nanoparticles than the label-free cells which resulted in fewer free-nanoparticles across the substrate. These qualities collectively amount to a molecular architecture that is favorable for SERS, resembling a sort of 'ankle monitor' which helps to digitalize this microbiology. Consistent nanoparticle-contact with the cells enabled a sort of 'dragnet' for mass collections of chemical data during SERS imaging. Bacteria cell populations can be surveilled *en masse* using the Raman system, in this respect. This is an important concept when considering real field applications of this kind. Nanoparticle depositions are often at the mercy of nature and physics when deployed upon a substrate. Raman systems should be innovated in ways which promote nanoparticle contact with the analyte for comprehensive analyses of unknown microbial ecosystems for the tracking of cell locations among a population.

5.4.3. SERS images of label-free vs. labeled bacteria cells

We previously showed that 3-mercaptophenylboronic acid produces light contrasting effects when bound to bacteria cells which aid in their optical analyses (Pearson et al., 2017; Pearson et al., 2018). We applied this concept to analyze individual bacteria cells using higher magnifications (Fig. 20). Label-free bacteria were difficult to bring into focus at the single-cell level using optical microscopy. Labeled bacteria cells exhibited a dark appearance and enabled higher magnification analyses without the need for immersion oil. Depending on the substrate, however, bacteria cells will not always be visible using optical microscopy. The precision of SERS imaging among single bacteria cells is critical to the accuracy of this approach. Optical microscopy concepts are

important to pair with SERS imaging and were utilized to validate detection signals during this study.

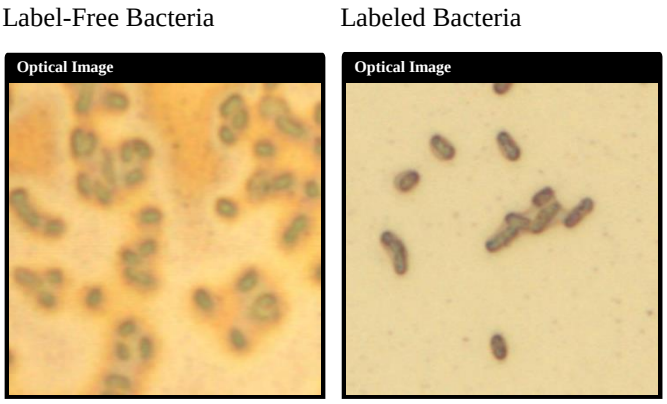

Figure 20: Bacteria cells which were brought under focus using an optical microscope. Label-free bacteria were difficult to bring into focus at higher magnification, compared to labeled cells which exhibited a darker, sharper appearance.

SERS investigations proved that the spatial resolution of our approach was sufficient for the detection of single bacteria cells (Fig. 21). The data was confirmed for conclusively using optical microscopy. The chemical image *accuracy* of bacterial distributions was similar for both the label-free and labeled cell populations. However, the *precision* of the chemical images was stronger for labeled bacteria than label-free cells. Lower precision among label-free populations can be attributed to lesser nanoparticle contact and the lower cell concentration of adenine-related compounds (*i.e.* 735 cm^{-1} peak), compared to the high cell concentration of the chemical label. The precision of the approach is suitable for single cell analyses, with the caveat being the need to manually locate the cells for alignment under the laser line; a 'needle in the haystack' effect when it comes to *in situ* labelling or more complex substrates.

SERS is resemblant to that of a voting system. Higher quantities of Raman-compatible molecules, which are vicinal to noble metal nanoparticles, will yield higher spectral peaks when contacted by a monochromatic light source. Label-based Raman imaging of bacteria populations therefore present sharp spectral differences between the cells and their substrate, resulting in tighter geographic precision (Fig. 22). Label-free analyses rely on natural molecular components which are less concentrated than chemical reagents, resulting in lower peak intensities which can fall below the spectroscopic detection threshold. SERS is more challenging when targeting bacteria than molecular reagents, due to the inherent biochemical diversity of natural cells and their physical distribution as a population of complex microstructures.

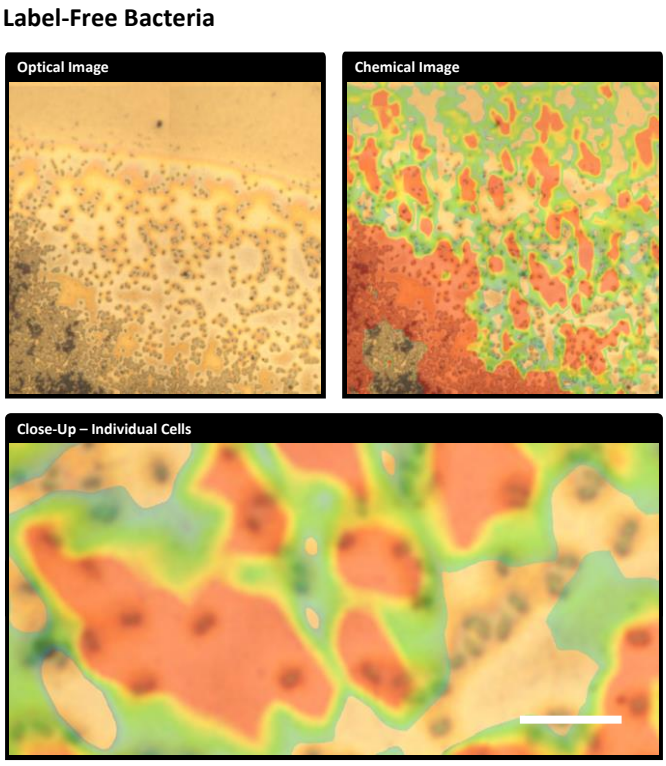

Figure 21: Bacteria cells surveilled using SERS without a chemical label. Many bacteria were not registered by the Raman system. Individual cells were detected but with less precision than labeled cells. Scale bar represents 15 μm length.

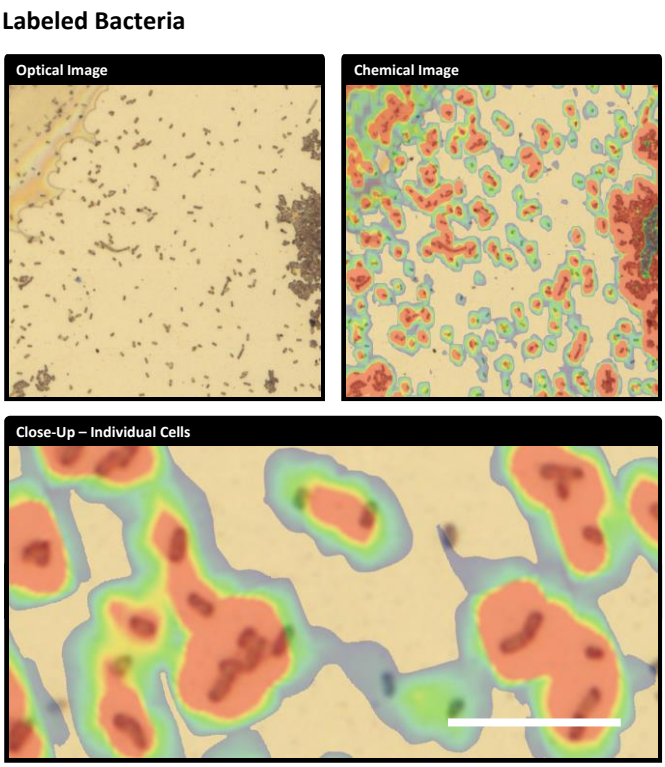

Figure 22: Bacteria cells individually surveilled using SERS. Coating bacteria with Raman-active labels enabled the digital tracking of cellular distributions among whole microbial populations. Scale bar represents 15 µm length.

A broader investigation into the imaging of label-free bacteria cells revealed the process to be time-dependent *in vitro* (Fig. 23). A time-lapse approach to imaging revealed higher pixel quantities of 735 cm^{-1} Raman shifting among the sample. However, the bacteria cell population and spectral peak height at 735 cm^{-1} were both unchanged. The experiment proved that the bacterial biochemistry, which produces the 735 cm^{-1} peak, is susceptible to diffusion outside of the cells. Interactions between the nanoparticles and signal molecules can be increased *in vitro* with time. Chen et al. (2018) noticed a similar trend in the supernatant of *Neisseria gonorrhoeae* but not *Chlamydia trachomatis*, suggesting that the trend is not universal to all bacteria species. The data is suitable for biochemical characterization but is less suitable for cell tracking. This approach might be especially useful for the monitoring or imaging of cell-to-cell communications by means of SERS. Label-free approaches to SERS-based bacterial detection are clearly fruitful but do face measurable limitations during quantitative image analyses.

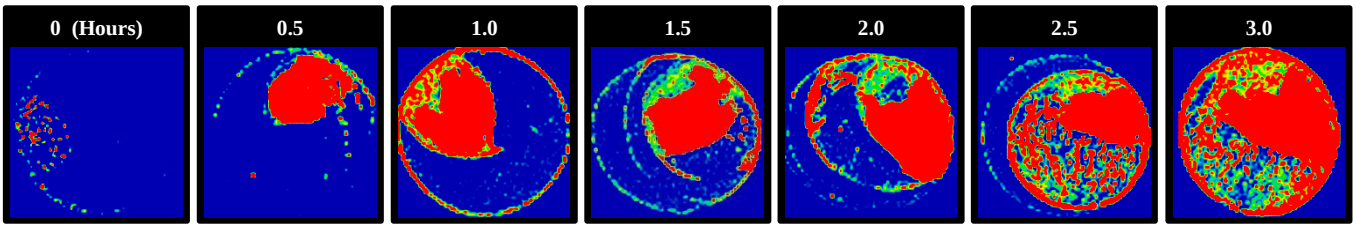

Figure 23: Label-free bacteria populations produced different results, depending on the duration in which they were suspended within colloidal gold (Au) nanoparticles. SERS spectra and bacteria cell populations were unchanged.

5.4.4. Multicomponent cellular analysis using two labels

Raman systems are capable of simultaneously imaging multiple analytes (Peters et al., 2017). We demonstrated that this function can be utilized to differentiate between live and dead bacteria cells (Fig. 24). Live and dead bacteria cells were exposed to propidium iodide and 3-MPBA labels. Spectra of dead bacteria produced strong signals among the 1400 cm^{-1} region, proving that propidium iodide was retained at higher concentrations within dead cells. Live bacteria cells did not produce spectral peaks in this region. All bacteria produced 3-MPBA peaks which enabled us to indiscriminately image total bacteria populations, as well as discriminate between live and dead cells. Propidium iodide is used in fluorescent microscopy as an indicator of dead cells (Crowley et al. 2016) and its Raman spectra did not overlap with that of 3-MPBA. Multicomponent Raman imaging is currently only applicable for analytes which produce spectra that are distinguishable from each other within the same mixture.

Multiple bacteria can be coated separately with *different* labels for multicomponent discrimination using Raman spectroscopy. We demonstrate another important concept in which multiple bacteria were coated using the *same* labels to yield different results. Multicomponent Raman imaging of bacteria will likely involve target-specific labels as the concept progresses forward. However, we wanted to make the case that non-specific labels also serve an important role in Raman imaging. Two important limitations of this approach were discovered during our analyses. We found that propidium iodide produced stronger Raman signals using nanoparticles from one commercial distributor vs. another. SERS nanoparticles should therefore be consistent with the goals of the user and are not always a ‘one size fits all’ solution to enhancement.

The second limitation that we encountered with propidium iodide was that the pixel size needed to be set to 2 µm for SERS imaging. There is potential for overlap between spectral collections at this range. Smaller pixel sizes yield higher-resolution images, but they also take longer to render larger surface areas within the system. Finally, the propidium iodide spectra presented broader horizontal features which resembled background noise, rather than the sharp vertical peaks that were evident using the 3-MPBA chemical label. The Raman system is less adept at identifying broader spectral features which exhibit lower peak intensities. Multicomponent SERS labelling procedures should favor sharp spectral peaks which produce spectra which are easily distinguishable among bacterial mixtures.

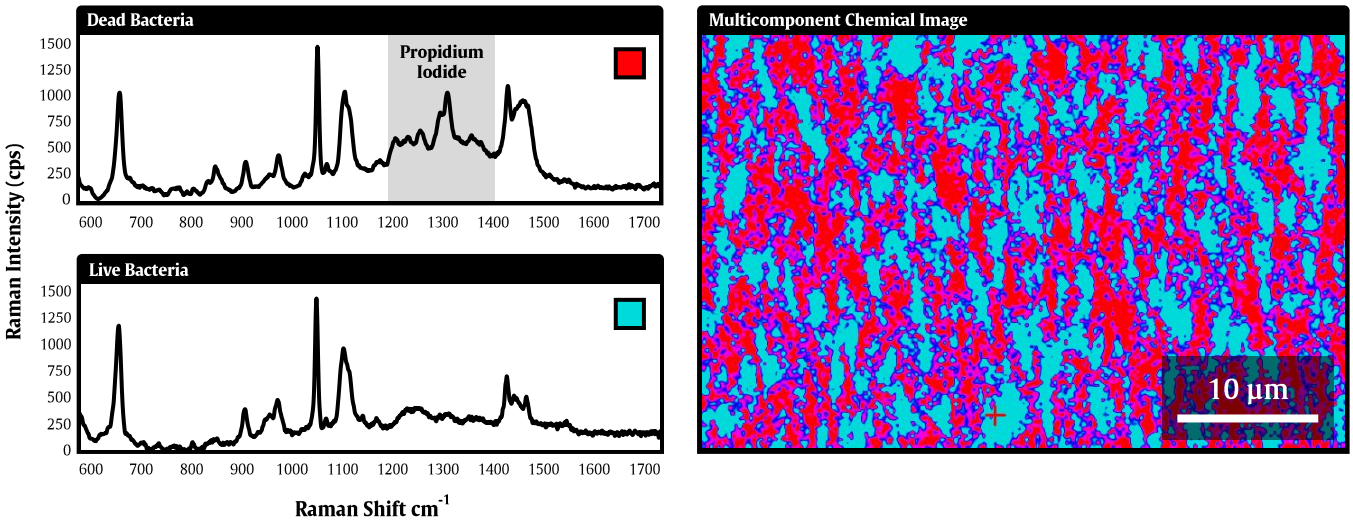

Figure 24: SERS spectra which are representative of bleach-inactivated and live bacteria cells that were labeled with propidium iodide and 3-mercaptophenylboronic esters. SERS imaging is capable of discriminating multiple labels when their corresponding spectra can be distinguished within the digital system.

5.5. Conclusions

Bacteria labelling enhanced the precision and versatility of SERS imaging. Molecular labelling also improved the optical properties of bacteria cells in ways which helped to verify the accuracy of SERS images using the same instrument. Multiple Labels were combined to discriminate live and dead bacteria cells within a mixture. Broader peaks were less favorable than sharp peaks when simultaneously mapping multiple labels among a population of bacteria. SERS analyses of label-free bacteria provided opportunities for biochemical profiling which were improved *in vitro* through time-dependent diffusion that enhanced nanoparticle interactions. Nanoparticle cell-contact yields are a primary bottleneck that requires optimization before SERS analyses can reach wider field investigations of bacteria in nature.

CHAPTER 6

SURFACE-ENHANCED RAMAN SPECTROSCOPIC ANALYSES OF BACTERIA CELLS DIRECTLY WITHIN PLANT TISSUES

6.1. Abstract

A real-time method to surveil mass bacterial communities directly *in situ* is reported. Surface-enhanced Raman spectra were collated *en masse* to generate panoramic chemical images of bacteria populations. Bacteria cells were coated in 3-mercaptophenylboronic acid for complexation with gold (Au) nanoparticles. This molecular architecture enhanced the detection of scattered Raman photon frequencies which were indicative of bacteria cells. The approach was successfully employed to indiscriminately monitor mass bacteria populations directly among plant tissue.

6.2. Introduction

Bacterial analyses were founded upon microscopy but have evolved to higher *ex situ* technologies. *In situ* observations of bacteria remain limited to electron micrographs and cellular fluorescence. Electron micrographs of bacteria provide ultra-high-definition visual insight below the nanoscale but the analysis is statuesque in nature and involves protracted sample preparation. Cellular fluorescence enables the real-time analysis of bacteria but most species do not fluoresce without an artificial stain. The scale of fluorescent analyses is also limited to the microscopic field-of-view and the characteristic qualities of the substrate are generally lost due to the dark-field nature of the approach.

Recent technological advancements in Raman imaging have allowed us to overcome important restraints in the surveillance of
bacterial communities *in situ*.

Raman imaging merges the chemical qualities of an analyte with the physical characteristics of its substrate based on real-time spectroscopic computations. The resolution of this approach is generally compromised between pixel size (*i.e.* distance between spectral collection sites) and mapping surface area (*i.e.* overall chemical image size) due to the slow spectral collection speed of the instrument and mechanical limitations of the microscope stage. Improvements have been made to the Raman system which now allow for sweeping surveillance of condensed nanoscale Raman collection sites (*i.e.* smaller pixels) which span a broader inch-scale (*i.e.* larger images and sample sizes). The system is no longer confined to one microscopic field-of-view and can now rapidly generate high-definition, panoramic chemical images of an analyte in real-time directly *in situ*.

We and others have utilized boronic acids as Raman indicators of bacterial presence within a sample. Phenylboronic acids possess vicinal diol-groups which can form stable complexes with surrounding polyols via esterification. Bacteria cells possess a variety of polyols along the outer-membrane surface which enables their envelopment in phenylboronic acids. Thiols and gold (Au) nanoparticles form a strong Au–S bond. Mercaptophenylboronic acids can therefore bridge together Au-nanoparticles and bacteria cells to construct functionalized enhancers of Raman photon-scattering. We hypothesized that bacterial communities could be surveilled *en masse* based on Raman scattering of mercaptophenylboronic acid/Au-nanoparticle interactions directly *in situ*. This approach

would expand the visual capacity of bacterial surveillance efforts in natural substrates beyond what is accessible using current microbiological analyses. We report the successful implementation of this concept by monitoring mass bacterial communities in real-time directly among plant tissue.

6.3. Materials and Methods

6.3.1. Bacterial culture and handling conditions

Escherichia coli O157:H7 (non shiga-toxin producing strain: 043888; American Type Culture Collection®, Rockville, Maryland, USA) cells were propagated using tryptic soy agar (Becton, Dickinson and Company, Difco™, Franklin Lakes, New Jersey, USA) at 37 ˚C. Individual colonies were then transferred to 10 mL of tryptic soy broth (Becton, Dickinson and Company). Broth cultures were incubated 37 ˚C with 125 rpm shaking until stationary growth. Broth cultures were then adjusted to a predetermined turbidity (optical density absorbance at 600 nm λ) using a spectrophotometer (BioSpec-mini, Shimadzu Corp., Kyoto, Japan) to ensure that consistent cell quantities were utilized during experimentation. Bacteria cultures were used for experimentation at the same growth stage throughout this study. Experimental cultures were adjusted to Log 8 CFU mL^{-1} for each inoculation, unless adjusted for tenfold differences in cell population. Supernatants were separated from each bacterial culture via centrifugation at 9,000 rpm for 3 min. Bacterial pellet masses were then resuspended in ammonium bicarbonate [800 µL, 50 mM] (Thermo Fisher Scientific Inc., Waltham, Massachusetts, USA). The cultures were washed-free of tryptic soy broth exactly three times by the approach.

6.3.2. Sample preparation for SERS analyses of bacteria among plant tissues

3-mercaptophenylboronic acid (3-MPBA) (AstaTech Inc., Bristol, Pennsylvania, USA) was employed as a SERS label for the detection of bacteria cells. The reagent first dissolved in absolute ethanol (200 proof) (Thermo Fisher Scientific Inc.) for high concentration [110 mM] storage in a 4 °C refrigerator. 3-MPBA (100 µL) was added to the ammonium bicarbonate-based bacterial suspension to achieve cellular labeling. Sodium hydroxide [100 mM] (Thermo Fisher Scientific Inc.) was administered for mixing at five 20 µL increments to drive esterification of 3-MPBA to the bacteria cells. The final solutions (1 mL) thereby consisted of a known *E. coli* cell concentration, ammonium bicarbonate [40 mM], 3-MPBA [10 mM], and sodium hydroxide [10 mM]. A solution containing ammonium bicarbonate [50 mM] and sodium hydroxide [10 mM] was then utilized as a rinse solution following the bacteria-rinsing procedure that was described previously, to remove unbound 3-MPBA from the sample. The bacteria pellet was finally suspended in a spherical bare Au-nanoparticle colloid (50nm ø) [0.20 mg mL^{-1}, 2 mM sodium citrate] (nanoComposix Inc., San Diego, California, USA) to enhance the Raman scattering of 3-MPBA during SERS bacterial analyses. Each model plant tissue (spinach leaves, cantaloupe, peanuts) was purchased from a local retailer of fresh, organic produce and was washed three times with ultrapure water from a Millipore water purification system (Millipore Co., Burlington, Massachusetts, USA). The same water from the purification system was utilized to evaluate bacterial attachment following rinse water applications. Each plant tissue was fixed in place upon a microscope slide glass. Bacteria samples were administered at 100 µL upon each plant substrate and the inocula were dried under room temperature (23 ˚C) incubation within a 1300 Series Class II,

Type A2 Biological Safety Cabinet (Thermo Fisher Scientific Inc.) before SERS analyses were performed. Bacteria were injected through the stem of spinach leaves for SERS profiling within the depth of the solid substrate using a Gastight® 1750 glass syringe (Hamilton Co., Reno, Nevada, USA).

6.3.3. Raman instrumentation and data analyses

Each sample was aligned with a Raman laser using a 20x/0.40NA magnification objective lens for SERS spectral collections using a DXRxi Raman Imaging Microscope System (Thermo Fisher Scientific Inc.). Each spectrum was generated based on photon scattering patterns from a 3mW, 780 nm (λ) laser line, following 0.1 sec sample exposures through a 50 µm slit aperture. Depth-profiling within leaf guard cells was achieved using higher laser powers at deeper z-coordinates. Each inocula was imaged near their entirety using the OMNICxi Raman Imaging Software v1.6 (Thermo-Nicolet, Madison, Wisconsin, USA). Laser exposures occurred at approximately 2.38 µm (ø) using 40 µm pixel steps. Maps were constructed based on the 998 cm^{-1} Raman shift within the SERS spectra of 3-MPBA. Raman intensity threshold values were variable depending on individual spectral trends and the collection region.

6.4. Results and Discussion

6.4.1. Raman spectral information

3- and 4-mercaptophenylboronic acids were comparatively evaluated for their efficacy as chemical indicators of bacterial presence during Raman imaging. Raman spectroscopy confirmed that 3-mercaptophenylboronic acid emits two major peaks at the

998 cm^{-1} and 1070/1090 cm^{-1} positions. These peaks are indicative of an in-plane benzene breathing mode and C–S stretching. In-plane v_{18a} C–H bond-bending occurs when phenylboronic acids are esterified to a substrate while being simultaneously excited by a Raman laser line. A third peak is therefore evident at the 1024 cm^{-1} position if 3-mercaptophenylboronic acid is complexed between Au-nanoparticles and bacteria cells. These observations were consistent when screening bacteria upon both substrates of interest. Raman imaging of bacteria cells using 4-mercaptophenylboronic acid was variable between substrates. Several spectral peaks were expressed among 4-mercaptophenylboronic acid samples on Au-coated slide glasses that were absent during plant tissue analyses. Binding between Au-nanoparticles and bacteria cells among plant tissue could not be differentiated against unbound Au-nanoparticles using 4-mercaptophenylboronic acid. 4-mercaptophenylboronic acid peaks provide unique bacteriological insight upon Au-coated glass but Raman analyses proved that 3-mercaptophenylboronic acid is more suitable for *in situ* chemical imaging of bacteria cells among natural substrates.

Bacteria cells indiscriminately registered 3-mercaptophenylboronic acid Raman signals regardless of their taxonomic classification (data not shown). Chemical images were generated for bacteria populations above approximately Log 3 cells/mm^2 but the spatial resolution of this approach is compatible with single cell detection. This approach offers new perspective into microbiological analyses by bridging the gap between volumetric and surface area -based analyses of bacteria cells. Cellular distributions are inconsistent among the substrate and volumetric analyses therefore offer limited insight into the relationship between cell populations and substrate geography. Raman chemical

imaging proved that bacteria populations can be surveilled *in situ* in a manner that is scaled to the size of the cells and is nondestructive to their substrate.

Microbial analyses generally require that an analyte be isolated from a solid substrate by homogenization in solution before any further analyses can be realized. Raman analyses of substrate-internalized microorganisms have so far been limited to liquid samples. Solid matrices generally inhibit the analysis of microorganisms *in situ* because photon-scattering-based depth profiling is generally only possible within transparent substrates. Liquid homogenate is therefore ideal for *in situ* Raman analyses of microorganisms which have been internalized within solid materials. Raman lasers can penetrate certain solid matrices for direct analyses but this level of imaging is only possible if noble metal nanoparticles –used to enhance Raman scattering– can sufficiently interact with the intended analyte. Solid matrices therefore prevent adequate nanoparticle-access to bacteria if the cell is situated within the depth of the substrate itself. Au-nanoparticles were recently identified as suitable enhancers of Raman signals within the depth of spinach leaves and possess the ability to penetrate leaf tissues. Au-nanoparticles are also compatible with the collection of bacterial Raman spectra *in situ* and such analyses can be strengthened with the application of phenylboronic acids. Internalized bacteria were Raman imaged within plant stoma cavities to illustrate the application of this approach during depth surveillance profiling.

6.4.2. Imaging bacterial populations within spinach leaves

Edible green leaves cause more foodborne illnesses than any other food group. Spinach leaves were therefore an appropriate model to demonstrate our proof-of-concept.

Our approach can mass-surveil bacteria populations directly upon foods that are of interest to public health (Figure 25). Bacterial analyses of this nature typically require the removal of bacteria from the food matrix for *ex situ* experimentation. There is certainly value to *ex situ* studies of bacteria, but the approach lacks direct insight into original ecosystem. Fluorescent and electron microscopic approaches enable scientists to study bacteria *in situ*. However, these approaches are limited to a maximum field-of-view of approximately 300 μm for visual analyses. Bacteria are generally indistinguishable above that threshold by these approaches. Our data proves that Raman spectroscopy offers visual insight into microbial ecosystems well-above the millimeter scale. Raman images also possess spectral data for each pixel of the image offering users multi-dimensional, chemical-metadata rather than optics alone.

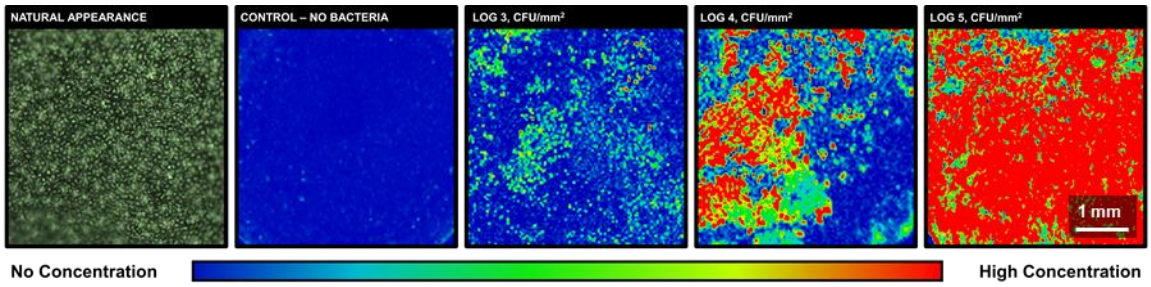

Figure 25: Various concentrations of *E. coli* were tagged with 3-mercaptophenylboronic acid to demonstrate that Raman imaging can be utilized to surveil bacteria populations *en masse* directly among plant tissues.

Raman systems are equipped with depth-profiling capabilities which have traditionally been employed to scan coarse surfaces. We and others have utilized this feature to perform z-stack Raman analyses of various x-y coordinates at different substrate depths. Here, we show that our approach enables the visualization of bacteria cells which are internalized within edible leafy greens (Figure 26). The approach is not limited to guard cell cavities in plant tissues, but it can be more challenging to achieve internalized signals in dense tissues. We therefore concluded that the ventral portion of green leaves are the most suitable for these analyses. Guard cells are more abundant on the bottom of leaves and air spaces within spongy mesophyll allow more light to penetrate the substrate for detection. Palisade parenchyma cells are more dense than spongy cells and stoma cavities are less abundant on the top of leaves. This is often attributed to plant evolution as a protective mechanism against sunshine-induced moisture loss.

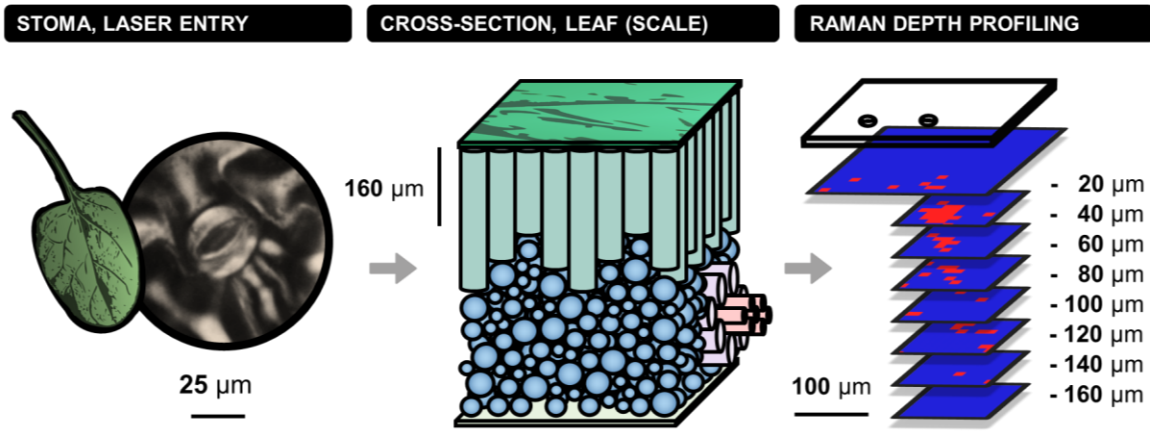

Figure 26: Labelled bacteria were screened within the depth of spinach leaves to demonstrate the potential for internalized bacterial analyses. Guard cells were the strongest point-of-entry to collect this data with a Raman laser. The stoma are generally more abundant on the bottom-side of leaves and the tissue tends to be more transparent, aiding in this type of microbial Raman detection.

Raman spectra were collected across symmetric quadrilateral distributions on an xy-plane at various z-coordinates which spanned the local position of guard cells. Laser miliwattage was incrementally increased respective to analytical depth within the substrate. The data were converged to establish two-dimensional maps which were representative of bacterial demographics within the plant tissue at specific depths. The two-dimensional maps were collated via z-stacking to display a three-dimensional atlas framework which represented bacteria cells as they existed within the internal matrix of the substrate. Internalized bacteria could be monitored *in situ* as deep as about 140 μm within plant tissue. Mature spinach leaves generally range from approximately 400-500 μm in overall thickness. Comprehensive analyses of bacteria which are internalized throughout spinach leaves are therefore possible when thinner leaves (*i.e.* 300 μm) are analyzed from both the dorsal and ventral habitus of the sample. Bacteria within larger leaves cannot be analyzed throughout the entirety of the leaf depth using the current approach. These analyses can be more target-specialized respective to internal tissues (*e.g.* palisade parenchyma or spongy mesophyll) and Raman depth signals proved to be strongest among the ventral habitus of the leaf due likely to the higher optical transparency of the tissue.

Arguments can be made that this approach to Raman imaging is less accurate than surface mapping. There is no way to definitively rule-out overlapping signals at various depth coordinates. Furthermore, there is a clear limitation to the depth at which Raman analyses could be achieved by this approach. Mature spinach leaves are known to grow more than two-thirds thicker than the maximum achievable depth signal shown here. Users can profile depth signals of leaves from both the dorsal and ventral coordinates.

However, leaves are sensitive to temperature and their structural qualities are quickly reduced outside of controlled refrigeration. It is therefore important that leaves always be anchored within a plastic petri dish that contains water along the bottom surface; otherwise, the integrity of the leaf tissue will warp and dry in a short-time. This is a critical point because Raman analyses enable us to study bacteria in fresh leaves. Electron microscopic approaches require dry substrates which, in this case, means that leaves need to be freeze dried and fixed in a statuesque state. The images tell us a lot about bacteria themselves, but the ecosystem is less-true to nature in this form. Our Raman imaging approach offers scientists a new gateway to study microbial ecosystems in complex solid, moist matrices.

No alternative *in situ* surveillance strategy can match the chemical precision or panoramic-scale of this approach. Alternative strategies are limited to visual speculation and lack the chemical validation that is indigenous to Raman spectroscopic analyses. Unlike optical surveillance approaches, *in situ* Raman surveillance is not reliant on the distribution of an analyte among a substrate. Inconsistent distributions of an analyte generally discourage *in situ* analyses due to their innate invisibility. Raman surveillance can now overcome this limitation through sweeping, dragnet spectral collections across unprecedented surface areas. Through this approach, we generated chemical images which detailed the inconsistent distribution of bacteria cells respective to their plant tissue substrate. Chemical analyses of this nature will act as the foundation of digitized microbiology. Efforts to refine this approach for the study of specific species, cell migration patterns, cellular communications, and biological responses to stimuli among a variety of relevant substrates are currently underway.

6.4.3. Imaging bacterial adhesion among cantaloupe

Raman imaging offered profound new visual insight into bacterial ecosystems as they exist among contaminated cantaloupe (Figure 27). *Escherichia coli* populations transitioned inward from cantaloupe surfaces toward crevices among the epidermal net surrounding the melon. Foodborne illness risks among cantaloupe are therefore increased respective to the duration at which each melon is neglected rinse applications. Cantaloupe surfaces are strongly hydrophobic and are thus easier to clean immediately following contamination rather than later when bacteria have found shelter below the hydrophobic epidermal network or within porous cavities throughout the epidermal net. SERS proved that the immediate rinsing of contaminated cantaloupe resulted in substantial decreases in bacteria populations. More bacteria endured rinse washes when contaminated cantaloupe were left untreated for 24 hours. Raman imaging proved that bacteria were able to bore into microcavities within the outer net surrounding the melon which aided in their brace against rinse washing. The data suggests that bacteria survival upon cantaloupe is more sustainable circling the circumference of the epidermal net compartments rather than upon the net itself. Bacterial contaminants are therefore a higher food safety risk in the days following bacterial exposure if rinse applications are ignored.

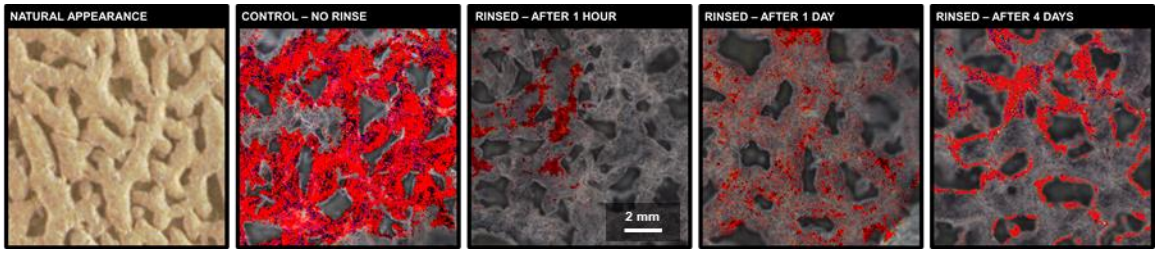

Figure 27: Labelled bacteria cells were Raman surveilled upon cantaloupe tissues to demonstrate the potential for this method in evaluating rinse-wash efficacy. Clear trends emerged with respect to the duration of unwashed contamination and bacterial adherence. No alternative method will offer this level into bacterial population surveillance directly within plant tissues.

6.4.4. Structural limitations when imaging bacteria among plant tissues

Raman imaging of bacteria among peanuts proved that the approach is highly sensitive to the incident point-of-contact (Figure 28). Cells can conclusively be detected and imaged by means of Raman scattering on complex plant structures. However, deep concavities and changes in surface structure resulted in significant data losses. The z-coordinate is therefore conclusively sensitive to optical calibration and the substrate must be in-focus to collect data. Peanuts consistently vary in size and shape, rendering their Raman analyses rather challenging. The peanut must be oriented by the user in such a way that a significant portion of the legume is in-focus on the x-y plane.

Raman depth profiling proved that z-axis structural limitations can be overcome. The hurdle requires multiple x-y images to be collected at various z-coordinates to comprehensively merge the information. There is a drawback in terms of experimental duration, as the user is essentially running the same experiment several times over. However, the approach offers scientists the opportunity to mass-surveil entire bacterial populations directly *in situ* among high-risk foods. No alternative method provides this type of information.

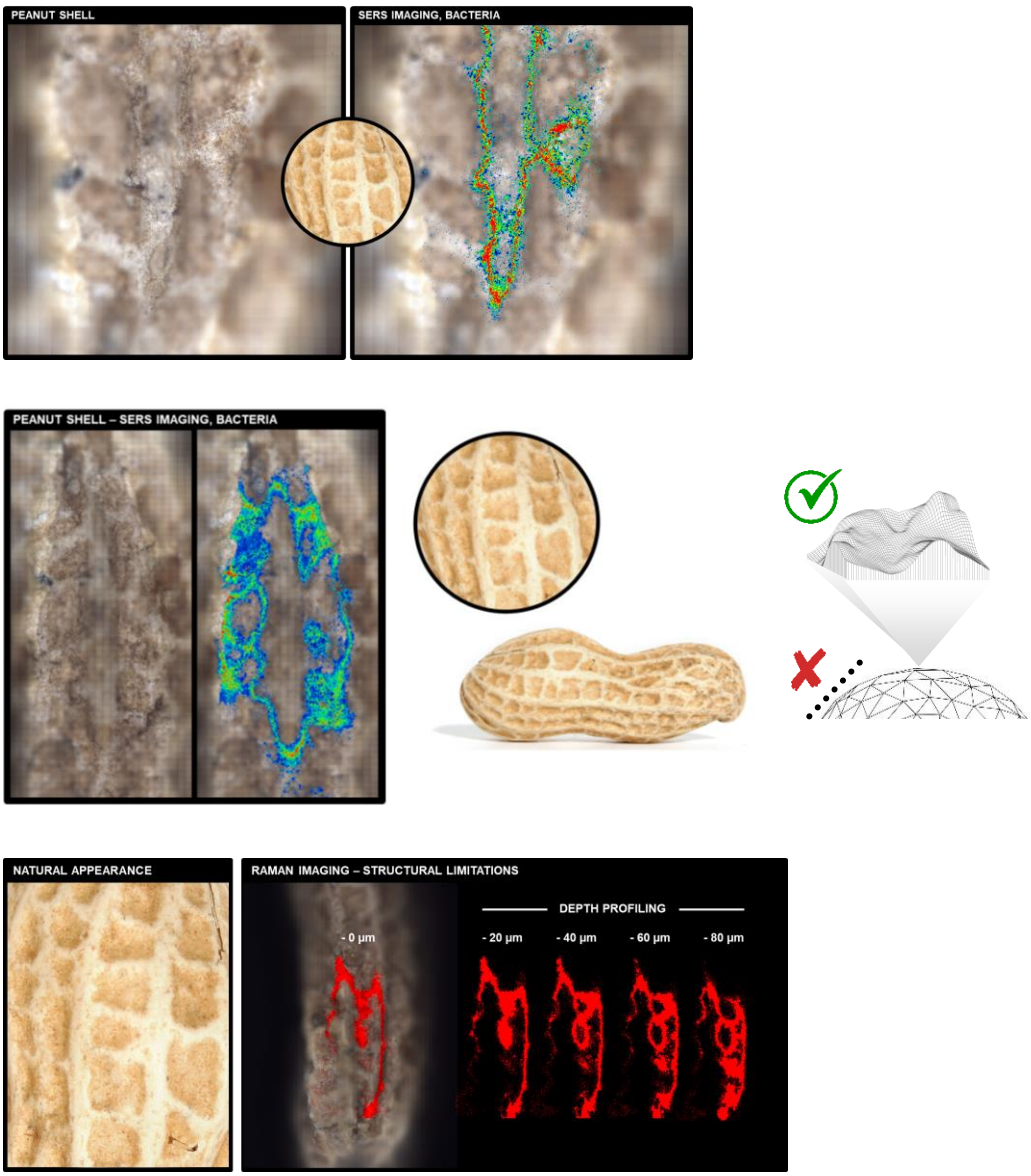

Figure 28: Peanuts were contaminated with bacteria to assess the ability of the Raman instrument to surveil cell populations among highly complex structures. There is conclusive evidence that minor structural changes are not inhibitory to the analysis. However, major physical changes will cause the instrument to move out-of-focus and the light incident will not be compatible with detection. Thus, depth profiling of complex structures can be employed to overcome this limitation.

6.5. Conclusions

We have proven, in concept and application, that bacteria can be monitored in real-time within a solid substrate directly *in situ* using surface-enhanced Raman spectroscopy. The present method can offer new insight into the behavior of bacteria directly in their natural ecosystem. Further applications of this method will help elucidate the nature of bacteria in plant tissues. Bacterial surveillance within plant tissues *in situ* will allow us to identify potential promoters or vulnerabilities in bacterial viability which can be exploited to improve modern agriculture or public safety.

CHAPTER 7

SUMMARY

Bacterial growth curves are important blueprints that need to be followed judiciously when making quantitative assessments of cell populations based on Raman light-scattering. Raman instruments will not distinguish between whole-cells, duplicate cells, damaged cells, or inactive cells without specialized, optimized protocols. We strictly adopted this responsibility when analyzing bacterial populations, herein. Labelling of bacteria cells with 3-mercaptophenylboronic esters is a known concept among Raman spectroscopy circles. However, we elucidated and overcame important vulnerabilities to the method that would have otherwise prevented further innovation of the approach. We also compared the data to label-free efforts to demonstrate the challenges of translating the experiment to real-field applications, such as those regarding plant tissues. Sodium hydroxide incorporation greatly enhanced bacterial coating with the boronic acid and prevented hydrolysis under rinse-washing. Thus, the approach was conclusively suitable for the evaluation of rinse-washing efficacy by means of Raman light-scattering. We demonstrated, with visual evidence that is inherent to Raman imaging, that contamination duration is directly related to bacterial adhesion to cantaloupe surfaces. Longer exposure of bacteria to cantaloupe increases the likelihood that bacteria will be eaten by the end-consumer, regardless of rinse-washing. There are structural limitations to the approach that is define in this dissertation; such as that of complex peanut shapes causing out-of-focus data collections. However, these challenges

can be overcome using the same depth profiling function on the surface of complex structures that we used to screen for internalized bacteria within plant tissues. No alternative method will offer this level into bacterial population surveillance directly within plant tissues.

REFERENCES

1. Alexander TA, Pellegrino PM, Gillespie JB, 2003. Near-infrared surface-enhanced-Raman-scattering-mediated detection of single optically trapped bacterial spores. Appl. Spectrosc., 57(11): 1340-1345. Link
2. Baena JR, Lenl B, 2004. Raman spectroscopy in chemical bioanalysis. Curr. Opin. Chem. Biol., 8(5): 534-539. Link
3. Bebu A, Szabó L, Leopold N, Berindean C, David L, 2011. IR, Raman, SERS and DFT study of amoxicillin. J. Mol. Struc., 993(1-3): 52-56. Link
4. Cam D, Keseroglu K, Kahraman M, Sahin F, Culha M, 2009. Multiplex identification of bacteria in bacterial mixtures with surface-enhanced Raman scattering. J. Raman Spectrosc., 41(5): 484-489. Link
5. Carlson HK, Iavarone AT, Gorur A, Yeo BS, Tran R, Melnyk RA, Mathies RA, Auer M, Coates JD, 2012. Surface multiheme *c*-type cytochromes from *Therminocola potens* and implication for respiratory metal reduction by Gram-positive bacteria. Proc. Natl. Acad. Sci., 109(5): 1702-1707. Link
6. Centers for Disease Control and Prevention (CDC), 2006. Ongoing multistate outbreak of *Escherichia coli* serotype O157:H7 infections associated with consumption of fresh Spinach – United States, September 2006. Morbidity and Mortality Weekly Report, 55: 1045 – 1046.
7. Centers for Disease Control and Prevention (CDC), 2010. CDC reports 1 in 6 get sick from foodborne illnesses each year [Press Release]. Retrieved from: http://bit.ly/2eLdjS4.

8. Chan JW, Esposito AP, Talley CE, Hollars CW, Lane SM, Huser T, 2004. Reagentless identification of single bacterial spores in aqueous solution by confocal laser tweezers Raman spectroscopy. Anal. Chem., 76(3): 599-603. Link
9. Chen, H.-Y., Guo, D., Gan, Z.-F., Jiang, L., Chang, S., Li, D.-W., 2019. A phenylboronic-based SERS nanoprobe for detection and imaging of intracellular peroxynitrite. Microchim. Acta 186, 11. Link
10. Chen, Y., Premasiri, W.R., Ziegler, L.D., 2018. Surface enhanced Raman spectroscopy of Chlamydia trachomatis and Neisseria gonorrhoeae for diagnostics, and extra-cellular metabolomics and biochemical monitoring. Sci. Rep. 8, 5163. Link
11. Cheng H-W, Huan S-Y, Wu H-L, Shen G-L, Yu R-Q, 2009. Surface-enhanced Raman spectroscopic detection of a bacteria biomarker using gold nanoparticle immobilized substrates. Anal. Chem., 81(24): 9902-9912. Link
12. Cheng I-F, Chen T-Y, Lu R-J, Wu H-W, 2014. Rapid identification of bacteria utilizing amplified dielectrophoretic force-assisted nanoparticle-induced surface-enhanced Raman spectroscopy. Nanoscale Res. Lett., 9: 324. Link
13. Chisanga M, Muhamadali H, Ellis DI, Goodacre R, 2018. Surface-enhanced Raman scattering (SERS) in microbiology: Illumination and enhancement of the microbial world. Appl. Spectrosc., 72(7): 987-1000. Link
14. Chu H, Huang Y, Zhao Y, 2008. Silver nanorod arrays as a surface-enhanced Raman scattering substrate for foodborne pathogenic bacteria detection. Appl. Spectrosc., 62(8): 922-931. Link
15. Colniță A, Dina NE, Leopold N, Vodnar DC, Bogdan D, Porav SA, David L, 2017. Characterization and discrimination of Gram-positive bacteria using Raman

spectroscopy with the aid of principle component analysis. Nanomaterials, 7(248): doi:10.3390/nano7090248. Link

16. Cowcher DP, Xu Y, Goodacre R, 2013. Portable, quantitative detection of Bacillus bacterial spores using surface-enhanced Raman scattering. Anal. Chem., 85(6): 3297-3302. Link
17. Craig AP, Franca AS, Irudayaraj J, 2013. Surface-enhanced Raman spectroscopy applied to food safety. Annu. Rev. Food Sci. Technol., 4: 369-380. Link
18. Crowley, L.C., Scott, A.P., Marfell, B.J., Boughaba, J.A., Chojnowski, G., Waterhouse, N.J., 2016. Measuring cell death by propidium iodide uptake and flow cytometry. Cold Spring Harb. Protoc. 7, 647-651. Link
19. Çulha M, Adigüzel A, Yazici MM, Kahraman M, Slahin F, Güllüce M, 2008. Characterization of thermophilic bacteria using surface-enhanced Raman scattering. Appl. Spectrosc., 62(11): 1226-1232. Link
20. Culha M, Kahraman M, Çam D, Sayın I, Keseroğlu K, 2010. Rapid identification of bacteria and yeast using surface-enhanced Raman scattering. Surf. Interface Anal., 42(6-7): 462-465. Link
21. De Marchi, S., Bodelón, G., Vázquez-Iglesias, L., Liz-Marzán, L.M., Pérez-Juste, J., Pastoriza-Santos, I., 2019. Surface-enhanced Raman scattering (SERS) imaging of bioactive metabolites in mixed bacterial populations. Appl. Mater. Today 14, 207-215. Link
22. Dina NE, Zhou H, Colniță A, Leopold N, Szoke-Nagy T, Coman C, Haisch C, 2017. Rapid single-cell detection and identification of pathogens by using surface-enhanced Raman spectroscopy. Analyst, 142(10): 1782-1789. Link

23. Dong C, Yan Z, Kokx J, Chrisey DB, Dinu CZ, 2012. Antibacterial and surface-enhanced Raman scattering (SERS) activities of AgCl cubes synthesized by pulsed laser ablation in liquid. Appl. Surf. Sci., 258(23): 9218-9222. Link
24. Driskell JD, Seto AG, Jones LP, Jokela S, Dluy RA, Zhao Y-P, Tripp RA, 2008/. Rapid microRNA (miRNA) detection and classification via surface-enhanced Raman spectroscopy (SERS). Biosens. Bioelectron., 24(4): 917-922. Link
25. Dutta RK, Sharma PK, Pandey AC, 2009. Surface enhanced Raman spectra of *Escherichia coli* cells using ZnO nanoparticles. Dig. J. Nanomater. Biostruct., 4(1): 83-87. Link
26. Efrima S, Zeiri L, 2008. Understanding SERS of bacteria. J. Raman Spectrosc., 40(3): 277-288. Link
27. Fan C, Hu Z, Mustapha A, Lin M, 2011. Rapid detection of food- and waterborne bacteria using surface-enhanced Raman spectroscopy coupled with silver nanosubstrates. Appl. Microbiol. Biotechnol., 92(5):
28. Fan Z, Senapati D, Khan SA, Singh AK, Hamme A, Yust B, Sardar D, Ray PC, 2013. Popcorn-shaped magnetic core-plasmonic shell multifunctional nanoparticles for the targeted magnetic separation and enrichment, label-free SERS imaging, and photothermal destruction of multidrug-resistant bacteria. Chem. Eur. J., 19(8): 2839-2847. Link
29. Food and Agricultural Organization of the United Nations, 2009. How to feed the world in 2050: Executive Summary. Conference: High-level expert forum, Rome, Italy.
30. Gao, S., Pearson, B., He, L., 2018. Mapping bacteria on filter membranes, an innovative SERS approach. J. Microbiol. Meth. 147, 69-75. Link

31. Goeller LJ, Riley MR, 2007. Discrimination of bacteria and bacteriophages by Raman spectroscopy and surface-enhanced Raman spectroscopy. Appl. Spectrosc., 61(7): 679-685. Link

32. Gopinath A, Boriskina SV, Reinhard BM, Dal Negro L, 2009. Deterministic aperiodic arrays of metal nanoparticles for surface-enhanced Raman scattering (SERS). Optics Express, 17(5): 3741-3753. Link

33. Golabi, M., Kuralay, F., Jagar, W.H.E., Beni, V., Turner, A.P.F., 2017. Electrochemical bacterial detection using poly(3-aminophenylboronicacid)-based imprinted polymer. Biosens. Bioelectron. 93, 87-93. Link

34. Gracie K, Correa E, Mabbott S, Dougan JA, Graham D, Goodacre R, Faulds K, 2014. Simultaneous detection and quantification of three bacterial meningitis pathogens by SERS. Chem. Sci., 5(3): 1030-1040. Link

35. Guicheteau, J., Christesen, S., Emge, D., Tripathi, A., 2010. Bacterial mixture identification using Raman and surface-enhanced Raman chemical imagin. J. Raman Spectrosc. 41, 1632-1637. Link

36. Guven B, Basaran-Akgul N, Temur E, Tamer U, Boyacı İH, 2011. SERS-based sandwich immunoassay using antibody coated magnetic nanoparticles for *Escherichia coli* enumeration. Analyst, 136(4): 740-748. Link

37. Halvorson RA, Vikesland PJ, 2010. Surface-enhanced Raman spectroscopy (SERS) for environmental analyses. Environ. Sci. Technol., 44(20): 7749-7755. Link

38. Harz M, Rösch P, Peschke K-D, Ronneberger O, Burkhardt H, Popp J, 2005. Micro-Raman spectroscopic identification of bacterial cells of the genus *Staphylococcus* and dependence on their cultivation conditions. Analyst, 130(11): 1543-1550. Link

39. Hering K, Cialla D, Ackermann K, Dörfer T, Möller R, Schneidewind H, Mattheis R, Fritzche W, Rösch P, Popp J, 2008. SERS: A versatile tool in chemical and biochemical diagnostics. Anal. Bioanal. Chem., 390(1): 113-124. Link
40. Hu, Q., Tay, L.-L., Noestheden, M., Pezacki, J.P., 2007. Mammalian cell surface imaging with nitrile-functionalized nanoprobes: Biophysical characterization of aggregation and polarization anisotropy in SERS imaging. J. Am. Chem. Soc. 129, 14-15. Link
41. Hudson SD, Chumanov G, 2009. Bioanalytical applications of SERS (surface-enhanced Raman spectroscopy). Anal. Bioanal. Chem., 394(3): 679-686. Link
42. Iwatsuki, S., Nakajima, S., Inamo, M., Takagi, H.D., Ishihara, K., 2007. Whis is reactive in alkaline solution, boronate ion or boronic acid? Kinetic evidence for reactive trigonal boronic acid in an alkaline solution. Inorg. Chem. 46, 354-356. Link
43. Izake EL, 2010. Forensic and homeland security applications of modern portable Raman spectroscopy. Forensic Sci. Int., 202(1-3): 1-8. Link
44. Jarvis RM, Brooker A, Goodacre R, 2004. Surface-enhanced Raman spectroscopy for bacterial discrimination utilizing a scanning electron microscope with a Raman spectroscopy interface. Anal. Chem., 76(17): 5198-5202. Link
45. Jarvis RM, Brooker A, Goodacre R, 2006. Surface-enhanced Raman scattering for the rapid discrimination of bacteria. Faraday Discuss., 132: 281-292. Link
46. Jarvis RM, Goodacre R, 2004. Discrimination of bacteria using surface-enhanced Raman spectroscopy. Anal. Chem., 76(1): 40-47. Link

47. Jarvis RM, Goodacre R, 2004. Ultra-violet resonance Raman spectroscopy for the rapid discrimination of urinary tract infection bacteria. FEMS Microbiol. Lett., 232(2): 127-132. Link

48. Jarvis RM, Goodacre R, 2008. Characterisation and identification of bacteria using SERS. Chem. Soc. Rev., 37(5): 931-936. Link

49. Jarvis RM, Law N, Shadi IT, O'Brien P, Lloyd JR, Goodacre R, 2008. Surface-enhanced Raman scattering from intracellular and extracellular bacterial locations. Anal. Chem., 80(17): 6741-6746. Link

50. Kahraman M, Keseroğlu K, Culha M, 2011. On sample preparation for surface-enhanced Raman scattering (SERS) of bacteria and the source of spectral features of the spectra. Appl. Spectrosc., 65(5): 500-506. Link

51. Kahraman M, Yazici MM, Şahin F, Bayrak OF, Culha M, 2007. Reproducible surface-enhanced Raman scattering spectra of bacteria on aggregated silver nanoparticles. Appl. Spectrosc., 61(5): 479-485. Link

52. Kahraman M, Yazici MM, Sahin F, Culha F, 2007. Experimental parameters influencing surface-enhanced Raman scattering of bacteria. J. Biomed. Opt., 12(5): 054015. Link

53. Kahraman M, Yazici MM, Şahin F, Çulha M, 2008. Convective assembly of bacteria for surface-enhanced Raman scattering. Langmuir, 24(3): 894-901. Link

54. Kahraman M, Zamaleeva AI, Fakhrullin RF, Culha M, 2009. Layer-by-layer coating of bacteria with noble metal nanoparticles for surface-enhanced Raman scattering. Anal. Bioanal. Chem., 395(8): 2559-2567. Link

55. Kao P, Malvadkar NA, Cetinkaya M, Wang H, Allara DL, Demirel MC, 2008. Surface-enhanced Raman detection on metalized nanostructured poly)*p*-xylylene) films. Adv. Mater., 20(18): 3562-3565. Link

56. Kataoka, K., Miyazaki, H., 1994. Sensitive glucose-induced change of the lower critical solution temperature of Poly[N,N-(dimethylacrylamide)-co-3-(acrylamido)-phenylboronic acid] in physiological saline. Macromolecules. 27, 1061-1062. Link

57. Knauer M, Ivleva NP, Niessner R, Haisch C, 2010. Optimized surface-enhanced Raman scattering (SERS) colloids for the characterization of microorganisms. Anal. Sci., 26(7): 761-766. Link

58. Knauer M, Ivleva NP, Niessner R, Haisch C, 2012. A flow-through microarray cell for the online SERS detection of antibody-captured *E. coli* bacteria. Anal. Bioanal. Chem., 402(8): 2663-2667. Link

59. Kneipp K, Wang Y, Kneipp H, Perelman LT, Itzkan I, Dasari RR, Feld MS, 1997. Single molecule detection using surface-enhanced Raman scattering (SERS). Physical Review Letters, 78(9): 1667 – 1670. Link

60. Ko, J., Park, S.-G., Lee, S., Wang, X., Mun, C., Kim, S., Kim, D.-H., Choo, J., 2018. Culture-free detection of bacterial pathogens on plasmonic nanopillar arrays using rapid Raman mapping. ACS Appl. Mater. Interfaces 10, 6831-6840. Link

61. Kotanen CN, Martinez L, Alvarez R, Simecek JW, 2016. Surface enhanced Raman scattering spectroscopy for detection and identification of microbial pathogens isolated from human serum. Sens. Biosensing Res., 8: 20-26. Link

62. Kudelski A, 2008. Analytical applications of Raman spectroscopy. Talanta, 76(1): 1-8. Link

63. Larkin, J.D., Bhat, K.L., Markham, G.D., Brooks, B.R., Schaefer, H.F., Bock, C.W., 2006. Structure of the boronic acid dimer and the relative stabilites of its conformers. J. Phys. Chem. A 110, 10633-10642. Link

64. Laucks ML, Sengupta A, Junge K, Davis EJ, Swanson BD, 2005. Comparison of psychro-active arctic marine bacteria and common mesophilic bacteria using surface-enhanced Raman spectroscopy. Appl. Spectrosc., 59(10): 1222-1228. Link

65. Le Ru, E.C., Etchegoin, P.G., 2012. Single-molecule surface-enhanced Raman spectroscopy. Annu. Rev. Phys. Chem. 63, 65-87. Link

66. Lee, S., Chon, H., Lee, J., Ko, J., Chung, B.H., Lim, D.W., Choo, J., 2014. Rapid and sensitive phenotypic marker detection on breast cancer cells using surface-enhanced Raman scattering (SERS) imaging. Biosens. Bioelectron. 51, 238-243. Link

67. Li M, Xu J, Romero-Gonzalez M, Banward SA, Huang WE, 2012. Single cell Raman spectroscopy for cell sorting and imaging. Curr. Opin. Biotech., 23(1): 56-63. Link

68. Lin D, Qin T, Wang Y, Sun X, Chen L, 2014. Graphene oxide wrapped SERS tags: Multifunctional platforms toward optical labeling, photothermal ablation of bacteria, and the monitoring of killing effect. ACS Appl. Mater. Inter., 6(2): 1320-1329. Link

69. Lin H-Y, Huang C-H, Hsieh W-H, Liu L-H, Lin Y-C, Chu C-C, Wang S-T, Kuo I-T, Chau L-K, 2014. On-line SERS detection of single bacterium using novel SERS nanoprobes and a microfluidic dielectrophoresis device. Small, 10(22): 4700-4710. Link

70. Liu T-Y, Tsai K-T, Wang H-H, Chen Y, Chen Y-H, Chao Y-C, Chang H-H, Lin C-H, Wang J-K, Wang Y-L, 2011. Functionalized arrays of Raman-enhancing nanoparticles for capture and culture-free analysis of bacteria in human blood. Nat. Commun., 2(538): DOI: 10.1038/ncomms1546. Link

71. Liu Y, Chen YD, Nou X, Chao K, 2007. Potential of surface-enhanced Raman spectroscopy for the rapid identification of *Escherichia coli* and *Listeria monocytogenes* cultures on silver colloidal nanoparticles. Appl. Spectrosc., 61(8): 824-831. Link
72. Liu Y, Zhou H, Hu Z, Yu G, Yang D, Zhao J, 2017. Label and label-free based surface-enhanced Raman scattering bacteria detection: A review. Biosens. Bioelectron., 94: 131-140. Link
73. Lucier G, Allshouse J, and Lin B-W, 2004. Factors affecting spinach consumption in the United States. Electronic Outlook Report from the Economic Research Service, VGS-300-01.
74. Luo S, Lin M, 2007. A portable Raman system for the identification of foodborne pathogenic bacteria. J. Rapid Methods Autom. Microbiol., 16(3): 238-255.
75. Madiyar FR, Bhana S, Swisher LZ, Culbertson CT, Huang X, Li J, 2015. Integration of a nanostructured dielectrophoretic device and a surface-enhanced Raman probe for highly sensitive rapid bacteria detection. Nanoscale, 7(8): 3726-3736. Link
76. McNay G, Eustace D, Smith WE, Faulds K, Graham D, 2011. Surface-enhanced Raman scattering (SERS) and surface-enhanced resonance Raman scattering (SERRS): A review of applications. Appl. Spectrosc., 65(8): 825-837. Link
77. Mosier-Boss PA, 2017. Review on SERS of bacteria. Biosensors, 7(51): doi:10.3390/bios7040051. Link
78. Murakami, H., Akiyoshi, H., Wakamatsu, T., Sagara, T., Nakashima, N., 2000. Electrochemical saccharide recognition by a phenylboronic acid-terminated redox active self-assembled monolayer on a gold electrode. Chem. Lett. 29, 940-941. Link

79. Naja G, Bouvrette P, Hrapovic S, Luong JHT, 2007. Raman-based detection of bacteria using silver nanoparticls conjugated with antibodies. Analyst, 132(7): 679-686. Link

80. Neugebauer U, Rösch P, Schmitt M, Popp J, Julien C, Rasmussen A, Budich C, Deckert V, 2006. On the way to nanometer-sized information of the bacterial surface by tip-enhanced Raman spectroscopy. Chem. Phys. Chem., 7(7): 1428-1430. Link

81. Nishiyabu, R., Kubo, Y., James, T.D., Fossey, J.S., 2011. Boronic acid building blocks: tools for sensing separation. Chem. Commun. 4, 1106-1123. Link

82. Oleson AP, Spies KB, Browning AC, Soneral PAG, Lindquist NC, 2017. Chemically imaging bacteria with super-resolution SERS on ultra-thin silver substrates. Sci. Rep., 7: 9135. Link

83. Otsuka, H., Uchimura, E., Koshino, H., Okano, T., Kataoka, K., 2003. Anomalous binding profile of phenylboronic acid with N-Acetylneuraminic acid (Neu5Ac) in aqueous solution with varying pH. J. Am. Chem. Soc. 125, 3493-3502. Link

84. Pahlow S, Meisel S, Cialla-May D, Weber K, Rösch P, Popp J, 2015. Isolation and identification of bacteria by means of Raman spectroscopy. Adv. Drug Deliv. Rev., 89: 105-120. Link

85. Painter JA, Hoekstra RM, Ayers T, Tauxe RV, Braden CR, Angulo FJ, Griffin PM, 2013. Attribution of foodborne illnesses, hospitalizations, and deaths to food commodities by using outbreak data, United States, 1998-2008. Emerging Infectious Diseases, 19(3): 407 – 415. Public Law 11-35, 2011. 111th Congress, HR 2751. 124 STAT. 3885 – 3973.

86. Paipetis, A., Vlattas, C., Galiotis, C., 1996. Remote laser Raman microscopy (ReRaM. 1-Design and testing of a confocal microprobe. J. Raman Spectrosc. 27, 519-526. Link

87. Park, H., Lee, S., Chen, L., Lee, E.K., Shin, S.Y., Lee, Y.H., Son, S.W., Oh, C.H., Song, J.M., Kang, S.H., Choo, J., 2009. SERS imaging of HER2-overexpressed MCF7 cells using antibody-conjugated gold nanorods. Phys. Chem. Chem. Phys. 11, 7444-7449. Link
88. Patel IS, Premasiri WR, Moir DT, Ziegler LD, 2008. Barcoding bacterial cells: a SERS-based method for pathogen identification. J. Raman Spectrosc., 39(11): 1660-1672. Link
89. Pearson, B., Mills, A., Tucker, M., Gao, S., McLandsborough, L., He, L., 2018. Rationalizing and advancing the 3-MPBA SERS sandwich assay for rapid detection of bacteria in environmental and food matrices. Food Microbiol. 72, 89-97. Link
90. Pearson, B., Wang, P., Mills, A., Pang, S., McLandsborough, L., He, L., 2017. Innovative sandwich assay with dual optical and SERS sensing mechanisms for bacterial detection. Anal. Methods 9, 4732-4739. Link
91. Peters, C., Wolff, L., Haase, S., Thien, J., Brands, T., Koß, H.-J., Bardow, A., 2017. Multicomponent diffusion coefficients from microfluidics using Raman microspectroscopy. Lab Chip 16, 2768-2776. Link
92. Preciao-Flores S, Wheeler DA, Tran TM, Tanaka Z, Jiang C, Barboza-Flores M, Qian F, Li Y, Chen B, Zhang JZ, 2011. SERS spectroscopy and SERS imaging of *Shewanella oneidensis* using silver nanoparticles and nanowires. Chem. Commun., 47(14): 4129-4131. Link
93. Premasiri WR, Gebregziabher Y, Ziegler LD, 2011. On the difference between surface-enhanced Raman scattering (SERS) spectra of cell growth media and whole bacterial cells. Appl. Spectrosc., 65(5): 493-499. Link

94. Premasiri WR, Lee JC, Sauer-Budge A, Théberge R, Costello CE, Ziegler LD, 2016. The biochemical origins of the surface-enhanced Raman spectra of bacteria: a metabolomics profiling by SERS. Anal. Bioanal. Chem., 408(17): 4631-4647. Link
95. Primasiri WR, Moir DT, Klempner MS, Krieger N, Jones G, Ziegler LD, 2005. Characterization of the surface enhanced Raman scattering (SERS) of bacteria. J. Phys. Chem. B, 109(1): 312-320. Link
96. Prucek R, Ranc V, Kvítek L, Panáček A, Zbořil R, Kolář M, 2012. Reproducible discrimination between Gram-positive and Gram-negative bacteria using surface enhanced Raman spectroscopy with infrared excitation. Analyst, 137(12): 2866-2870. Link
97. Rao, N.Z., Larkin, J.D., Bock, C.W., 2016. A comparison of the structure and bonding in the aliphatic boronic R–B(OH)2 and borinic R–BH(OH) acids (R=H; NH2, OH, and F): a computational investigation. Struct. Chem. 27, 1081-1091. Link
98. Ravindranath SP, Henne KL, Thompson DK, Irudayaraj J, 2011. Raman chemical imaging of chromate reduction sites in a single bacterium using intracellularly grown gold nanoislands. ACS Nano, 5(6): 4729-4736. Link
99. Ryder AG, 2005. Surface enhanced Raman scattering for narcotic detection and applications to chemical biology. Curr. Opin. Chem. Biol., 9(5): 489-493. Link
100. Sauer-Budge AF, Ziegler LD, Premasiri WR, Klapperich CM, Lee JC, 2012. Rapid bacteria diagnostics via surface-enhance Raman microscopy. Spectroscopy, 27(6): s8-s21. Link

101. Schmid, T., Opilik, L., Blum, C., Zenobi, R., 2013. Nanoscale chemical imaging using tip-enhanced Raman spectroscopy: A critical review. Angew. Chem. Int. Ed. 52, 5940-5954. Link

102. Sengupta A, Laucks ML, Dildine N, Drapala E, Davis EJ, 2005. Bioaerosol characterization by surface-enhanced Raman spectroscopy (SERS). J. Aerosol. Sci., 36(5-6): 651-664. Link

103. Sengupta A, Mujacic M, Davis J, 2006. Detection of bacteria by surface-enhanced Raman spectroscopy. Anal. Bioanal. Chem., 386(5): 1379-1386. Link

104. Shanmukh S, Jones L, Driskell J, Zhao Y, Dluhy R, Tripp RA, 2006. Rapid and sensitive detection of respiratory virus molecular signatures using a silver nanorod array SERS substrate. Nano Lett., 6(11): 2630-2636. Link

105. Sivanesan A, Witkowska E, Adamkiewicz W, Dziewit Ł, Kamińska A, Waluk J, 2014. Nanostructured silver-gold bimetallic SERS substrates for selective identification of bacteria in human blood. Analyst, 139(5): 1027-1043. Link

106. Stephen KE, Homrighausen D, DePalma G, Nakatsu CH, Irudayaraj J, 2012. Surface enhanced Raman spectroscopy (SERS) for the discrimination of *Arthrobacter* strains based on variations in cell surface composition. Analyst, 137(18): 4280-4286. Link

107. Sun, F., Bai, T., Zhang, L., Ella-Menye, J.R., Liu, S., Nowinski, A.K., Jiang, S., Yu, Q., 2014. Sensitive and fast detection of fructose in complex media via symmetry breaking and signal amplification using surface-enhanced Raman spectroscopy. Anal. Chem. 86, 2387-2394. Link

108. Sundaram J, Park B, Kwon Y, Lawrence KC, 2013. Surface enhanced Raman scattering (SERS) with biopolymer encapsulated silver nanosubstrates for rapid detection of foodborne pathogens. Int. J. Food Microbiol., 167(1): 67-73. Link

109. Sundaram J, Park B, Kwon Y, Lawrence KC, 2013. Surface enhanced Raman scattering (SERS) with biopolymer encapsulated silver nanosubstrates for rapid detection of foodborne pathogens. International Journal of Food Microbiology, 167(1): 5221 – 5225.

110. Szafranksi, C.A., Tanner, W., Laibinis, P.E., Garrell, R.L., 1998. Surface-enhanced Raman spectroscopy of aromatic thiols and disulfides on gold electrodes. Langmuir. 14, 3570-3579. Link

111. Tian ZQ, 2005. Surface-enhanced Raman spectroscopy: Advancements and applications. J. Raman Spectrosc., 36(6-7): 466-470. Link

112. Tomson B, 2013. Vegetables big culprit in food illness. The Wall Street Journal, Life: January 29.

113. Tripp RA, Dluhy RA, Zhao Y, 2008. Novel nanostructures for SERS biosensing. Nano Today, 3(3-4): 31-37. Link

114. United States Department of Agriculture (USDA), 2016. Vegetables 2015 Summary, page(s) 39 and 56.

115. United States Food & Drug Administration (FDA), 2016. FDA Food Safety Modernization Act (FSMA). Retrieved from: http://www.fda.gov/Food/GuidanceRegulation/FSMA/

116. Vo-Dinh T, Houck K, Stokes DL, 1994. Surface-enhanced Raman gene probes. Anal. Chem., 66(20): 3379-3383. Link

117. Vo-Dinh T, Stokes DL, Griffin GD, Volkan M, Kim UJ, Simon MI. Surface-enhanced Raman scattering (SERS) method and instrumentation for genomics and biomedical analysis. J. Raman Spectrosc., 30(9): 785-793. Link

118. Walter A, März A, Schumacher W, Rösch P, Popp J, 2011. Towards a fast, high specific and reliable discrimination of bacteria on strain level by means of SERS in a microfluidic device. Lab Chip, 11(6): 1013-1021. Link

119. Wang H, Zhou Y, Jiang X, Sun B, Zhu Y, Wang H, Su Y, He Y, 2015. Simultaneous capture, detection, and inactivation of bacteria as enabled by a surface-enhanced Raman scattering multifunctional chip. Angew. Chem. Int. Ed., 54(17): 5132-5136. Link

120. Wang, P., Pang, S., Pearson, B., Chujo, Y., McLandsborough, L., 2017. Rapid concentration detection and differentiation of bacteria in skimmed milk using surface enhanced Raman scattering mapping on 4-mercaptophenylboronic acid functionalized silver dendrites. Anal. Bioanal. Chem. 409, 2229-2238. Link

121. Weise E and Schmit J, 2007. Spinach recall: 5 faces. 5 agonizing deaths. 1 year later. USA Today, Money: September 24.

122. Willets KA, 2009. Surface-enhanced Raman scattering (SERS) for probing internal cellular structure and dynamics. Anal. Bioanal. Chem., 394(1): 85-94. Link

123. Wu X, Xu C, Tripp RA, Huang Y-W, Zhao Y, 2013. Detection and differentiation of foodborne pathogenic bacteria in mung bean sprouts using field deployable label-free SERS devices. Analyst, 138(10): 3005-3012. Link

124. Wu X, Xu C, Tripp RA, Huang YW, Zhao Y, 2013. Detection and differentiation of foodborne pathogenic bacteria in mung bean sprouts using field deployable label-free SERS devices. Analyst, 138(10): 3005-3012. Link

125. Xue, Y., Li X., Li H., Zhang, W., 2014. Quantifying thiol-gold interactions towards the efficient strength control. Nat. Commun. 5, 4348. Link

126. Yamamoto YS, Ishikawa M, Ozaki Y, Itoh T, 2014. Fundamental studies on enhancement and blinking mechanism of surface-enhanced Raman scattering (SERS) and basic applications of SERS biological sensing. Front. Phys., 9(1): 31-46. Link

127. Yan B, Thubagere A, Premasiri WR, Ziegler LD, Negro LD, Reinhard BM, 2009. Engineered SERS substrates with multiscale signal enhancement: Nanoparticle cluster arrays. ACS Nano, 3(5): 1190-1202. Link

128. Yang D, Zhou H, Dina NE, Haisch C, 2018. Portable bacteria-capturing chip for direct surface-enhanced Raman scattering identification of urinary tract infection pathogens. R. Soc. Open Sci., 5: 180955. Link

129. Yang L, Yan B, Premasiri WR, Ziedgler LD, Negro LD, Reinhard BM, 2010. Engineering nanoparticle cluster arrays for bacterial biosensing: The role of the building block in multiscale SERS substrates. Adv. Funct. Mater., 20(16): 2619-2628. Link

130. Yang T, Zhang Z, Zhao B, Hou RY, Kinchla A, Clark JM, He L, 2016. Real-time and *in situ* monitoring of pesticide penetration in edible leaves by surface-enhanced Raman scattering mapping. Analytical Chemistry, 88(10): 5243-5250. Link

131. Yang X, Gu C, Qian F, Li Y, Zhang JZ, 2011. Highly sensitive detection of proteins and bacteria in aqueous using surface-enhanced Raman scattering and optical fibers. Anal. Chem., 83(15): 5888-5894. Link

132. Zeiri L, Bronk BV, Shabtai Y, Czégé J, Efrima S, 2002. Silver metal induced surfaced enhanced Raman of bacteria. Colloids Surf. A Physicochem. Eng. Asp., 208(1-3) 357-362. Link

133. Zeiri L, Bronk BV, Shabtai Y, Eichler J, Efrima S, 2004. Surface-enhanced Raman spectroscopy as a tool for probing specific biochemical components in bacteria. Appl. Spectrosc., 58(1): 33-40.

134. Zeiri L, Efrima S, 2005. Surface-enhanced Raman spectroscopy of bacteria: The effect of excitation wavelength and chemical modification of the colloidal milieu. J. Raman Spectrosc., 36(6-7): 667-675. Link

135. Zhang L, Xu J, Mi L, Gong H, Jiang S, Yu Q, 2012. Multifunctional magnetic-plasmonic nanoparaticles for fast concentration and sensitive detection of bacteria using SERS. Biosens. Bioelectron., 31(1): 130-136. Link

136. Zhang X, Young MA, Lyandres O, Van Duyne RP, 2005. Rapid detection of an anthrax biomarker by surface-enhanced Raman spectroscopy. J. Am. Chem. Soc., 127(12): 4484-4489. Link

137. Zhao X, Li M, Xu Z, 2018. Detection of foodborne pathogens by surface enhanced Raman spectroscopy. Front. Microbiol., 9: 1236. Link

138. Zhang, Y., Hong, H., Myklejord, D.V., Cai, W., 2011. Molecular imaging with SERS-active nanoparticles. Small 23, 3261-3269. Link

139. Zheng J and He L, 2014. Surface-enhanced Raman spectroscopy for the chemical analysis of food. Comprehensive Reviews in Food Science and Food Safety, 13(3): 317 – 328.

140. Zhou H, Yang D, Ivleva NP, Mircescu NE, Niessner R, Haisch C, 2014. SERS detection of bacteria in water by *in situ* coating with Ag nanoparticles. Anal. Chem., 86(3): 1525-1533. Link

141. Zhou H, Yang D, Ivleva NP, Mircescu NE, Schubert S, Niessner R, Wieser A, Haisch C, 2015. Label-free *in situ* discrimination of live and dead bacteria by surface-enhanced Raman scattering. Anal. Chem., 87(13): 6553-6561. Link